ADDIS ABABA UNIVERSITY

SCHOOL OF GRADUATE STUDIES

DISSOLUTION ENHANCEMENT OF ALBENDAZOLE USING SOLID DISPERSION TECHNIQUE

BEZA TESHOME (B.PHARM)

JUlY 2016

DISSOLUTION ENHANCEMENT OF ALBENDAZOLE USING SOLID DISPERSION TECHNIQUE

A Thesis Submitted to School of Graduate Studies of Addis Ababa University in Partial Fulfillment of the Requirements for the Degree of Master of Science in Pharmaceutics

By

Beza Teshome (B.Pharm)

Under the Supervision of Prof. Tsige Gebre-Mariam and Dr.Fitsum Feleke, Department of Pharmaceutics and Social Pharmacy, School of Pharmacy, Addis Ababa University.

JULY 2016

DISSOLUTION ENHANCEMENT OF ALBENDAZOLE USING SOLID DISPERSION TECHNIQUE

By

Beza Teshome (B.Pharm)

Department of Pharmaceutics and Social Pharmacy

School of pharmacy

Approved by:	Signature	Date
Prof. Tsige Gebre-Mariam (Advisor)	_____	_____
Dr. Fitsum Feleke (Advisor)	_____	_____
Dr. Nisha Mary Joseph (Examiner)	_____	_____
Dr. Kaleab Asres (Examiner)	_____	_____

ACKNOWLEDGEMENTS

Above all, Thanks to the Almighty God for giving me all the courage and patience.

It is a pleasure and privilege for me to express my sincere gratitude to my esteemed advisors Professor Tsige Gebre-Mariam and Dr. Fitsum Feleke for their continuous encouragement and valuable suggestions throughout the period of this work.

I am extremely grateful to Ethiopian Pharmaceuticals Manufacturing Share Company (EPHARM) for providing all the facilities during the study period. I convey my gratitude and warm thanks to the staff members in R & D and QA especially Mr. Tilahun Mekuria for whole hearted support and generous help. I am also thankful to East Africa Trading PVT LTD Company for providing samples of Albendazole.

My special gratitude also goes to Ato Fekade Tefera, the staff members of the Departments of Pharmaceutics & Social Pharmacy, classmates and friends who have contributed a lot to the successful accomplishment of this study. I am indebted to my beloved family for their continuous support and encouragement throughout the study period.

I would also like to acknowledge Addis Ababa University for providing me scholarship and sponsoring my study.

ACRONYMS

2D	Two dimensional
3D	Three dimensional
ABZ	Albendazole
ABZ-SO	Albendazole sulfoxide
API	Active pharmaceutical ingredient
ASON	Albendazole sulfone
BCS	Biopharmaceutics Classification System
BD	Bulk density
BZD	Benzimidazol
CDER	Center for Drug Evaluation and Research
CI	Carr's Index
CYP	Cytochrome P450
DSC	Differential Scanning Calorimetry
FDA	Food and Drug Administration
FMO	Flavin mono-oxygenases
FTIR	Fourier Transform Infrared spectroscopy
GI/GIT	Gastro-intestinal/Gastro-intestinal tract
HPMC	Hydroxypropyl methylcellulose
HPMCAS	Hydroxypropyl methylcellulose acetate succinate
HCL	Hydrochloric acid
HR	Hausner Ratio
MCC	Microcrystalline cellulose
M.p	Melting point
MW/MWs	Molecular weight/Molecular weights
NaOH	Sodium hydroxide
PEG/PEGs	Polyethylene glycol/Polyethylene glycols
PM/PMs	Physical mixture/Physical mixtures
PVP	Polyvinyl pyrrolidone K-30
RSM	Response surface methodology
SAC /SACs	Surface-active carrier/carriers

SCF	Supercritical fluids
SD/SDs	Solid dispersion/ Solid dispersions
SSG	Sodium starch glycolate
TD	Tapped density
Tg	Glass transition temperature
USP/NF	United States Pharmacopeia/National Formulary

TABLE OF CONTENTS

Contents **Page**

LIST OF TABLES

LIST OF FIGURES

ABSTRACT

Albendazole (ABZ) is a benzimidazol (BZD) derivative with broad spectrum of activity against human and animal helminth parasites. However, its poor water solubility gives rise to formulation problems and reduced bioavailability. These problems can be reduced by increasing the dissolution rate of the drug using different approaches such as solid dispersions (SDs).

This study was designed to formulate ABZ loaded SDs with improved dissolution profiles. For this purpose, binary and ternary SDs were prepared by kneading and solvent evaporation methods using the hydrophilic carriers such as polyethylene glycol 4000 (PEG), polyvinyl pyrrolidone K-30 (PVP) and hydroxypropyl methylcellulose 5 cps (HPMC) and the surfactant polysorbate 80. To prepare binary SDs, the carriers were used in three drug: carrier proportions (1:0.5, 1:1, 1:2), where as in case of ternary SDs, polysorbate 80 was added at 0.1 proportion of the pure drug for all proportions of the carriers used. Physical mixtures (PMs) containing the above mentioned carriers were similarly prepared for comparison purpose.

Fourier Transformer Infrared Spectroscopy (FTIR) studies of the samples stored for 2 months revealed interaction through hysdrogen bonding between the drug and the carriers. Differential Scanning Calorimetry (DSC) of the PMs and SDs indicated decreased crystallinity of the drug. Dissolution profiles of ABZ were remarkably improved from the binary and ternary SDs as well as from ternary PMs than the pure drug (4.50% within 60 min). The rate and extent of dissolution was significantly higher in the ternary systems than the binary systems ($p < 0.5$). Solvent evaporation method demonstrated the highest dissolution profile. The ternary SD of ABZ with PEG and polysorbate 80 at a ratio of 1:2:0.1 prepared with solvent evaporation technique showed the highest dissolution profile with 100% of the drug released within 60 min. The SDs with PEG showed higher dissolution profiles than with PVP in both the SDs prepared by kneading and solvent evaporation techniques. From the SDs prepared by kneading method, the highest drug release was observed with the carrier HPMC (88.8% of the drug being released with 60 min) followed by PEG (81.4%). In all the formulations the release of ABZ was shown to increase with increasing carrier proportions.

The prepared SDs were characterized for flow properties and compressibility. Tablets of selected SDs were prepared by direct compression method and evaluated for their quality attributes. The results revealed that the major factors that affect the SDs and tablet characteristics are carrier to drug ratio, the amount of microcrystalline cellulose (MCC) and compression force. Thus, 3 factors, two level (2^3) full factorial experimental design was selected to investigate the effects of the selected factors on the various responses such as flow property, compressibility and drug release in 10 min and 60 min. Accordingly, the various models describing the relationship of the selected variables were obtained using Design-Expert 9.0.6 software and the optimum area was determined. The optimal points for the responses were found to be 55.09% for amount of ABZ released within 10 min, 81.27% for amount of ABZ released within 30 min, 29.48° for angle of repose, 94.60 N for hardness and 0.62% for friability when the factors are set at compression force of 14.03 KN, carrier to drug ratio of 1.98 and concentration of MCC of 23.57%. The validity of obtained optimal point was confirmed experimentally. Evaluation of the optimized formulation showed successful formulation of ABZ SD tablets. The release profiles of the optimized tablet formulation were superior to marketed tablets. Thus, it can be concluded that the dissolution of ABZ is significantly enhanced by SD technique.

Key Words: Albendazole; HPMC; Kneading; PEG; Physical mixture; Polysorbate 80; PVP; Solid dispersion; Solvent evaporation

1. INTRODUCTION

Oral drug delivery is preferred for most drugs due to its several advantages like greater flexibility in design and high patient compliance (Vaskula *et al.*, 2012). The vast majority of orally administered drugs are intended to be absorbed from the gastro-intestinal tract (GIT). The slowest step in the series of rate processes that controls the overall rate and extent of appearance of drug in the systemic circulation is called the rate limiting step. The particular rate limiting step may vary from drug to drug (Giri *et al.*, 2010). The rate limiting step for most of the pharmaceutical formulations is low solubility and dissolution (Gawai *et al.*, 2013: Rajesh *et al.*, 2011)

The idea of permeability and solubility characteristics had been helpful to classify the drug under four classes prescribed by biopharmaceutics classification system (BCS) (Thorat *et al.*, 2011). The BCS groups poorly soluble compounds as Class II, compounds which feature poor solubility and high permeability and Class IV, compounds which feature poor solubility and poor permeability. Those drugs dissolve slowly, poorly and irregularly, and hence pose serious delivery challenges, like incomplete release from the dosage form, poor bioavailability, increased food effect and high inter-patient variability (Nagabandi *et al.*, 2011) .

In addition, poorly water-soluble drugs often require high doses in order to reach therapeutic plasma concentrations after oral administration. Improvement in the extent and rate of dissolution is highly desirable for such compounds, as this can lead to an increased and more reproducible oral bioavailability, and subsequently to clinically relevant dose reduction and more reliable therapy (Tejas *et al.*, 2010).

A possible strategy to improve solubility and, thus, bioavailability, without modifying drug chemical structure, strictly connected to therapeutic properties is to act on drug physical properties (Simone *et al.*, 2012). Especially for Class II substances, the bioavailability may be enhanced by increasing the solubility and dissolution rate of the drug in the gastro-intestinal (GI) fluids (Thorat *et al.*, 2011).

1.1. Solid dispersion (SD)

Enhancement of bioavailability of hydrophobic drugs is one of the major challenges in drug development (Anupama *et al.*, 2011a). Over the years, a number of techniques have been developed to improve the dissolution of poor water soluble drugs, such as inclusion complexation, salt formation, cogrinding, solubilization, and particle size reduction (Akiladevi *et al.*, 2011; Rupal *et al.*, 2009).

Among other techniques SD is one of the popular methods to enhance dissolution rate (Jahan *et al.*, 2011). This technique has been used by various researchers who have reported encouraging results with different drugs. The first drug whose rate and extent of absorption significantly enhanced using this technique was sulfathiazole by Sekiguchi and Obi (Sekiguchi and Obi, 1961). With accelerated increase in the number of FDA-approved products in recent years, SD is now firmly established as a platform technology for the formulation of poorly-soluble drugs (Huang and Dai, 2014). Few examples of SDs available in market are Sporanox® (iterconazole), Intelence® (etravirine), Prograf® (tacrolimus), Crestor® (rosuvastatin), Gris-PEG® (griseofulvin) and Cesamet® (nabilone) (Mahapatra *et al.*, 2012).

The term SD refers to a group of solid products consisting of at least two different components, generally a hydrophilic matrix and a hydrophobic drug. The matrix can be either crystalline or amorphous. The drug can be dispersed molecularly, in amorphous particles (clusters) or in crystalline particles.

1.1.1. Types of solid dispersion

1.1.1.1 Physicochemical classification of solid dispersions

I. Simple eutectic mixture

A simple eutectic mixture consists of two compounds that are completely miscible in the liquid state but only to a very limited extent in the solid state (Chowdary *et al.*, 2014). An eutectic mixture of a sparingly water soluble drug and a highly water soluble carrier may be regarded thermodynamically as an intimately blended physical mixture of its two crystalline component (Varma *et al.*, 2012).

Solid eutectic mixtures are usually prepared by rapid cooling of a co-melt of the two compounds in order to obtain a physical mixture of very fine crystals of the two components. When an eutectic mixture is exposed to water or gastrointestinal fluids, the soluble carriers dissolve rapidly leaving very fine crystalline state that will rapidly go into solution. Due to increased surface area of the insoluble compound, an enhanced dissolution rate and hence an increased oral absorption is obtained (Giri *et al.*, 2010).

II. Solid solutions

Solid solution consists of a solid solute dissolved in a solid solvent. The particle size in solid solution is reduced to molecular level. It was reported that a solid solution of a poorly soluble drug in a fast dissolving carrier achieves a faster dissolution rate than an eutectic mixture because the drug particle size is reduced to its absolute minimum as it is molecularly dispersed in the carrier in a solid solution. Solid solutions can be classified by two methods. According to the extent of miscibility of the two components, they may be classified as continuous or discontinuous (Patidar *et al.*, 2011b).

In continuous solid solutions, the two components are miscible in the solid state in all proportions. Theoretically, this means that the bonding strength between the two components is stronger than the bonding strength between the molecules of each of the individual components. Solid solutions of this type have not been reported in the pharmaceutical literature to date. In discontinuous solid solutions, the miscibility or solubility of one component in the other is limited (Chowdary *et al.*, 2014).

III. Glass solutions and suspensions

A glass solution, also known as an amorphous solution, is a homogeneous system in which a glassy or a vitreous form of the carrier solubilizes drug molecules (Giri *et al.*, 2010). A glass suspension refers to a mixture in which precipitated particles are suspended in a glassy solvent. The glassy state is characterized by transparency and brittleness below the glass transition temperature. Glasses do not have sharp melting points; instead, they soften progressively on heating. The lattice energy, which represents a barrier to rapid dissolution, is much lower in glass solutions than in solid solutions (Patidar *et al.*, 2011b).

An important disadvantage of glass solutions is that the glassy state is metastable compared to the crystalline state. Depending on its physicochemical properties and storage conditions a glass can convert into a crystalline solid. Crystallization from the amorphous state over practical time scales can be prevented by keeping the operating temperature below (glass transition temperature) $T_{g,}$ by reducing the water content or by raising the T_g of the system using additives with high T_g values (Giri *et al.*, 2010).

V. Amorphous precipitations in a crystalline carrier

The difference between this group of SDs and the simple eutectic mixture is that the drug is precipitated out in an amorphous form in the former as opposed to a crystalline form in the latter (Kaur *et al.*, 2012).

1.1.1.2 Classifications of solid dispersion on the basis of carrier used

I. First generation

First generation SDs were prepared using crystalline carriers such as urea and sugar, which were the first carriers to be employed in SD. They have the disadvantage of forming crystalline SD, which are thermodynamically more stable and did not release the drug as quickly as amorphous ones (Kaur *et al.*, 2012).

II. Second generation

In the 1960s, it was reported that amorphous SD was more effective than crystalline SD because of the thermodynamic stability. Therefore the second generation SDs contained amorphous carriers which are mostly polymers that can be fully synthetic, which include Polyvinylpyrrolidone (Kalyanwat and Patel, 2010) polyethyleneglycols (Chauhan *et al.*, 2005; Dabbagh and Taghipour, 2007; Venkatesh *et al.*, 2008) and polymethacrylates. The other is natural product based polymers, which is composed of cellulose derivatives like hydroxypropylmethylcellulose (Arunachalam *et al.*, 2011) ethylcellulose or hydroxypropylcellulose or starch derivates, like cyclodextrins (Kim *et al.*, 2011).

Polyethylene glycols

Polyethylene glycols (PEGs) are polymers of ethylene oxide (Fig. 1.1), with a molecular weight (MW) usually falling in the range 200-300,000 (Nikghalb *et al.*, 2012). For the manufacture of SDs and solutions, PEGs with molecular weights of 1,500-20,000 are usually employed (Mahapatra *et al.*, 2012). As the MW rises, so does the viscosity of the PEGs (Nikghalb *et al.*, 2012).

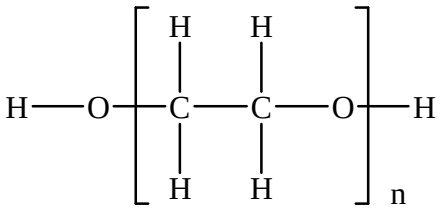

Figure 1.1: Molecular structure of PEG

Their solubility in water is generally good, but reduces with MW. A meticulous advantage of PEGs for the SDs include good solubility in numerous organic solvents (Nikghalb *et al.*, 2012), low toxicity and wide drug compatibility (Anupama *et al.*, 2011b). The melting point (M.p.) of the PEGs of interest lies under 65 ^{0}C in every case (e.g. the M.p. of PEG 1000 is 30-40 ^{0}C, the M.p. of PEG 4,000 is 50-58 ^{0}C and the M.p. of PEG 20,000 is 60-63 ^{0}C). Additional attractive features of the PEGs include their ability to solubilize some compounds and also to improve compound wettability (Nikghalb *et al.*, 2012).

PEGs are widely used in a variety of pharmaceutical formulations. Generally, they are regarded as nontoxic and nonirritant materials. Orally higher-molecular-weight PEGs are not significantly absorbed from the GIT. Absorbed PEGs are excreted largely unchanged in the urine, although low molecular weight may be partially metabolized (Rowe *et al.*, 2006).

Polyvinylpyrrolidone

Polymerization of vinyl pyrrolidone leads to polyvinyl pyrrolidone (PVP) of MWs ranging from 2,500 to 3,000,000 (Manohara *et al.*, 2014) . Depending upon the conditions of polymerization,

PVP can be prepared in a variety of MWs expressed by the so called “K-values” (Eq. 1.1), which are based on viscosity measurements (Chadha *et al.*, 2006).

$$K\ value = \frac{\left[(300C\ logZ + (C+1.5C\ logZ)^2)^{1/2} + 1.5C\ logZ - C\right]}{(0.15C + 0.003C^2)} \qquad \text{Eq. 1.1}$$

Where Z is the viscosity of PVP at a concentration C relative to water

PVP is mainly used as a binder in tablet formulations but it also increases the dissolution of the active ingredient. The soluble PVP grades are useful for preparing solid solutions and dispersions because of their good hydrophilization properties, universal solubility and ability to form water soluble complexes (Kadajji *et al.*, 2011) .

The structure of PVP consists of the polymeric unit of lactam with an internal amide bond (Fig. 1.2) which is polar and of a highly water soluble functional group making PVP highly hydrophilic. This water solubility can improve dispersed drug's wettability. Therefore, oral bioavailability would be improved by taking SDs prepared with PVP. It has high solubility in both water and broad ranges of organic solvents. Therefore the solvent method is adjustable to SD using this carrier (Kim *et al.*, 2011).

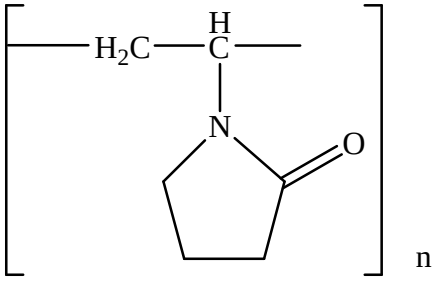

Figure 1.2: Molecular structure of PVP

PVP is also able to prevent crystallization of amorphous drug. This is mostly offered by antiplasticizing effect of PVP and by its surface adsorption and efficient steric hindrance for nucleation and crystal growth (Chadha *et al.*, 2006). Because of these advantages, PVP is the most commonly used polymer as carrier in making SDs. The toxicity of PVP is not problematic

at all in per oral SD formulations since the possibility to be absorbed in the GIT is low because of the comparatively large MW (Kim *et al.*, 2011).

Hydroxypropylmethylcellulose (HMPC)

HPMC (Fig. 1.3) is mixed ethers of cellulose, in which 16.5-30% of the hydroxyl groups are methylated and 4 - 32% is derivatized with hydroxypropyl groups. The MW of the HPMC ranges from about 10,000 to 1,500,000 and they are soluble in water and mixtures of ethanol with dichloromethane and methanol with dichloromethane (Nikghalb *et al.*, 2012).

HPMC products vary chemically and physically. The major chemical differences are in degree of methoxyl substitution, moles of hydroxypropoxyl substitution, and degree of polymerization. Varying ratios of hydroxypropyl and methyl substitution in different products influence properties such as organic solubility and thermal gelation temperature of aqueous solutions and swelling behavior (Gafourian *et al.*, 2007).

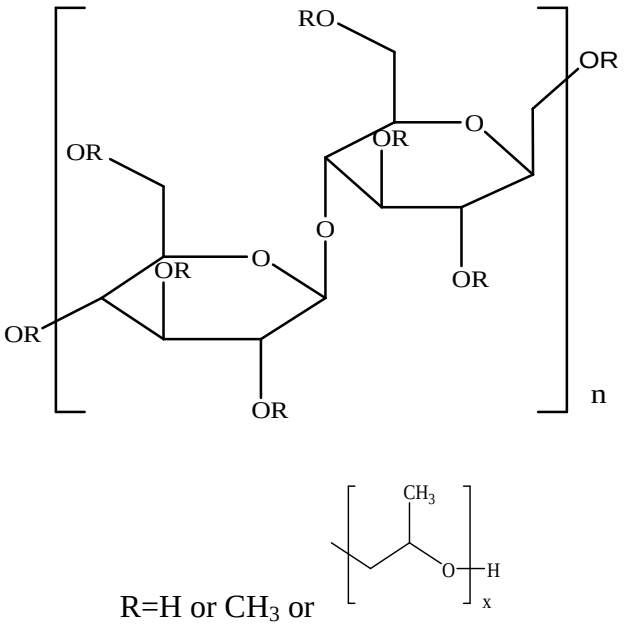

Figure 1.3: Molecular structure of HPMC

III. Third generation

Some studies evidenced that the dissolution rate may be improved using carriers, which possess surface activity or self-emulsifying properties. These third generation SDs showed to be more efficient for bioavailability enhancement and more stable SDs owed mainly to a reduction of drug recrystallization (Castro *et al.*, 2010).

A surface-active carrier (SAC) may be preferable in almost all cases for the SD of poorly water-soluble drugs. A commonly used surfactant, Polysorbate 80, when mixed with solid PEG, has also been reported to be an alternative SAC. Polysorbate 80 is liquid at room temperature; it forms a solid matrix when it is mixed with a PEG because it incorporates within the amorphous regions of PEG solid structure. The PEG-polysorbate carriers have been found to enhance dissolution and bioavailability of drugs from the SD. Other important SACs include poloxamers, Gelucire 44/14 and Vitamin E R-alpha-tocopheryl polyethylene glycol 1000 succinate (TPGS) (Dhirendra *et al.*, 2009).

1.1.2. Preparation of solid dispersions

Various preparation methods for SDs have been reported in the literature. These methods deal with the challenge of mixing a matrix and a drug, preferably on a molecular level, while matrix and drug are generally poorly miscible (Tiwari *et al.*, 2009). The methods used to prepare SDs include melting, solvent evaporation and kneading (Shinde *et al.*, 2010). Modifications of these methods and combination of them have also been used.

I. Solvent evaporation method

Tachibana and Nakamura were the two researchers who firstly applied solvent evaporation method for the preparation of SDs (Tachibana and Nakamura, 1965). The first step in the solvent method is the preparation of a solution containing both matrix material and drug. The second step involves the removal of solvent(s) resulting in the formation of a SD. The first challenge is to mix both drug and matrix in one solution, which is difficult when they differ significantly in polarity. To minimize the drug particle size in the SD, the drug and matrix have to be dispersed in the solvent as fine as possible, preferably in the dissolved state in one solution (Dhirendra *et*

al., 2009). Methods for solvent evaporation can be sub-classified as follows; vacuum drying, spray drying, freeze drying (lyophilization), and supercritical fluid evaporation (SCF). Vacuum drying is often used in the solvent evaporation method. A mixture of the drug and carrier is evaporated in a vacuum. Then, the manufactured SD is kept in a desiccator until the residual solvent is extirpated (Kim *et al.*, 2011).

Spar drying is an established method that is initiated by atomizing suspensions or solutions into fine droplets followed by a drying process, resulting solid particles. The process allows rapid drying, production of fine, dust free powder as well as agglomerated ones to precise specifications (Masters, 1991).

The other method is freeze drying method (lyophilization), which has been thought of a molecular mixing technique. The drug and carrier are co-dissolved in a common solvent, frozen and sublimed to obtain a lyophilized molecular dispersion (Patidar *et al.*, 2011a). The merit of this method is nominal thermal problems. What is more important is that possibility of phase separation is minimized. However, because the freezing point of most organic solvents is quite low, it is difficult to sublime the organic solvent completely (Kim *et al.*, 2011).

On the other hand, supercritical fluid method is also often used as the solvent evaporation method. Carbon dioxide is currently the most commonly used supercritical fluid. Because of its low critical temperature (31.06°C) and low critical pressure (7.38 MPa), it is suitable to precipitate heat-sensitive drugs (Arunachalam *et al.*, 2011). In the context of manufacturability, rate of cooling and solvent removal is stringently controlled, resulting in acceptable batch to batch variation (Kalyanwat and Patel, 2010).

The main advantage of the solvent method is thermal decomposition of drugs or carriers can be prevented because of the relatively low temperatures required for the evaporation of organic solvents. However, some disadvantages are associated with this method such as higher cost of preparation, the difficulty in completely removing liquid solvent, possible adverse effect of traces of the solvent on the chemical stability and selection of a common volatile solvent (Hasnain and Nayak, 2012; Jahan *et al.*, 2011).

II. Melting method

Sekiguchi and Obi first proposed the melting or fusion method, to prepare fast release SD dosage forms. In this method, the PM of drug and water-soluble carrier is heated directly until it is melted. The melted mixture is then cooled and solidified in an ice bath under vigorous stirring until solidification. The final mass is crushed, pulverized and sieved (Sekiguchi and Obi, 1961).

The main advantages of this method are its simplicity and economy. Although frequently applied, the fusion method has serious limitations. Firstly, a major disadvantage is that the method is only applied when the drug and matrix are compatible and when they mix well at the heating temperature. When the drug and matrix are incompatible two liquid phases or suspension can be observed in the heated mixture which results in an inhomogeneous SD and this problem can be prevented by using surfactants (Giri *et al.*, 2010).

Secondly, a problem can arise during cooling when the drug matrix miscibility changes. In this case phase separation can occur. Indeed, it was observed that when the mixture was slowly cooled, crystalline drug occurred, whereas fast cooling yielded amorphous SDs. Thirdly, degradation of the drug and or matrix can occur during heating to temperatures necessary to fuse matrix and drug (Kommavarapu *et al.*, 2014).

The degradation of somewhat thermolabile drugs can be prevented by using melt extrusion method. In this method the drug/carrier mix is typically processed with a twin screw extruder. The drug/carrier mix is simultaneously melted, homogenized and then extruded and shaped as tablets, granules, pellets, sheets, sticks or powder. The intermediates can then be further processed into conventional tablets. An important advantage of the hot melt extrusion method is that the drug/carrier mix is only subjected to an elevated temperature for about 1 min (Sameer *et al.*, 2011).

The other method is melt agglomeration process in which the binder acts as a carrier. This process consists heating the binder, drug and excipients to a temperature above the melting point of the binder or by spraying a dispersion of drug in molten binder on the heated excipients by using a high shear mixer. The effect of binder type, method of manufacturing and particle size are critical parameters in preparation of SDs by melt agglomeration. It has been investigated that

the spray on procedure with PEG-3000, Poloxamer 188 and gelucire 50/13 attributed to immersion mechanism of agglomerate formation and growth. In addition, the melt in procedure also results in homogeneous distribution of drugs in agglomerate (Yadav and Tanwar, 2015).

III. Kneading method

A mixture of accurately weighed drug and carrier is wetted with solvent and kneaded thoroughly using a glass mortar. The paste formed is dried and sieved (Chowdary *et al.*, 2014).

1.1.3. Mechanisms of enhanced dissolution

The main reasons postulated for the observed improvements in the dissolution of insoluble drugs form SDs are as follows:

A. Reduction of particle size:

In case of glass, solid solution and amorphous dispersions, particle size is reduced to a minimum level. This can result in an enhanced dissolution due to an increase in the surface area (Chowdary *et al.*, 2014).

B. Solubilization effect:

A strong contribution to the enhancement of drug solubility is related to the drug wettability improvement verified in SDs. It was observed that even carriers without any surface activity, such as urea improved drug wettability. Carriers with surface activity, such as cholic acid and bile salts are used, which can significantly increase the wettability property of a drug. Moreover, carriers can influence the drug dissolution profile by direct dissolution or co-solvent effects (Dhirendra *et al.*, 2009).

C. Particles with higher porosity

Particles in SDs have been found to have a higher degree of porosity. The increase in porosity also depends on the carrier properties; for instance, SDs containing linear polymers produce larger and more porous particles than those containing reticular polymers and, therefore, results

in a higher dissolution rate. The increased porosity of SD particles also hastens the drug release profile (Dhirendra *et al.*, 2009).

D. Drugs in amorphous state

The enhancement of drug release can usually be achieved if the drug is in its amorphous state, because no energy is required to break up the crystal lattice during the dissolution process as is the case in crystalline substances. In SDs, drugs are presented as supersaturated solutions after system dissolution, and it is speculated that if drugs precipitate it is as a metastable polymorphic form with higher solubility than the most stable crystal form (Thakur *et al.*, 2014).

E. Interactions of the drug with carrier functional groups

Konno and Taylor reported that hydrogen bonding interactions existed in felodipine SDs with PVP, hydroxypropyl methylcellulose acetate succinate (HPMCAS), and HPMC where all polymers were able to maintain the amorphous state of the drug even at low excipient concentrations (Konno and Taylor, 2006). Tantishaiyakul *et al.*'s studies, the intermolecular hydrogen bonding between piroxicam and PVP in their SDs was also confirmed by FTIR (Tantishaiyakul *et al.*, 1999).

F. Complex formation:

In SD, a drug forms a complex with an inert soluble carrier in solid state. The availability of the drug depends on the solubility and stability constant of the compound or complex and the absorption rate of the drug. It is suggested that the dissolution rate and oral absorption can be enhanced by formation of water soluble complex with high dissolution constant. One of the most frequently used complex carriers are within the class of Cyclodextrins (Sapkal *et al.*, 2013).

Limitations

Despite the extensive research that revealed the advantages of SDs, their application in the market is limited (Kim *et al.*, 2011) because of the drawbacks such as problems in scale up, stability of the drug and vehicle (changes in crystalline) and (Ankush *et al.*, 2011) requirement of high percentage of carrier materials (Ankush *et al.*, 2011; Okonogi and Puttipipatkhachorn,

2006; Thakur *et al.*, 2014). However, these problems have been surmounted to some extent by some possible solutions. For instance, there have been substantial improvements in the manufacturing methods. In addition combined carriers can be used instead of using high amounts of single carrier material. This approach not only reduces the amount of carrier material required but also increases the drug dissolution (Ankush *et al.*, 2011).

To make up for the stability problem, using polymers that can make certain cross-links or hydrogen bonding with the drug and reduce its nucleation rate is being actively studied (Kim *et al.*, 2011). It is recognized that the majority of drugs contain hydrogen-bonding sites, consequently, several studies have shown the formation of ion–dipole interactions and intermolecular hydrogen bonding between drugs and polymers, and the disruption of the hydrogen bonding pattern characteristic to the drug crystalline structure (Sapkal *et al.*, 2013).

1.2. Albendazole (ABZ)

ABZ, methyl [5- (propylthio)-1-*H*-benzimidazol-2yl] carbamate (Fig. 1.4) is a BZD derivative with broad spectrum of activity against human and animal helminth parasites (Alanazi *et al.*, 2007). It was first approved for treatment of helminthic infections in sheep in 1977 and subsequently approved for human use in 1983. In general, most ascariasis, trichuriasis, enterobiasis and hookworm infections can be successfully treated with single dose ABZ and strongyloidiasis with multiple doses of ABZ. ABZ has also been used in the treatment of capillariasis, gnathostomiasis, trichostrongyliasis, hydatidosis, taeniasis, neurocysticercosis, and the tissue nematodes cutaneous larval migrans, toxicariasis, trichinosis and filariasis (in combination with other anthelmintics) (Anupama *et al.*, 2011a).

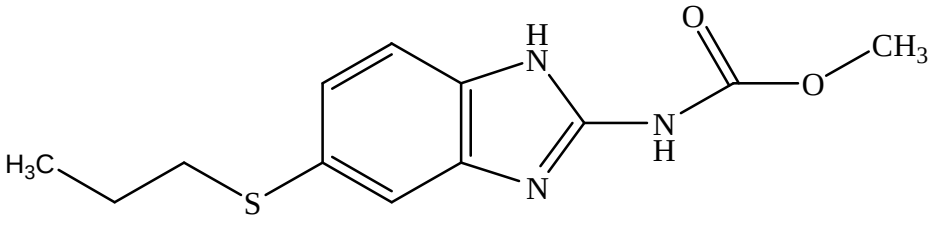

Figure 1.4: Methyl [5-(propylthio)-1*H*-benzimidazol-2-yl] carbamate (Albendazole)

1.2.1. Physicochemical characteristics of albendazole

ABZ is a white to faintly yellowish (USP30-NF25, 2007), odorless powder with poor flow property. It has a molecular weight of 265.34 g mol^{-1} and the molecular formula is C12H15N3O2S. It is a Class II BCS substance, with low solubility and high permeability (Cavalcanti *et al.*, 2012). The M.p of ABZ is 209°C and its solubility constant (n-octanol) at neutral pH is 0.75 ± 0.2 (g/ml) (Castro *et al.*, 2010). ABZ is practically insoluble in water (Pranzo *et al.*, 2010) and most organic solvents (ethanol), properties that influence its absorption and behavior in the body (El Harti *et al.*, 2014). It is freely soluble in anhydrous formic acid; very slightly soluble in ether and in methylene chloride (USP30-NF25, 2007).

X-ray diffraction revealed that ABZ showed crystalline behavior and the absence of polymorphism. Scanning electron microscopy also showed crystals of different sizes and shapes with a strong tendency to aggregate (Cavalcanti *et al.*, 2012).

Due to their chemical features, all the BZD drugs are sensitive to light, with behavior common to all members of this class of compounds. The amine derivative from hydrolysis of the carbamic group has been reported to be the main photo-degradation product (Yagoub *et al.*, 2013).

Following storage for one and two months, ABZ expressed noticeable change in assay down to 85.3 and 74.6%, respectively. It showed high photosensitivity in solution but a reliable stability in solid form and when exposed to a temperature up to 50 °C. The thermal degradation test, performed under temperatures from 20 to 50 °C, demonstrated a very high stability both in solid and solution form. These temperature values were considered a reliable range that can be reached in the drug storages of the tropical lands. These results confirmed that the degradation process was caused just by light and not by high temperature (Yagoub *et al.*, 2013).

1.2.2. Pharmacokinetics and pharmacodynamics of albendazole

Several studies suggest that only limited absorption of BZD anthelmintics are achieved in cats, dogs and humans, owed mainly to their low dissolution rate on the gastric fluid (Castro *et al.*, 2010). The intestinal absorption of ABZ in human has been shown to be < 5% (Fernando *et al.*, 2011).

After oral administration, ABZ is metabolized rapidly by flavin mono-oxygenases (FMO) and by the hepatic microsomal cytochrome P450 (CYP) into the chiral metabolite albendazole sulfoxide [(+)-ABZ-SO; (-)-ABZ-SO)], which possess anthelmintic activity, and into the non-chiral metabolite albendazole sulfone (ASON) which lacks pharmacologic activity (Eslami *et al.*, 2006; Mahler *et al.*, 2008; Marques *et al.*, 2002). As it undergoes very rapid first pass metabolism in all species, the unchanged drug has not been reliably detected in plasma. Plasma levels of the initial oxidized metabolites (the sulphoxide (a) and sulphone (b)) (Fig. 1.5) in all species are much higher than the parent drug (El Harti *et al.*, 2014).

After an oral dose of 400 mg, peak plasma levels of ABZ-SO reach 0.04–0.55 mg/L, with great variation between individuals (Venkatesan, 1998). ABZ-SO is widely distributed throughout the body; it is 70% bound to plasma proteins. Clearance of the parent drug is very rapid in all species but that of the sulphoxide and sulphone metabolites is slower with a half-life of 8-12 h in man. Excretion occurs very largely as metabolites in bile. Only metabolites of ABZ are excreted in animals and man, as metabolism is very extensive (Dayan, 2003).

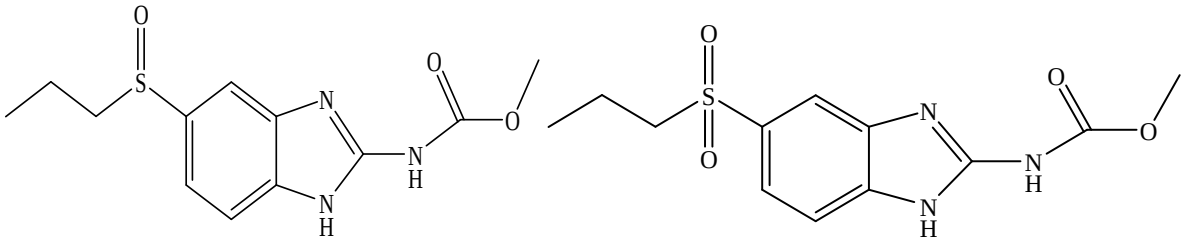

(a) (b)

Figure 1.5: Chemical structures of albendazole sulphoxide (a) and albendazole sulphone (b)

The anthelmintic activity of ABZ has been related to their selective antimitotic activity due to the preferential binding of these agents to helminthic tubulin over mammalian tubulin (Vazquez *et al.*, 2003). It is thought to act by blocking glucose uptake in the larva and adult stage of susceptible parasites, thereby depleting the energy stores and decreasing formation of ATP leading to immobilization and death of the parasite (El-Rahman *et al.*, 1999). ABZ induces the enzymes of the cytochrome P450 system responsible for its metabolism (Venkatesan, 1998). Increased systemic bioavailability of this drug was reported when the drug was co-administered

with a fatty meal, fruit juice, or taken as drug solution with co-solvent, or with surfactants (El-Badry *et al.*, 2008).

The incidence of side effects reported in the published literature on the use of ABZ for intestinal helminthiasis is very low, with only gastrointestinal side effects (Horton, 2000). When used in lengthy therapies such as for hydatoses and neurocysticercosis, ABZ can produce liver degeneration. Hence, it is not recommended for patients with hepatic problems. ABZ is teratogenic and embryotoxic and consequently cannot be administered to pregnant women. The safety of ABZ for children of less than two years has not yet been established (Moriwaki *et al.*, 2008).

1.3. Rationale for dissolution enhancement of albendazole

The low cost and broad spectrum activity of ABZ make it typically the drug of choice for treatment of several parasitic diseases (Moriwaki *et al.*, 2008). Several studies suggest that only limited absorptions are achieved in cats, dogs and humans, owed mainly to their low dissolution rate on the gastric fluid (Castro *et al.*, 2010). This property is a major disadvantage for the use of ABZ in the treatment of systemic helminthiasis. Furthermore, the lack of water solubility reduces flexibility for formulation and administration (Alanazi *et al.*, 2007) which is the major problem for pharmaceutical formulators to formulate it into solid dosage form. Therefore, to overcome the problem by improving its dissolution rate is an important goal.

1.4. Objectives

1.4.1. General objective

- To enhance the dissolution of ABZ using SD technique.

1.4.2. Specific objectives

- To prepare binary and ternary SDs of ABZ with selected carriers using kneading and solvent evaporation techniques;
- To study drug excipient interactions and DSC thermal behavior of the formulations;
- To study the dissolution of ABZ from the formulations prepared;
- To determine the effect of carrier type, drug to carrier ratio, preparation method and surfactant effect on the dissolution profile of ABZ; and
- To formulate and optimize tablets of selected SDs and compare the dissolution profile of the optimized formulation with marketed tablet.

2. EXPERIMENTAL

2.1. Materials

ABZ was a generous gift from East African Trading PLC. HPMC 5cp (Unival, china), PEG (Unival, china), PVP K-30 (Shangai Wellton, china), Polysorbate 80 (Tween 80), Microcrystalline Cellulose (Avicel PH 102, NB, Entrepreneurs. Nagpur, India), Sodium Starch Glycolate (China Associate Co. Ltd, Shenzhen, China), Colloidal Silicon Dioxide (Aerosil®) (Wacker Silicon, Germany), Magnesium Stearate (China Associate Co. Ltd, Shenzhen China), and other chemicals were kindly donated by Ethiopian Pharmaceuticals Share Company (EPHARM). ABZ 200mg tablet was purchased as a potential comparator. All chemicals and solvents used were of pharmaceutical grade. Distilled water was used throughout the study.

2.2. Methods

2.2.1. Preparation of solid dispersions

SDs of ABZ containing various proportions and type of carriers with and without surfactant (Table 2.1) were prepared using kneading and solvent evaporation methods as described below.

I. Kneading

In this method, first the carriers and the carriers mixture with surfactant were wetted with water (30% of the total formulation) for the SDs with PEG and PVP and (50% of the total formulation) for HPMC in mortar and pestle. Then the drug was incorporated and kneaded further for 30 min until a paste like consistency is formed. The mixture was then dried in a drying oven (Dry oven, Kendro, Germany) at 50 °C until the moisture content was less than 2% (as determined by Moisture Analizer, Mettler Toledo, Switzerland). Finally the dried mixture was stored in a desiccator for 48 h to remove residual moistures and the resulting solid was pulverized and sieved using 250 μm mesh sieve.

Table 2.1: Compositions and proportions of the drug, carriers and surfactant mixtures studied.

Formulation code	Drug	Carrier	Surfactant	Drug: Carrier: Surfactant	Methods of preparation	
					Kneading	Solvent evaporation
SD_{K1}	ABZ	PEG	--	1:0.5:0	kneading	--
SD_{K2}	ABZ	PEG	--	1:1:0	kneading	--
SD_{K3}	ABZ	PEG	--	1:2:0	kneading	--
SD_{K4}	ABZ	PEG	Polysorbate	1:0.5:0.1	kneading	--
SD_{K5}	ABZ	PEG	Polysorbate	1:1:0.1	kneading	--
SD_{K6}	ABZ	PEG	Polysorbate	1:2:0.1	kneading	--
SD_{SE1}	ABZ	PEG	--	1:0.5:0	--	solvent evaporation
SD_{SE2}	ABZ	PEG	--	1:1:0	--	solvent evaporation
SD_{SE3}	ABZ	PEG	--	1:2:0	--	solvent evaporation
SD_{SE4}	ABZ	PEG	Polysorbate	1:0.5:0.1	--	solvent evaporation
SD_{SE5}	ABZ	PEG	Polysorbate	1:1:0.1	--	solvent evaporation
SD_{SE6}	ABZ	PEG	Polysorbate	1:2:0.1	--	Solvent evaporation
SD_{K7}	ABZ	PVP	--	1:0.5:0	kneading	--
SD_{K8}	ABZ	PVP	--	1:1:0	kneading	--
SD_{K9}	ABZ	PVP	--	1:2:0	kneading	--
SD_{K10}	ABZ	PVP	Polysorbate	1:0.5:0.1	kneading	--
SD_{K11}	ABZ	PVP:	Polysorbate	1:1:0.1	kneading	--
SD_{K12}	ABZ	PVP	Polysorbate	1:2:0.1	kneading	--
SD_{SE7}	ABZ	PVP	--	1:0.5:0	--	solvent evaporation
SD_{SE8}	ABZ	PVP	--	1:1:0	--	solvent evaporation
SD_{SE9}	ABZ	PVP	--	1:2:0	--	solvent evaporation
SD_{SE10}	ABZ	PVP	Polysorbate	1:0.5:0.1	--	solvent evaporation
SD_{SE11}	ABZ	PVP	Polysorbate	1:1:0.1	--	solvent evaporation
SD_{SE12}	ABZ	PVP	Polysorbate	1:2:0.1	--	solvent evaporation
SD_{K13}	ABZ	HPMC	--	1:0.5:0	Kneading	--
SD_{K14}	ABZ	HPMC	--	1:1:0	Kneading	--
SD_{K15}	ABZ	HPMC	--	1:2:0	Kneading	--
SD_{K16}	ABZ	HPMC	Polysorbate	1:0.5:0.1	Kneading	--
SD_{K17}	ABZ	HPMC	Polysorbate	1:1:0.1	Kneading	--
SD_{K18}	ABZ	HPMC	Polysorbate	1:2:0.1	Kneading	--

Key: SD: solid dispersion, $_K$: kneading, $_{SE}$: solvent evaporation

II. Solvent evaporation

In this method 16 g of the drug and 16 g of the carrier mixture were dissolved in 100 ml of acidified ethanol (Hydrochloric acid (HCL), 6%) using an ultrasonic sonicator (Sonerex D2800, Berline) for 15 min. The surfactant was added into the solution in case of the ternary systems. The solvent was allowed to evaporate at 50 °C in drying oven (Dry oven, Kendro, Germany). To ensure the residual solvent was completely removed, the moisture content was analyzed and found to be less than 1%. The resulting SDs were stored in a desiccator, pulverized and sieved through a 250 µm mesh sieve.

2.2.2. Preparation of physical mixtures

PMs of the corresponding SDs were prepared (Table 2.2) by mixing the drug and the carriers with and without surfactant in a mortar until a homogeneous mixture is obtained (for 30 min). The resulting mixtures were sieved through a 250 µm mesh sieve.

Table 2. 2: Compositions and proportions of the drug, carriers and surfactant of PMs studied.

Formulation code	Drug	Carrier	Surfactant	Drug: Carrier: Surfactant
PM_1	ABZ	PEG	--	1:0.5:0
PM_2	ABZ	PEG	--	1:1:0
PM_3	ABZ	PEG	--	1:2:0
PM_4	ABZ	PEG	polysorbate	1:0.5:0.1
PM_5	ABZ	PEG	polysorbate	1:1:0.1
PM_6	ABZ	PEG	polysorbate	1:2:0.1
PM_7	ABZ	PVP	--	1:0.5:0
PM_8	ABZ	PVP	--	1:1:0
PM_9	ABZ	PVP	--	1:2:0
PM_{10}	ABZ	PVP	polysorbate	1:0.5:0.1
PM_{11}	ABZ	PVP	polysorbate	1:1:0.1
PM_{12}	ABZ	PVP	polysorbate	1:2:0.1
PM_{13}	ABZ	HPMC	--	1:0.5:0
PM_{14}	ABZ	HPMC	--	1:1:0
PM_{15}	ABZ	HPMC	--	1:2:0
PM_{16}	ABZ	HPMC	polysorbate	1:0.5:0.1
PM_{17}	ABZ	HPMC	polysorbate	1:1:0.1
PM_{18}	ABZ	HPMC	polysorbate	1:2:0.1

2.2.3. Estimation of drug content of solid dispersions and physical mixtures

Content uniformity study of the formulations was done by preparing standard and sample solutions according to the procedure stated in the USP (USP30-NF25, 2007). PMs & SDs equivalent to 400 mg of ABZ were taken and dissolved separately in 500 ml acidified methanol. The solutions were filtered using Whatman filter paper No.5 and diluted with 0.1N (Sodium hydroxide) NaOH. Drug content of the formulations was estimated spectrophotometrically by measuring the absorbance of the sample solution and the standard solution at the wavelengths of maximum and minimum absorbance at about 308 nm and 350 nm.

2.2.4. Determination of percent yield

The percent yield of the prepared ABZ SDs was determined by using the following equation:

Percent yield = (weight of prepared solid dispersion / weight of drug + carriers) x 100 Eq. 2.1

2.2.5. Dissolution study

The dissolutions of the pure drug, PMs and SDs were determined following the USP (USP30-NF25, 2007) method using dissolution apparatus 2. The paddle speed was set at 50 rpm and the temperature was maintained at 37 ± 0.5°C. The assayed amount of all the fromulations was equivalent to 400 mg of ABZ and 900 ml 0.1 N HCl solution was used as a dissolution medium. Ten ml aliquots were withdrawn at predetermined time intervals (at 3, 5, 10, 30, 60 min), and the same amount of fresh medium was replaced in order to keep the volume constant and to maintain sink condition in the vessel. The samples were filtered using Whatman filter paper No.5 and then diluted with 0.1N NaOH. The concentration of dissolved drug was measured using a UV–Vis spectrophotometer at 308 and 350 nm.

2.2.6. Evaluation of the formulations and statistical analysis

The FDA recommended model independent method, the similarity (*f2*) factors was used to evaluate the difference in dissolution profile between the pure drug and the prepared formulations. To compare the differences in dissolution profiles between formulations, the data was analyzed using Analysis of Variance (ANOVA) with Origin 8.5 (OriginLabTM Corporation,

USA) statistical software. At 95% confidence interval, p-values of ≤ 0.05 were considered statistically significant.

2.2.7. Drug-polymer interaction analysis

2.2.7.1. Fourier-transform infrared spectroscopy (FTIR)

Drug-excipient interaction study was carried out on SDs stored for two months using FTIR (FTIR-8400, Shimadzu, Japan). 5-10 mg of the samples were ground and mixed with an oily mulling agent (Nujol) in a mortar and pestle. The mixtures were then placed on the surface of a potassium bromide (KBr) plate and a second plate was placed on top of the two plates. The compressed plate was then placed in the infrared spectrometer and the spectra were recorded. The spectra were scanned over a frequency range of 4000 – 750 cm^{-1} with a resolution of 4 cm^{-1}. Background spectrum was collected before running the samples.

2.2.7.2. Thermal analysis

Samples were analyzed using DSC (DSC 200, Netzsch-Gerätebau GmbH, Selb, Germany). The samples were weighed (6 mg) and sealed in an aluminum pan and then scanned at a heating rate of 5°C /min between 25 - 240 °C under nitrogen gas, flowing at a rate of 100 ml/min. An empty aluminum pan was used as a reference.

2.2.8. Powder characteristics study of solid dispersions

Powder characteristics (flow properties, and compressibility) of the prepared formulations were determined as described below. Each experiment was done in triplicate and mean and the standard deviation were obtained.

2.2.8.1. Flow property study

Flow rate:

30 g of the Pure drug, PMs and SDs powder were transferred into a funnel which has 15 mm internal diameter at the bottom. The powder was allowed to flow through the funnel and the time was recorded. The flow rate was determined by dividing the amount of powder in gram (g) with the time (sec) it took to pass through the funnel.

Angle of repose:

Angle of repose was measured by using a fixed funnel method. Accordingly, 30 g of sample from 10 cm height were allowed to flow through a glass funnel orifice with an inner diameter of 15 mm. The angle of repose (θ, degree) was calculated by substituting the values of the base radius 'R' and pile height 'H' in Equation 2.2.

$$\text{Angle of repose } (\theta) = \tan^{-1} H/R \qquad \text{Eq. 2.2}$$

Hausner's Ratio (HR) and Carr's Index (CI)

Samples of 30 g of the prepared formulations were carefully introduced into a 250 ml graduated glass cylinder and the volume was measured. The bulk density (BD) of each formulation was then obtained by dividing the weight of samples by their respective volumes (Eq. 2.3). Then, the powder in the glass cylinder was tapped 500 times using tapped densitometer (ERWEKA, SVM 20, Germany). The volume was noted after tapping. The tapped density (TD) of each formulation was then obtained by dividing the weight of sample by the final tapped volume (Equation 2.4). Then, the HR and CI were calculated from bulk and tapped densities using Equation 2.5 and 2.6, respectively.

$$\text{BD} = \text{Weight of powder blend/volume of powder blend} \qquad \text{Eq. 2.3}$$

$$\text{TD} = \text{Weight of powder blend/tapped volume of powder blend} \qquad \text{Eq. 2.4}$$

$$\text{HR} = \text{TD/BD} \qquad \text{Eq. 2.5}$$

$$\text{CI} = (\text{TD-BD})/\text{TD}*100 \qquad \text{Eq. 2.6}$$

2.2.8.2. Compressibility study

The SDs powders were compressed at 10 and 20KN and compressibility was determined by measuring hardness and friability as a function of compression force.

2.2.9. Preparation and evaluation of tablets

The selected SDs (ternary SD of ABZ with PEG and polysorbate 80 (1:0.5:0.1 and 1:2:0.1) prepared with kneading method) were accurately weighed and mixed with excipients such as sodium starch glycolate (SSG), aerosil®, magnesium stearate and microcrystalline cellulose (MCC) (Table 2.3). The excipients were passed through a 250 μm sieve. SSG and MCC were mixed with the SDs in a TURBULA® Mixer (Willy A. Bachofen AG, Turbula®2TF, Basel, Switzerland) for 10 min at a speed of 49 rpm. Then aerosil® and magnesium stearate were added and mixed for additional 5 min. Powder characterization such as flow property and compressibility of the various powder blends, were determined using the methods described in section 2.2.8.1 and 2.2.8.2, respectively.

Table 2. 3: Compositions of powder blend for tablet compression.

Formulation code	Drug: Carrier: Surfactant	Composition of excipients (%)			
		Aerosil®	SSG	MCC	Magnesium stearate
F1	1:0.5:0.1	1	4	15	0.5
F2	1:0.5:0.1	1	4	20	0.5
F3	1:0.5:0.1	1	4	30	0.5
F4	1:2:0.1	1	4	15	0.5
F5	1:2:0.1	1	4	20	0.5
F6	1:2:0.1	1	4	30	0.5

Tablets were prepared by direct compression technique using a single punch machine (KORSCH XP1-K0010288, Berlin, Germany) at 10 and 20 KN compression force. The prepared tablets were evaluated 24 hrs after compression for content uniformity, hardness, friability, disintegration time and drug release.

2.2.9.1. Hardness test

The hardness of 10 randomly selected tablets were measured using hardness tester (CALEVA, THT 2). The hardness was determined by recording the crushing strength in Newton (USP30-NF25, 2007).

2.2.9.2. Friability study

The total weight of 20 tablets was recorded and the tablets were placed in a friability tester (Erweka, TAR20, Germany) and allowed to rotate at 20 rpm for 5 min. The tablets were removed and reweighed. The percentage loss in weight with respect to the initial value was used as a measure of friability (USP30-NF25, 2007).

2.2.9.3. Content uniformity

Content uniformity study of the tablets were done according to the procedure stated in the USP (USP30-NF25, 2007). Ten tablets from each batch were randomly selected and ground in mortar and pestle. Samples equivalent to 400 mg of ABZ were taken and dissolved separately in 500 ml acidified methanol. The solutions were filtered using Whatman filter paper No.5 and diluted with 0.1N NaOH. Drug content of the samples were estimated spectrophotometrically by measuring the absorbance of the sample solution and the standard solution at the wavelengths of maximum and minimum absorbance at about 308 nm and 350 nm.

2.2.9.4. Disintegration study

Disintegration time of tablets from each batch was determined as per the USP procedure in which six tablets were placed in a disintegration apparatus filled with 800 ml of distilled water maintained at 37 ± 2^{o}C (Erweka-ZT-3-4). The time of disintegration with no palpable mass remaining in the apparatus was recorded as the disintegration time (USP30-NF25, 2007).

2.2.9.5. Dissolution study

The dissolution of the tablets were determined following the USP (USP30-NF25, 2007) as per the procedure indicated in section 2.2.5.

2.2.10. Experimental design and optimization of ABZ tablet

Full factorial design was used to optimize the different responses (flow, compressibility and drug release) in which the three factors (compression force, percentage of MCC, and drug to carrier ratio) were studied at two level resulting in 8 experiments ($2^3 = 8$) (Table 2.4). The response values were subjected to multiple regression analysis using Design-Expert 8.0.7.1 software to

find out the relationship between the factors used and the response values obtained. Thus, a systematic optimization was carried out using response surface methodology where the response surface plot, the countor plot and the optimum area at which the desired responses were obtained.

Table 2. 4: Factors and their levels.

Factors	Levels	
	+1	-1
Drug/carrier (w/w)	2	0.5
Compression force (N)	20	10
Concentration of MCC (%)	30	20

2.2.11. Drug release kinetics and mechanism of drug release

Data obtained from in vitro release study of the optimized tablet formulation was fitted into various kinetic equations. The kinetic models used are zero order, first order, Higuchi equation, Hixson-Crowell and Korsmeyer-Peppas model (Equation 2.7-2.11).

Zero order release model

$$Q = Q_o - Kt \qquad \text{Eq. 2.7}$$

Where, Q is the amount of drug remaining in the dosage form at time t, Qo is the quantity of drug present initially in the dosage form and K is the zero order release constant.

First order release model

$$\ln Q = \ln Q_o - Kt \qquad \text{Eq. 2.8}$$

Where, Q is the amount of drug remaining in the dosage form at time t, Qo is the quantity of drug present initially in the dosage form, and K is the first order release constant.

Higuchi square root model

$$\frac{M_t}{M_|} \mathrm{X} Kt^{1/2}$$ Eq. 2.9

Where, Mt/M∞ is the fraction release of drug at time t, and K is rate constant.

Hixson-Crowell cube root model

$$Q^{1/3} \mathrm{X} Q_0^{1/3} \mathrm{Z} Kt$$ Eq. 2.10

Where Q is the amount of drug remaining in the dosage form at time t, Qo is the quantity of drug present initially in the dosage form and K is the rate constant for Hixson-Crowell rate equation.

In order to find out the mechanism of drug release, drug release data were fitted to the Korsmeyer-Peppas model (Equation 2.11).

$$\frac{M_t}{M_|} \mathrm{X} Kt^n$$ Eq. 2.11

Where Mt/M∞ is the fraction of drug released at time t, K is the rate constant and n is the release exponent that is used to characterize different release mechanisms (Dash *et al.*, 2010).

3. RESULTS AND DISCUSSION

3.1. Preparation of albendazole solid dispersions

This study focuses on enhancing the bioavailability of ABZ using highly drug loaded SDs of binary and ternary mixtures that consist of drug, a polymeric carrier and a surfactant. The three hydrophilic polymers (PEG, PVP and HPMC) were selected in this study because they have shown to enhance the dissolution profiles of different drugs (Alanazi *et al.*, 2007; Kim *et al.*, 2011).

There are different methods of preparing SDs and among the different methods kneading was considered because it has been shown to be an industrially feasible method (Venkatesh *et al.*, 2008). Solvent evaporation method was also considered since it has been shown to increase the dissolution profile of many drugs (Chhater and Praveen, 2013; Howlader *et al.*, 2012; Jahan *et al.*, 2011; Jatwani *et al.*, 2011; Jahan *et al.*, 2011). Melting method is another common method in SD preparation which is suitable for drugs and ingredients for which melting is very easy. While the lower melting point of PEG (50-58°C) (Nikghalb *et al.*, 2012) used in this study makes it possible to use this method, the higher melting point of ABZ (209°C) and the first stage decomposition of ABZ below its melting point that is 197.22 - 205.94 °C makes the method unsuitable (Cavalcanti *et al.*, 2012). Therefore, in this study kneading and solvent evaporation techniques were used.

ABZ is practically insoluble in water and alcohol (El Harti *et al.*, 2014) . It is very slightly soluble in ether and in methylene chloride but soluble in acidified methanol (USP30-NF25, 2007). Thus, In this study methanol was replaced by ethanol which is a less toxic alternative (Tiwari *et al.*, 2009) and acidified ethanol was used as a common solvent for both the drug and the carriers (PEG and PVP).

Besides, the solubility of the drug and the carriers was found to be dependent on the degree of acidity (percentage of HCl). Hence the drug and the carriers (PEG and PVP) were dissolved in ethanol of various acidity (i.e. 2, 4, 6, 8 and 10% HCL in ethanol). The results showed that as compared to the 2% solution the amount of ABZ dissolved increased more than 6 times (16 g/100ml) at 6% HCl. However, further increase in HCl percentage showed no significant

increase in amount of ABZ dissolved, rather the amount of PEG dissolved decreased and the viscosity of PVP increased. Therefore, the 6% solution was chosen as a common solvent for this study. However, the third carrier used in this study, HPMC, was found to be insoluble in acidified ethanol, consequently, in this study this carrier was used for kneading method only.

PMs were obtained by blending the components whose compositions are detailed in Table 2.2. PMs were included in the study, to assess the effect of preparation technique on dissolution profile of the drug apart from the effect of carriers used.

Moreover, one of the challenges of enhancing drug bioavailability using SD technology in pharmaceutical product development is that mostly a large amount of carrier is required to achieve the desired dissolution (Ankush *et al.*, 2011; Okonogi and Puttipipatkhachorn, 2006; Thakur *et al.*, 2014). Thus, in this study the level of carrier used was given due attention and the drug: carrier was maintained at 1:0.5, 1:1 and 1:2 (polysorbate 80 in 0.1 proportion was added to the ternary systems).

3.2. Drug content and percent yield

The quantity of ABZ in each formulation was determined using equation 3.1 (USP30-NF25, 2007).

$$\text{Amount of ABZ} = 25C\,(Au/As) \qquad \text{Eq. 3.1}$$

Where

C is concentration of USP ABZ RS in the standard solution (µg/ml); Au is the difference in absorbance between 308 nm and 350 nm from the sample solution; and AS is the difference in absorbance between 308 nm and 350 nm from the sample solution.

Percentage drug content was found to be within the range of 95.87 ± 0.71% to 99.15 ± 0.44%. This indicates that the drug was uniformly distributed throughout the prepared formulations. Percent yield of the SDs were also determined and results were found to be between the ranges of 90.00 ± 1.20% to 97.57 ± 1.10%. All determinations are the mean of three determinations.

3.3. Dissolution

Dissolution is a common characterization test used by the pharmaceutical industry to guide formulation design and to control product quality. It is often a required performance test for solid dosage forms, transdermal patches, and suspensions. Dissolution is also the only test that measures in vitro drug release as a function of time, which may reflect the reproducibility of the manufacturing process and, in some cases, the drug's in vivo performance. Dissolution is defined as the process by which solid substance enters in solvent to yield a solution. Simply, dissolution is a mass transfer from a solid surface to liquid phase (Ramesh, 2011).

In the dissolution study the percentage of ABZ released was determined according to USP (USP30-NF25, 2007) using UV spectrophotometer, where the amount of ABZ released is calculated using the equation 3.2. The amounts of drug released at 3, 5, 10, 30 and 60 min were calculated to study the release profile (Equation. 3.2).

Amount of ABZ released = 22.5C (Au/AS) Eq. 3.2

Where

C is concentration in µg/ml of ABZ in the standard solution (9 µg/ml);

Au is the difference in absorbance between 308 and 350nm of the solution under test

As is the difference in absorbance between 308 and 350 nm of the standard solution

Therefore, the standard solution was prepared in triplicate and the average difference in absorbance (As) between 308 and 350 nm was found to be 0.7069 with STD of 0.003. The dissolution profile for each formulation was plotted as percent released versus time (min).

During dissolution experiments it was noticed that all the binary and ternary SDs powder prepared with the three carriers settled to the bottom of the dissolution vessel. The PMs of the ternary system also settled instantly, whereas the binary PMs and the pure drug floated for a long period of time on the surface of the dissolution medium.

As can be seen in figure 3.1, the dissolution of ABZ was very insignificant with only 3.70% and 4.50% of the drug going into solution in 30 and 60 min, respectively. On the other hand, increase in dissolution profiles were observed in both PMs and SDs.

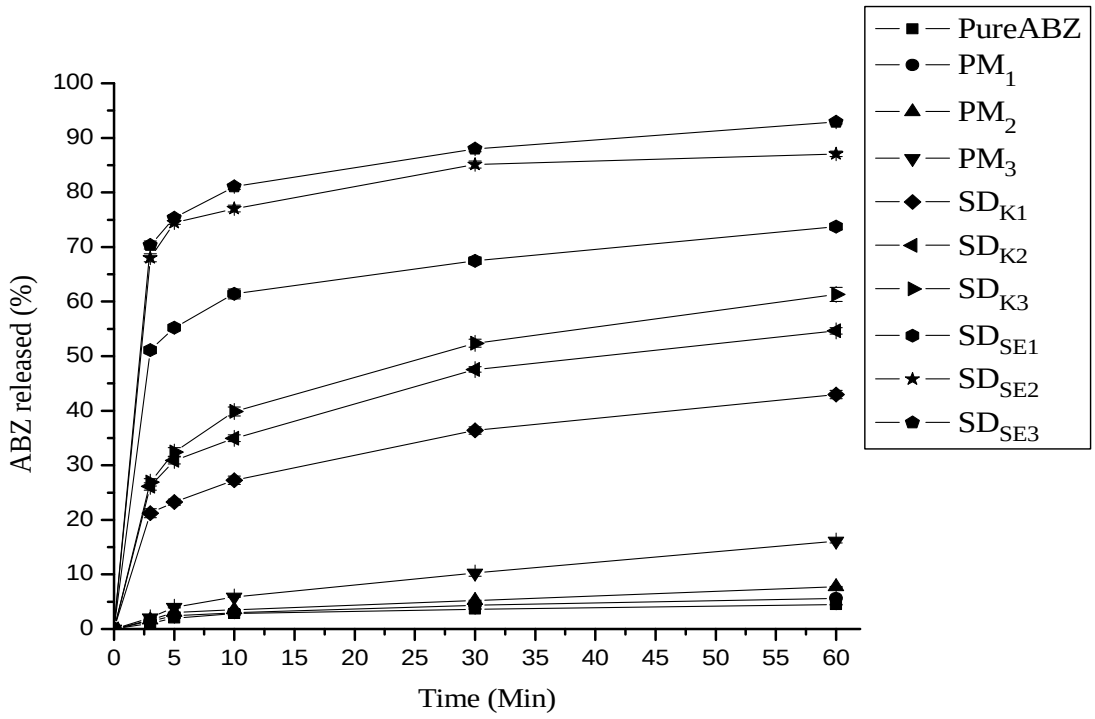

SDs: solid dispersions, PMs: physical mixtures, K: kneading, SE: solvent evaporation.

Figure 3. 1: Dissolution profile of ABZ from the binary PMs and SDs with PEG.

Different factors can be mentioned for the observed improvement in dissolution profile of this drug including the type and proportions of the hydrophilic carriers used in the preparation and the effect of the surfactant. The effect of the different factors was studied using the similarity factor *f2* metrics proposed by Moore and Flanner (Ma *et al.*, 1999). Similarity factor *f*2 is adopted by FDA Center for Drug Evaluation and Research (CDER) as an assessment criterion of similarity between different in vitro profiles. It is defined by Equation 3.3 (Ullah *et al.*, 2011).

$$f_2 = 50\log\left\{\left[1+\frac{1}{n}\sum_{t=1}^{n} w_t\left(R_t - T_t\right)^2\right]^{-0.5} \times 100\right\}$$

Eq. 3.3

Where Rt is the percentage dissolved at each time point for the reference formulation, Tt is the percentage dissolved at each time point for the test formulation, n is the number of dissolution

sample times. The similarity factor is 100 when the test and reference profiles are identical and approaches 0 as the dissimilarity increases. An *f2* value between 50 and 100 suggests that two dissolution profiles are similar and indicates a point-to-point difference of 10% or less (Bakshi *et al.*, 2012). The higher proportions of each carriers used was taken to compare the difference between each formulations and *p*-value was calculated to see the significance in difference.

3.3.1. Dissolution profiles of pure albendazole, physical mixtures and solid dispersions prepared using PEG

The release profiles of ABZ from the pure drug, PMs and SDs prepared using PEG alone as well as with the addition of polysorbate 80 are shown in Figs. 3.1 and 3.2, respectively. Taking ABZ as a reference, the *f*2 values were calculated for all the formulations prepared. The *f*2 values for the binary and ternary PMs and SDs with this carrier are listed in Table 3.1.

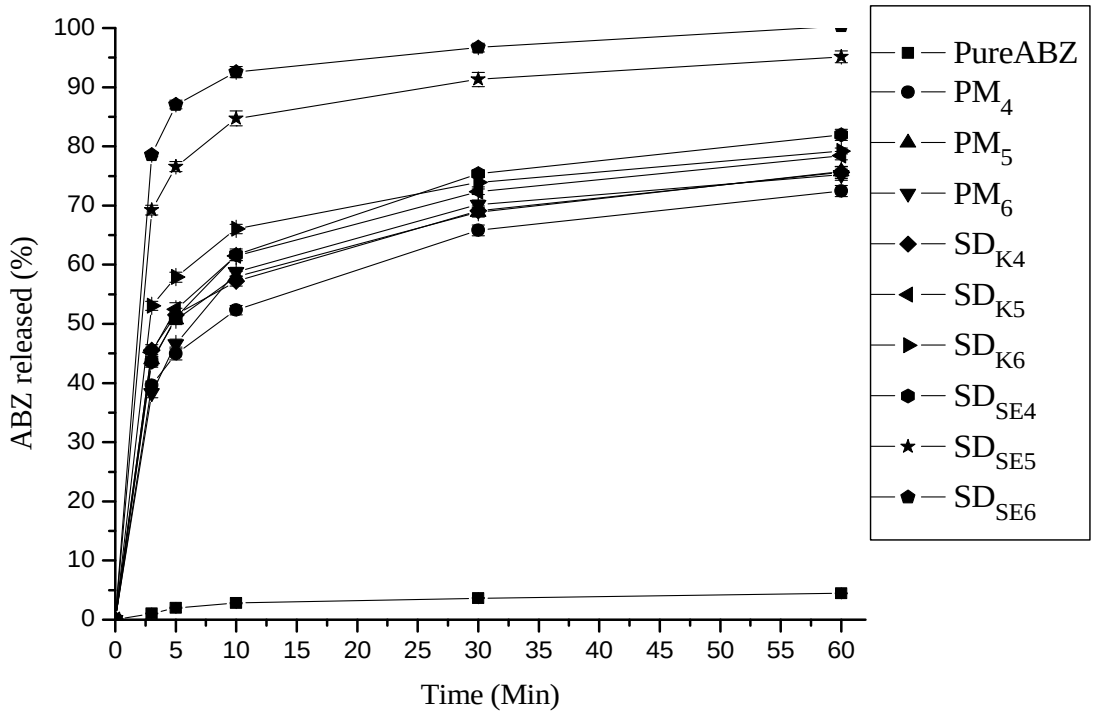

SDs: solid dispersions, PMs: physical mixtures, K: kneading, SE: solvent evaporation.

Figure 3. 2: Dissolution profile of ABZ from the ternary PMs and SDs with PEG.

From the results shown, the dissolution profiles of the pure drug and the binary PMs werefound to be similar (f2 > 50). However, an increase in dissolution rate and extent was observed with increasing carrier proportion. On the other hand the f2 values of the corresponding ternary PMs showed a remarkable improvment in dissolution profiles than the pure drug (Table 3.1). The differences from the binary PMs were also significant ($p < 0.05$). The drug released within 60 min from the ternary PMs was more than 4 folds as compared to the binary system. This result can be related to the wetting and solublizing effect of polysorbate 80.

Table 3. 1: Similarity factor *(f2)* values of binary and ternary PMs and SDs of ABZ with PEG in comparison to the pure drug.

Comparison	*f*2- values	Dissolution profile
PM_1 and Pure ABZ	96.02	Similar
PM_2 and Pure ABZ	84.99	Similar
PM_3 and Pure ABZ	59.99	Similar
PM_4 and Pure ABZ	13.61	Dissimilar
PM_5 and Pure ABZ	12.41	Dissimilar
PM_6 and Pure ABZ	11.98	Dissimilar
SD_{K1} and Pure ABZ	27.38	Dissimilar
SD_{K2} and Pure ABZ	21.43	Dissimilar
SD_{K3} and Pure ABZ	19.14	Dissimilar
SD_{K4} and Pure ABZ	11.88	Dissimilar
SD_{K5} and Pure ABZ	11.01	Dissimilar
SD_{K6} and Pure ABZ	10.6	Dissimilar
SD_{S1} and Pure ABZ	11.31	Dissimilar
SD_{S2} and Pure ABZ	6.02	Dissimilar
SD_{S3} and Pure ABZ	5.11	Dissimilar
SD_{S4} and Pure ABZ	9.76	Dissimilar
SD_{S5} and Pure ABZ	4.57	Dissimilar
SD_{S6} and Pure ABZ	2.65	Dissimilar

Key: SD: solid dispersion, $_K$: kneading, $_{SE}$: solvent evaporation

The *f*2 values of the SDs with kneading method showed the difference in dissolution profile between the pure drug and the SDs (both binary and ternary system). As compared to the corresponding PMs there was also a significant ($p < 0.5$) increase for both the binary and ternary systems. This can be associated with the intermeshing of the drug particles within the wetted hydrophilic carrier. Increased drug release was also shown with increasing carrier proportion associated with the increased interaction between the drug and the carrier.

There was a significant difference ($p < 0.5$) in dissolution rate and extent between the binary and ternary SDs with this method as observed for the PMs. For instance, there has been around 1.5 and 1.4 folds increase in the amount of the drug released for the ternary system at 30 and 60 min, respectively than the corresponding binary system. This could be partly attributed to the reduction in the surface tension between the drug and the dissolution medium due to the addition of Polysorbate 80, leading to higher interaction of drug to Polysorbate 80 and consequently to increased drug wettability. The increase in wettability was also practically observed by the immediate settling of the ternary PMs which was not the case for the binary PMs.

The dissolution profiles of SDs prepared using solvent evaporation, however, exhibited superior release compared to the other formulations where there was 51.09, 68.00 and 70.36% of the drug released in 3 min, for the 1:0.5, 1:1 and 1:2 proportions, respectively, and more than 80% of the drug was released for the 1:1 and 1:2 proportions within 30 min. This can be attributed to the molecular dispersion of drug in the carrier allowing the formation of solid solution.

The difference in dissolution profile between the binary and ternary system with solvent evaporation method was shown to be significant though less significant than kneading method as well as PMs.

3.3.2. Dissolution profiles of pure albendazole, physical mixtures and solid dispersions using PVP

Fig. 3.3 and 3.4 represents the effect of PVP on ABZ dissolution profile from its PMs and SDs. As can be seen in the figures, the dissolution profile of ABZ was improved by several folds both through physical mixing and preparation of SDs using kneading and solvent evaporation techniques.

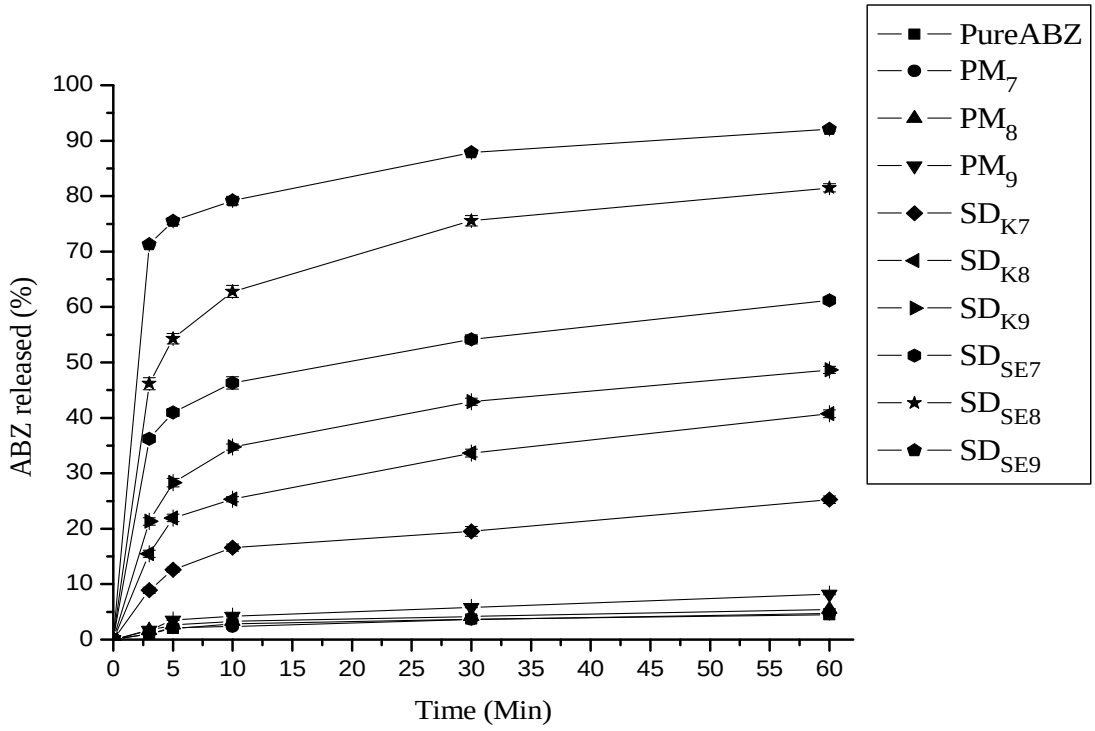

SDs: solid dispersions, PMs: physical mixtures, K: kneading, SE: solvent evaporation.

Figure 3. 3: Dissolution profile of ABZ from the binary PMs and SDs using PVP.

The *f* values were calculated and listed in Table 3.2. The difference in the amount released from binary PMs was found to be similar as compared to the pure drug which is similar to the binary PMs prepared using PEG. Even though there was increase in dissolution as the proportion of the carriers increase, with the maximum proportion used in this study it was found to be marginal (*f2* > 50). However the percent dissolute of the drug from the ternary PMs was found to be remarkably higher signifying the solubilizing effect of Polysorbate 80 (Fig 3.4).

The dissolution rate and extent of ABZ was shown to increase remarkably as compared to the PMs for both the binary and ternary SDs with kneading method which also indicates the effect of the preparation method on the dissolution.

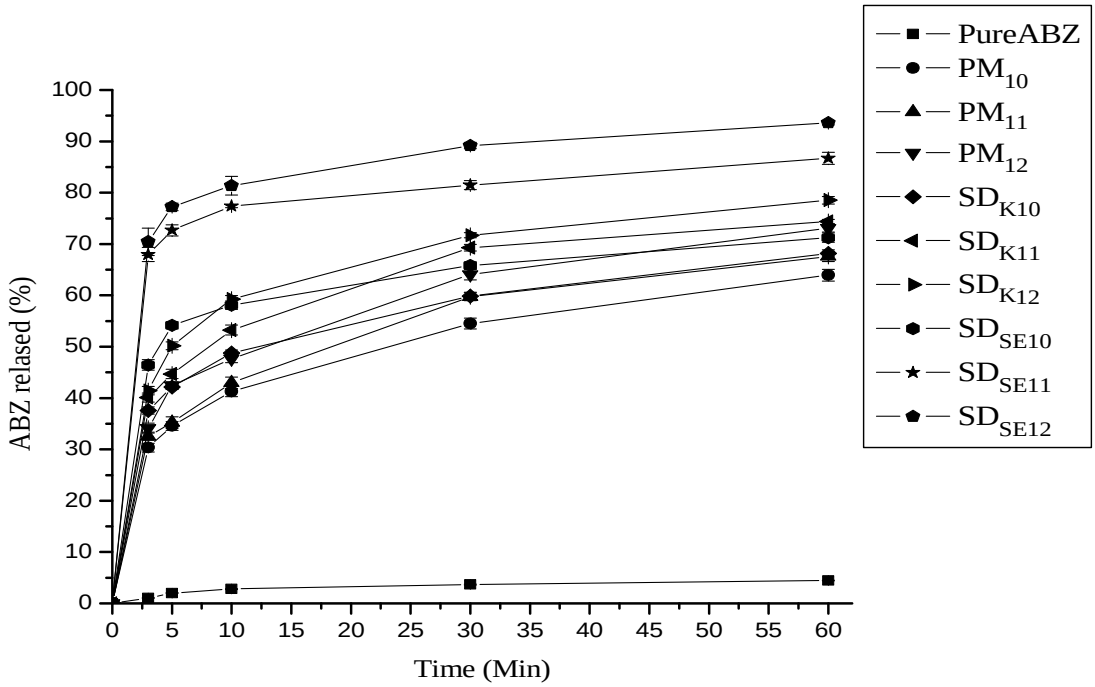

Key: SDs: solid dispersions, PMs: physical mixtures, K: kneading, SE: solvent evaporation.

Figure 3. 4: Dissolution profile of ABZ from the ternary PMs and SDs using PVP.

The SDs of PVP prepared with solvent evaporation technique have shown the highest amount of ABZ released as compared to the kneading method and PMs. Similar results were also shown for the SDs with the other carrier used (PEG). These results demonstrated the success of solvent evaporation method to enhance the dissolution of ABZ than the PMs and SDs with kneading method.

Even though the difference in dissolution profiles between the binary and ternary systems are significant ($p < 0.5$), the differences observed were higher for PMs than SDs. As also shown above with the other carrier used (PEG) the solubilizing effect of polysorbate 80 is more significant in PMs than SDs and more significant in SDs with kneading method than with solvent evaporation.

Table 3. 2: Similarity factor (f2) values of binary and ternary PMs and SDs of ABZ with PVP in comparison to the pure drug.

Combination	*f*2-metric values	Dissolution profile
PM_7 and pure ABZ	99.45	Similar
PM_8 and pure ABZ	96.02	Similar
PM_9 and pure ABZ	81.11	Similar
PM_{10} and pure ABZ	18	Dissimilar
PM_{11} and pure ABZ	16.6	Dissimilar
PM_{12} and pure ABZ	14.53	Dissimilar
SD_{K7} and pure ABZ	41.92	Dissimilar
SD_{K8} and pure ABZ	29.41	Dissimilar
SD_{K9} and pure ABZ	23.73	Dissimilar
SD_{K10} and pure ABZ	15.24	Dissimilar
SD_{K11} and pure ABZ	13.01	Dissimilar
SD_{K12} and pure ABZ	11.55	Dissimilar
SD_{S7} and pure ABZ	17.05	Dissimilar
SD_{S8} and pure ABZ	10.24	Dissimilar
SD_{S9} and pure ABZ	5.21	Dissimilar
SD_{S10} and pure ABZ	12.26	Dissimilar
SD_{S11} and pure ABZ	6.35	Dissimilar
SD_{S12} and pure ABZ	4.87	Dissimilar

Key: SD: solid dispersion, $_K$: kneading, $_{SE}$: solvent evaporation.

This decrease in the contribution of Polysorbate 80 in enhancing dissolution with preparation method can be associated with the fact that in SDs prepared with solvent evaporation method, the drug molecules are already found in molecular state so that once exposed to the dissolution medium they will dissolve immediately. This effect is also shown for the SDs prepared with kneading method since there could be molecular dispersion of the drug to some extent. On the other hand it is unlikely for the PMs to result in molecular dispersion of the drug. The wetting

effect of the surfactant would be able to create a favorable micro-environment around the particles facilitating the dissolution process.

To compare the effect of the type of carrier on dissolution enhancement the higher carrier proportion used was considered i.e. (drug: carrier) 1:2 for the binary system and (drug: carrier: surfactant) 1:2:0.1 for the ternary system. The effect of PEG was found to be higher ($p < 0.05$) than PVP for all the PMs and SDs prepared with kneading and solvent evaporation method.

3.3.3. Dissolution profiles of pure albendazole, physical mixtures and solid dispersions using HPMC

Figs. 3.5 and 3.6 represent the effect of HPMC on ABZ dissolution from its binary and ternary PMs and SDs. Like the case with PEG and PVP, the dissolution of ABZ has been increased by several folds for the ternary PMs and for both the binary and ternary SDs prepared by kneading method. The release rate and extent from the SDs was much better than the PMs. However, the dissolution profiles of the binary PMs were found to be similar to that of the pure drug (*f2* > 50) (Table 3.3).

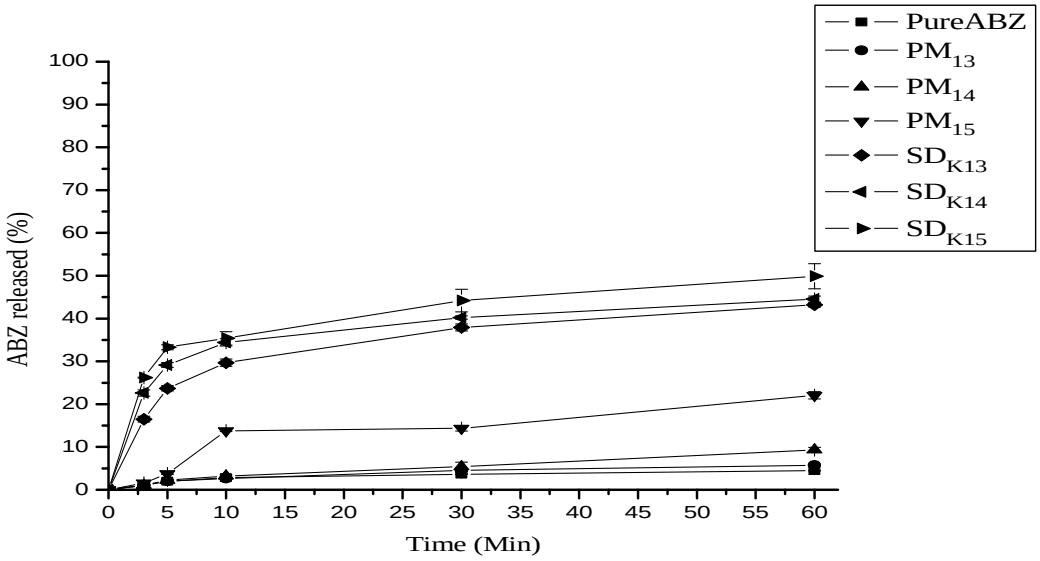

SDs: solid dispersions, PMs: physical mixtures, K: kneading.

Figure 3. 5: Dissolution profile of ABZ from the binary PMs and SDs prepared with HPMC.

Table 3. 3: Similarity factor (f2) values of binary and ternary PMs and SDs of ABZ with HPMC in comparison to the pure drug.

Formulation code	*f*2-values	Dissolution profile
PM_{13} and pure ABZ	95.69	Similar
PM_{14} and pure ABZ	79.83	Similar
PM_{15} and pure ABZ	51.95	Similar
PM_{16} and pure ABZ	16.66	Dissimilar
PM_{17} and pure ABZ	15.42	Dissimilar
PM_{18} and pure ABZ	15.16	Dissimilar
SD_{K13} and pure ABZ	27.12	Dissimilar
SD_{K14} and pure ABZ	24.67	Dissimilar
SD_{K15} and pure ABZ	21.77	Dissimilar
SD_{K16} and pure ABZ	10.36	Dissimilar
SD_{K17} and pure ABZ	9.48	Dissimilar
SD_{K18} and pure ABZ	7.16	Dissimilar

Key: PM: Physical mixture, SD: solid dispersion, $_K$: kneading

The addition of surfactant has shown a remarkable increase in dissolution profile (Fig. 3.6), the effect being signified on the PMs than the SDs, which is in agreement with the results obtained with the other carriers (PEG and PVP). The increase in dissolution rate and extent was proportional with the amount of the carrier used.

The observed increase in dissolution profile with increased carrier proportion, (as shown for all the carriers used in this study) can be explained as follows: If the ratio of drug to polymers is too high, molecularly dispersed state of the drug could change into crystalline state. On the other hand, if the carrier has much higher ratio to drug, then crystallization of drug can be prevented to some extent, leading to induction of solubilization and rapid release (Kim *et al.*, 2011).

Considering kneading method of preparation the ternary SD prepared with HPMC (SD_K18) has given the best dissolution profile than the SDs prepared with the other carriers (PEG and PVP) (Fig. 3.6). Around 67.00% of drug has been released within 5 min and 88.77% of the drug has

been released within one h. The PMs prepared with this carrier has also shown better release than with PEG and PVP showing the superiority of HPMC on improving drug release of ABZ.

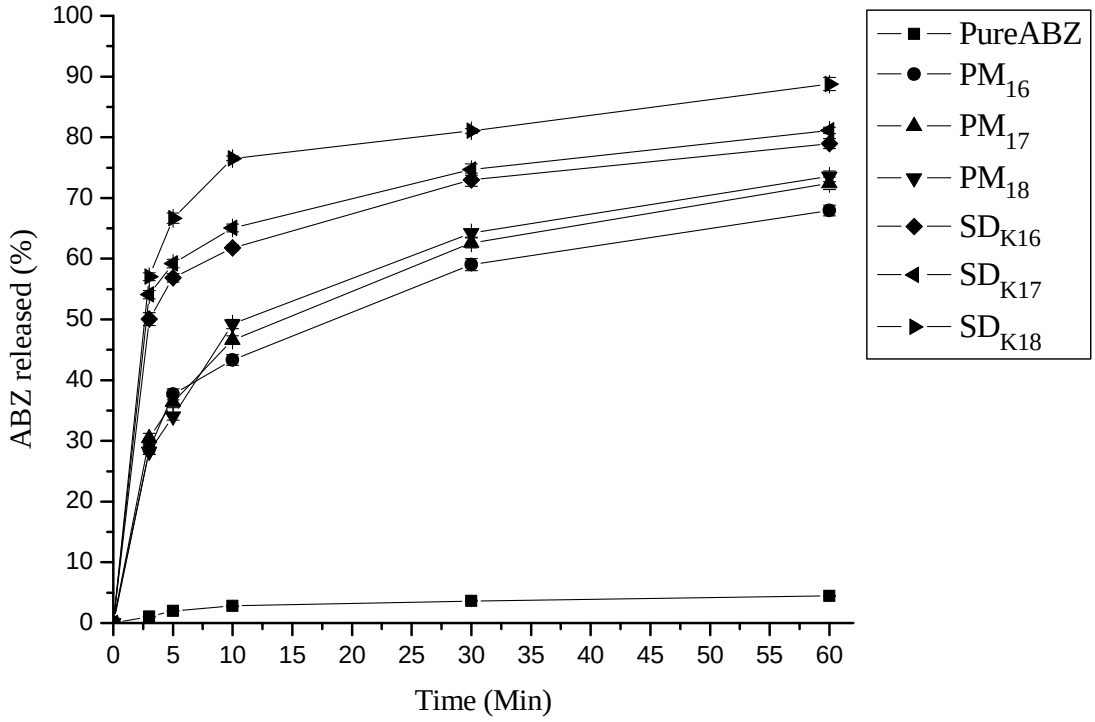

SDs: solid dispersions, PMs: physical mixtures, K: kneading.

Figure 3. 6: Dissolution profile of ABZ from the ternary PMs and SDs prepared with HPMC.

3.4. Drug-polymer interaction analysis

3.4.1. Fourier-transform infrared spectroscopy study

Among the various methodologies used to study drug excipient interactions, the commonest approaches include FTIR spectroscopy and DSC. FTIR study shows interaction between molecules at the level of functional groups (Biswas and Maity, 2011). In polymer blends, mixing of two components at the molecular level will cause changes in the oscillating dipole of the molecules (Akiladevi *et al.*, 2011). Structural changes and the lack of a crystal structure can lead to changes in the molecular bonding energy between functional groups, which can be detected by

FTIR Spectroscopy (Biswas and Maity, 2011). In this study, the ternary PMs and SDs in 1:1:0.1 (drug: carrier: surfactant) proportions were selected for FTIR analysis.

Changes in the FTIR spectrum are recorded as new bands, band disappearing, a shift or widening of the existing bands as well as a change in their intensity. Interactions observed between the SD components such as physical adsorption phenomenon, an effect of electrostatic force, hydrogen bond and vander Walls interactions are in general reversible, while the chemical interactions, including ion exchange, protonation, complexation are irreversible changes. Studies show that the degree of physical adsorption depends to similar extent on physicochemical properties of both SD components, i.e., both drug substance and excipients (Karolewicz *et al.*, 2012).

As can be seen in Fig. 3.7, the spectrum of pure ABZ showed characteristic peaks at 3311.55 cm^{-1} representing the amide NH bond and at 1712.67 cm^{-1} representing the ester C=O bond corresponding to the carbamate portion of the ABZ molecule. Another absorption band appeared at 1618.17 cm^{-1} representing the aromatic C=C bond. Besides, other absorption bands from the aliphatic hydrocarbon group at 2952.32 cm^{-1} and the ether bond,C-O streching at 1095.49 cm^{-1} were obtained.

The PM and SD prepared by kneading method showed all the characteristic peaks of ABZ except the SD showed a shift from 2952.32 cm-1 to 2916cm-1 corresponding to aliphatic hydrocarbon group of ABZ. There was disappearance of band at 3413.77 cm-1 which corresponds to OH stretching of PEG. Shift in C-H stretching of PEG from 2894.9 cm-1 to 2852 cm-1 has also been shown (Figs 3.8 and 3.9). The reason might be due to the interaction of aliphatic hydrocarbon group of ABZ with OH group of PEG through hydrogen bonding explaining the significant difference in enhancing dissolution between the PMs and the SDs with kneading method (See Section 3.3.1).

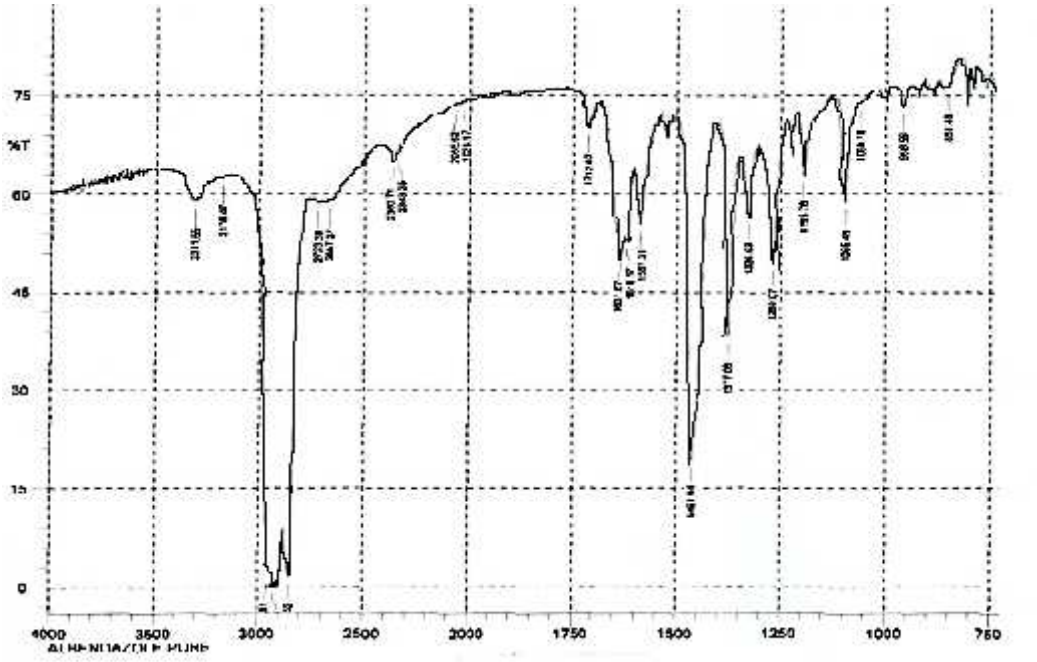

Figure 3. 7: FTIR spectrum of pure ABZ.

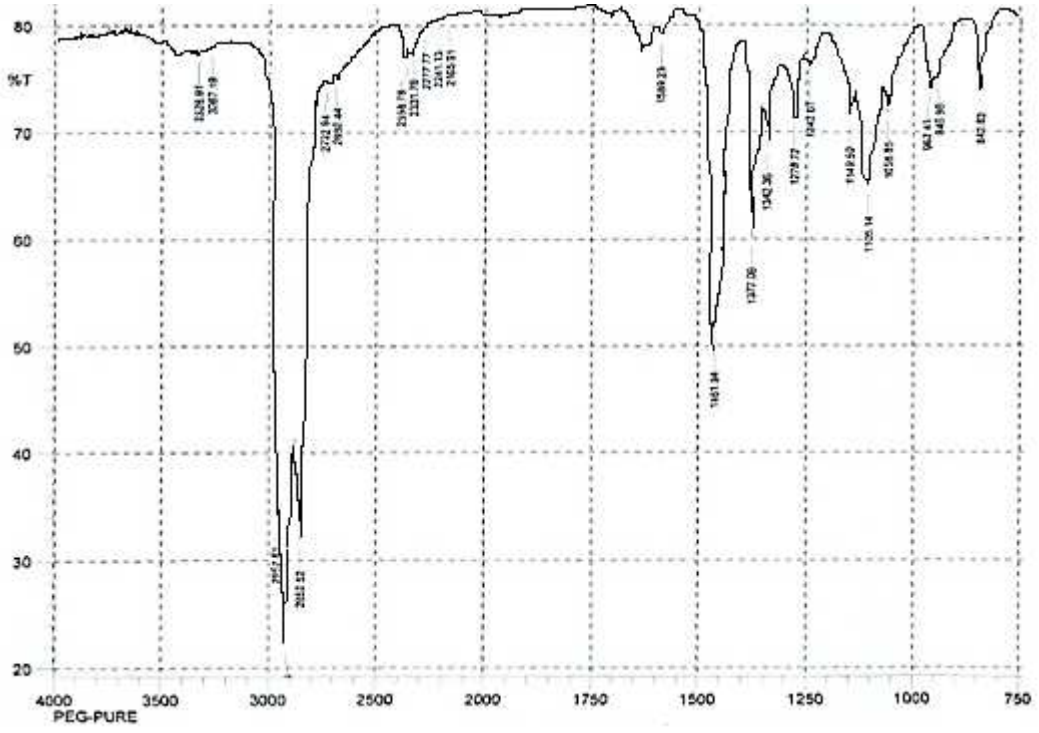

Figure 3.8: FTIR spectrum of PEG

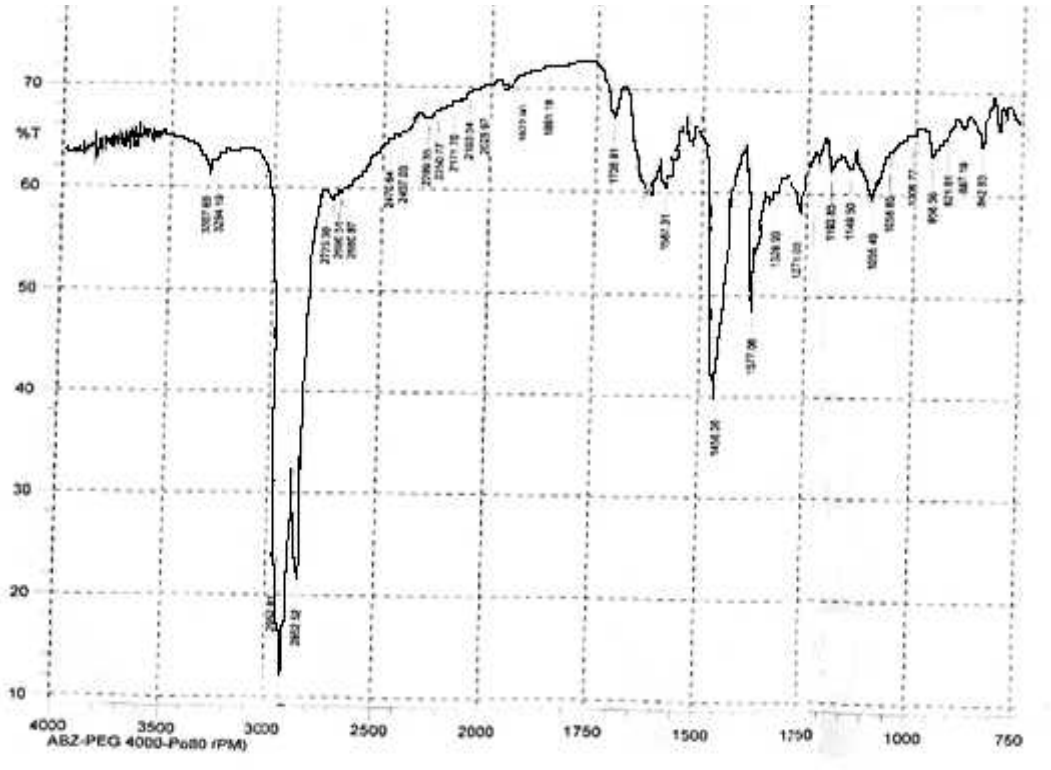

Figure 3. 8: FTIR spectrum of physical mixture of ABZ, PEG and polysorbate 80 in 1:1:0.1 ratios.

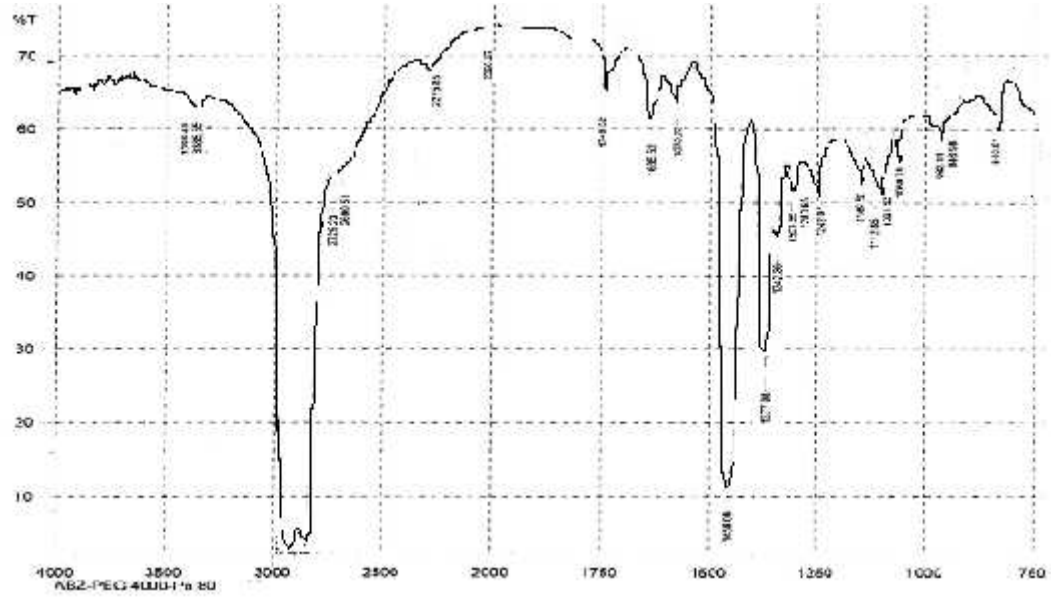

Figure 3. 9: FTIR spectrum of solid dispersion of ABZ, PEG and polysorbate 80 in 1:1:0.1 ratio prepared by kneading method.

The FTIR spectrum of SD with solvent evaporation technique showed disappearance of absorption bands at 3311.55 cm^{-1}, 1095.49 cm-1and 1618.17 cm^{-1} corresponding to amide NH, ether and aromatic C=C bonds of ABZ, respectively and 3413.77 cm^{-1} corresponding to OH stretching of PEG indicating an interaction between drug and the carrier. (Fig. 3.10).

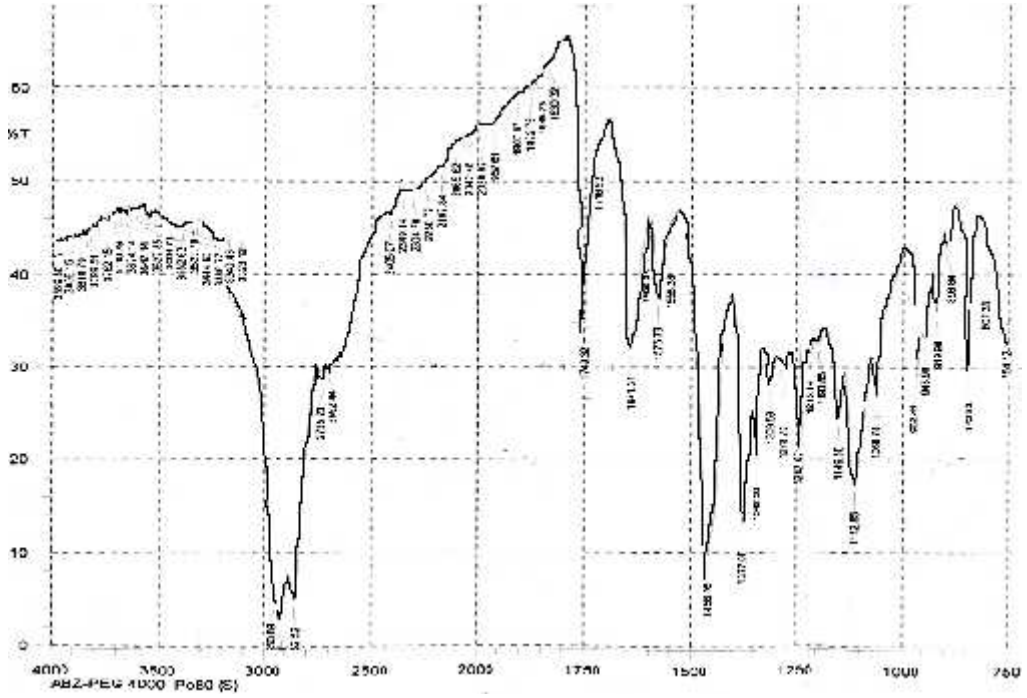

Figure 3. 10: FTIR spectrum of solid dispersion of ABZ, PEG and polysorbate 80 in 1:1:0.1 ratio prepared by solvent evaporation technique.

The PM of the drug in ternary system with PVP and polysorbate 80 showed all the characteristic peak of ABZ and PVP (Fig. 3.11). The spectra of PMs were similar to the spectra obtained by the mixture of polymer and the drug. This indicated that no interaction occurred with simple physical mixing of the drug and PVP. However the SD prepared using kneading method showed shifts in some of the characteristic peaks of ABZ and PVP including shifts from 3311.55 cm^{-1} to 3303.83 cm^{-1} representing the amide NH bond of ABZ and from 1290 cm^{-1} (C–N band for tertiary amines) to 1269.07 cm^{-1} of PVP (Fig. 3.12). PVP is known to be capable of forming H-bond either through the nitrogen or carbonyl group on the pyrrolidine ring (Akiladevi *et al.*, 2011). Here the nitrogen group might be responsible for the formation of hydrogen bonding with

amide NH bond of ABZ explaining the interaction demonstrated in DSC thermogram (See Section 3.4.2).

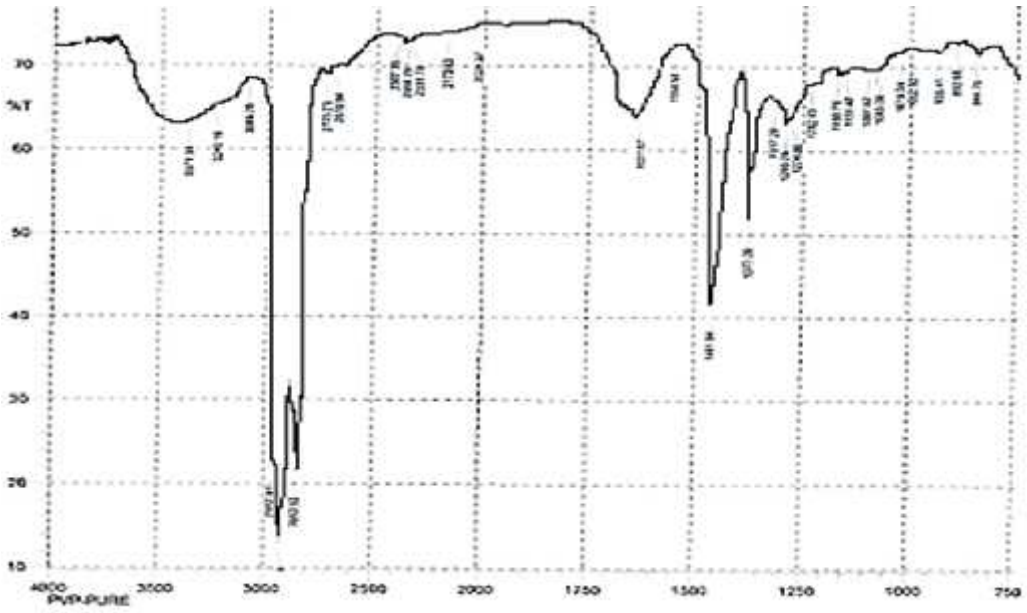

Figure 3. 11: FTIR spectrum of PVP.

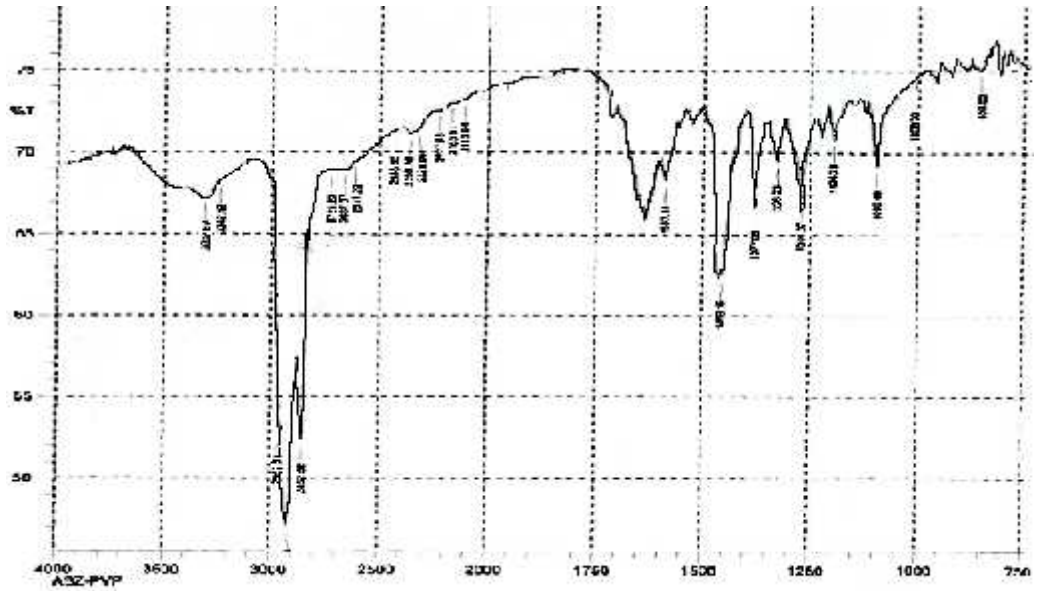

Figure 3. 12: FTIR spectrum of physical mixture of ABZ, PVP and polysorbate 80 in 1:1:0.1 ratios.

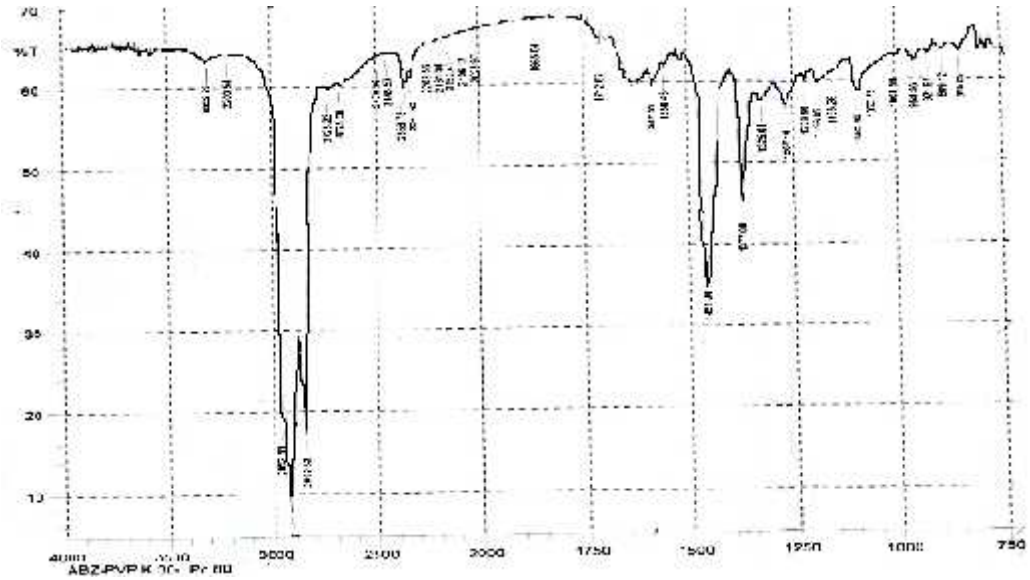

Figure 3. 13: FTIR spectrum of solid dispersion of ABZ, PVP and polysorbate 80 in 1:1:0.1 ratio prepared by kneading method.

The FTIR spectrum of SD of ABZ, PVP and polysorbate 80 (Fig. 3.13) prepared by solvent evaporation technique showed all the characteristic peaks of ABZ as well as the carrier which might be a sign of abcence of intraction.

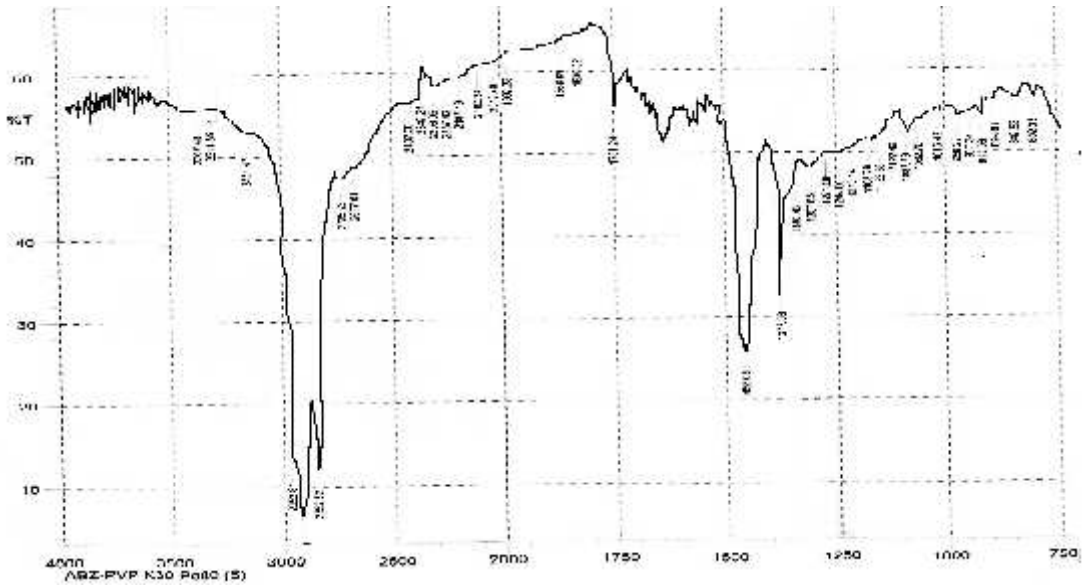

Figure 3. 14: FTIR spectrum of solid dispersion of ABZ, PVP and polysorbate 80 in 1:1:0.1 ratio prepared by solvent evaporation technique.

The PM and SD prepared by kneading using HPMC showed all the characteristics peaks of ABZ except there was a slight shift from 3311cm^{-1} (amide NH bond of ABZ) to 3299.98 and 3321.19 to the PM and SD, respectively. In both the PM and SD spectra, all the peaks of pure HPMC have appeared without any shift except for the disappearance of the peak between 3500-3400 cm^{-1} which corresponds to OH vibrational stretching (Figs 3.14 and 3.15). This indicates the formation of hydrogen bonding between the amide NH bond of ABZ and the OH group of HPMC. Thus, the formation of hydrogen bonding can explain the observed increase in dissolution (See Section 3.3.3) which is one of the mechanisms enhanced dissolution in SDs.

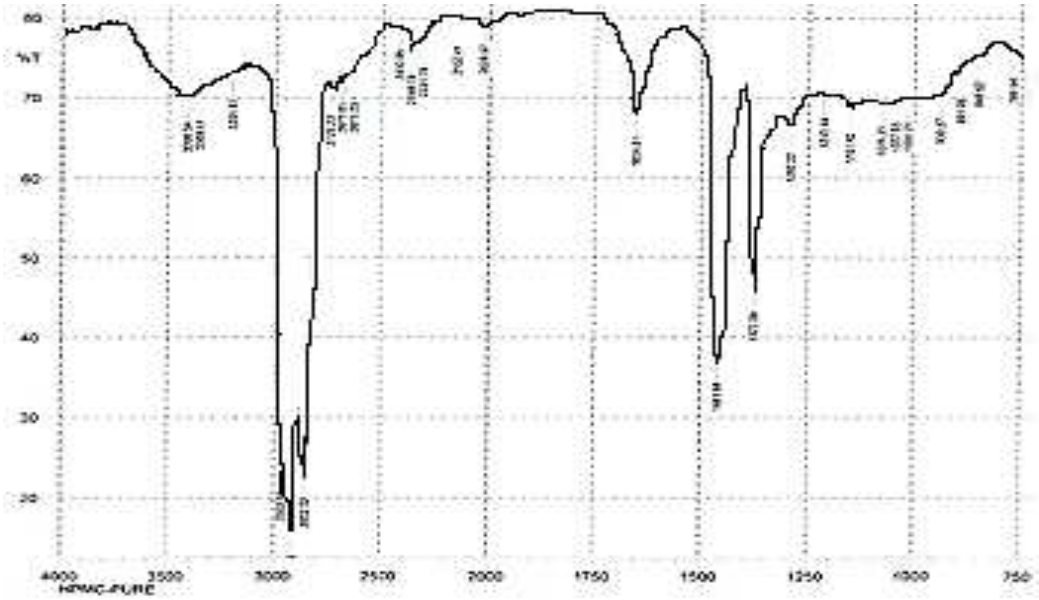

Figure 3. 15:FTIR spectrum of HPMC

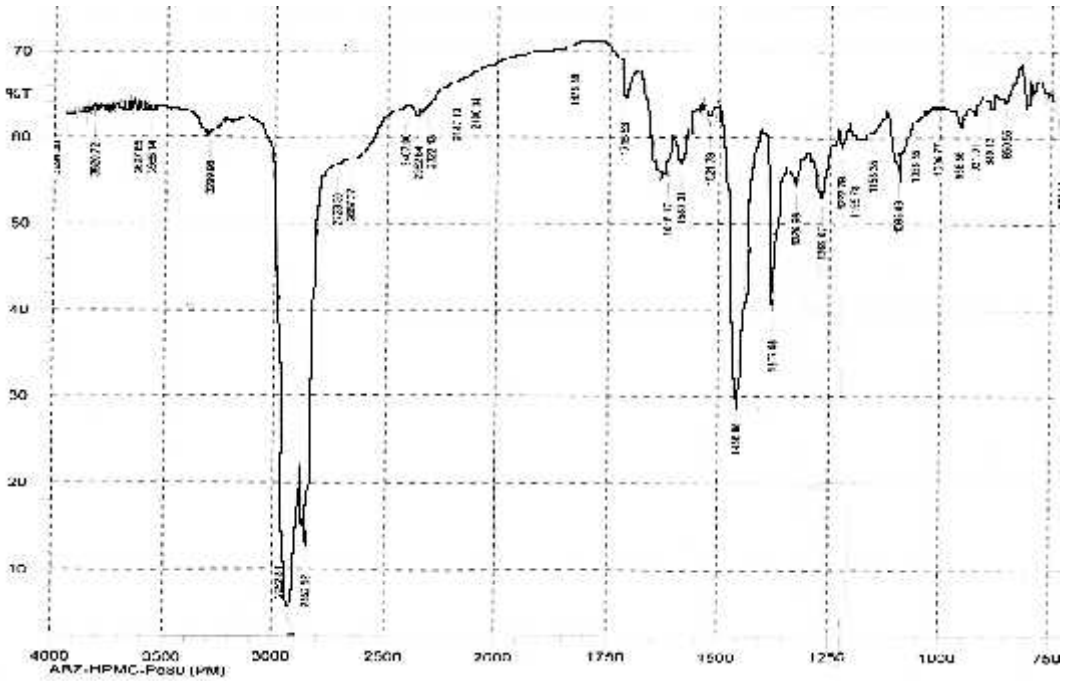

Figure 3. 16: FTIR spectrum of physical mixture of ABZ, HPMC and polysorbate 80 in 1:1:0.1 ratios.

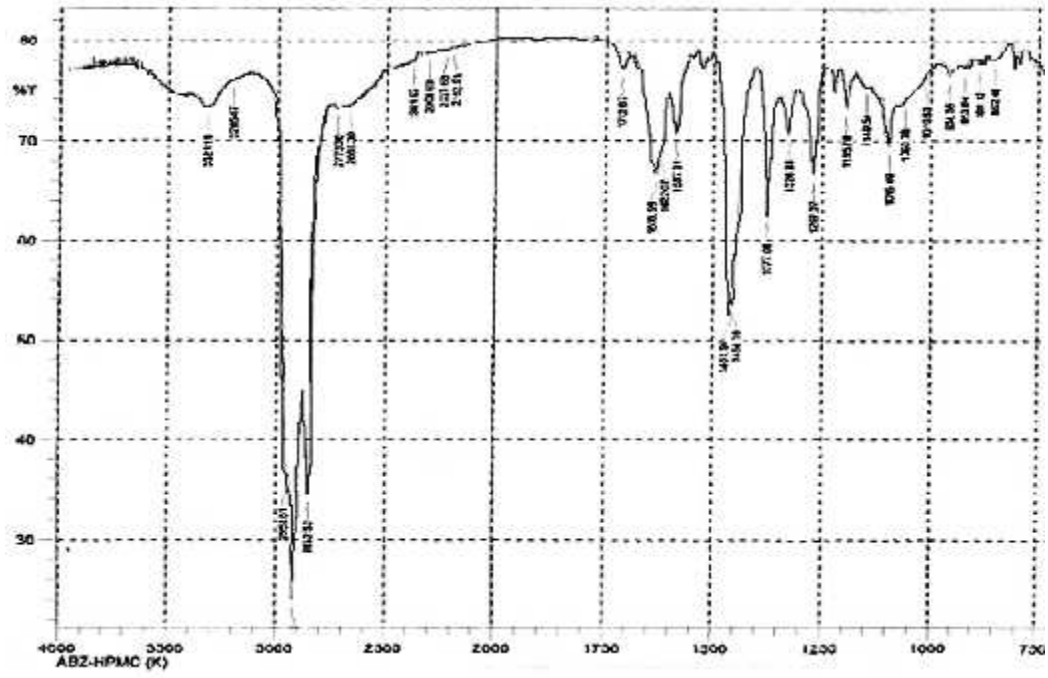

Figure 3. 17: FTIR spectrum of solid dispersion of ABZ, HPMC and polysorbate 80 in 1:1:0.1 ratio prepared by kneading method.

3.4.2. Thermal analysis

DSC detects the temperature at which thermal events occur. Thermal events can be a glass to rubber transition, (re)crystallization, melting or degradation (Dhirendra *et al.*, 2009). When the sample is heated peaks indicating changes in enthalpy and specific heat are recorded. Each peak refers to the specific thermal effect resulting from the process, such as crystallization or melting. The sample crystallization is confirmed by a sharp peak on the thermogram, indicating the exothermic nature of the transformation. On the other hand, the process of melting characteristic for samples with the crystalline structure only is detected as the endothermic peak on the thermogram. Peaks of the DSC curve associated with melting cannot be found for the amorphous forms. Lack of a peak related to SD melting on DSC indicates that the substance predominates in the amorphous form in the formulation (Karolewicz *et al.*, 2012).

Thermal analysis was done for the pure drug, the carriers and the ternary PMs and SDs in 1:1:0.1 (drug: carrier: surfactant) proportions. As can be seen in Figs 3.16 - 3.18, ABZ and PEG showed a single endothermic peak at 206.12 °C and 63.62 °C, respectively corresponding to their melting point. PVP and HPMC showed broad DSC endotherms ranging from 28.65 to 130.14 °C and 25.90 to 99.94 °C, respectively, which might be associated with the presence of residual moisture in those carriers. Polysorbate 80 is liquid at room temperature; therefore, no peak is expected under the experimental conditions used.

The DSC thermograms of the PM and SD prepared with PEG showed the characteristic peak of PEG related to its melting point with no additional peaks. However, as can be seen in Fig 3.16, ABZ peak has disappeared which could be due to the presence of the carrier that decreased the crystallinity and stabilizing the amorphous structure of the drug. This finding could explain the observed enhancement in the dissolution profiles of ABZ (See Section 3.3.1). On the other hand on the DSC thermogams of the SDs with PVP and HPMC, the peak of ABZ has shifted towards the lower temperature range from the peak of the pure ABZ (Figs 3.17 and 1.8). This shift could be as a result of interaction between ABZ and the carriers (PVP and HPMC) though the formation of hydrogen bond which is also shown on the FTIR study (See Section 3.4.1).

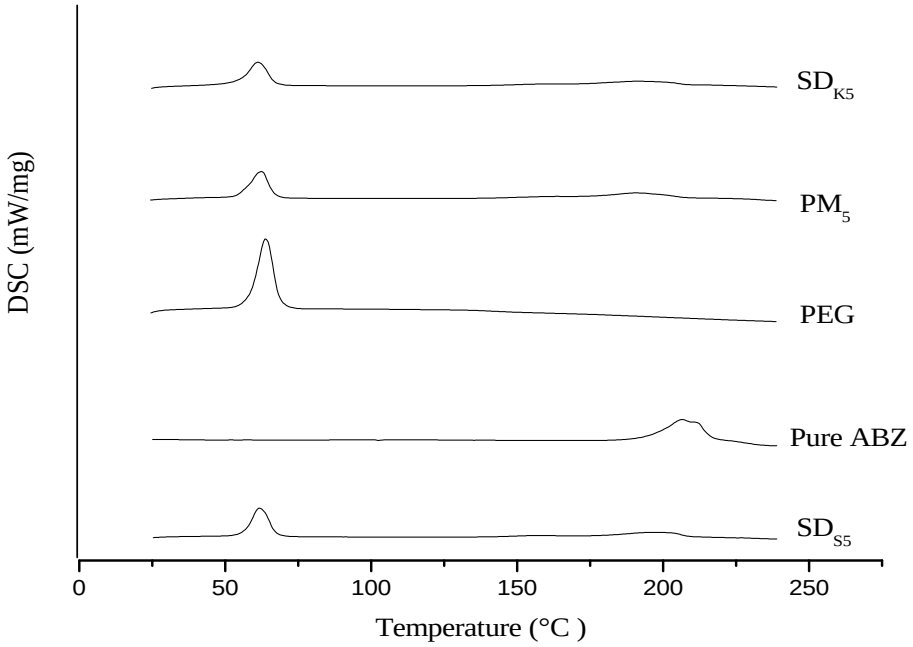

Figure 3. 18: DSC Thermogram of Pure ABZ, PEG, PM_5, SD_{K5} and SD_{S5} (Key: PM_5: Physical mixture of ABZ, PEG and polysorbate 80; SD_{K5}: Solid dispersion of ABZ, PEG and polysorbate 80 prepared by kneading method; SD_{S5}: Solid dispersion of ABZ, PEG and polysorbate 80 prepared by solvent evaporation method.

It has been reported that the shape of the peaks of the DSC thermogram and enthalpy may change due to the presence of impurity in the materials used for analysis. Thus, changes in the melting endotherm of the pure ABZ could be due to the mixing of the drug and the carriers, which lowers the purity of each component in the mixture and may not necessarily indicate potential incompatibility (Pehlivan *et al.*, 2011).

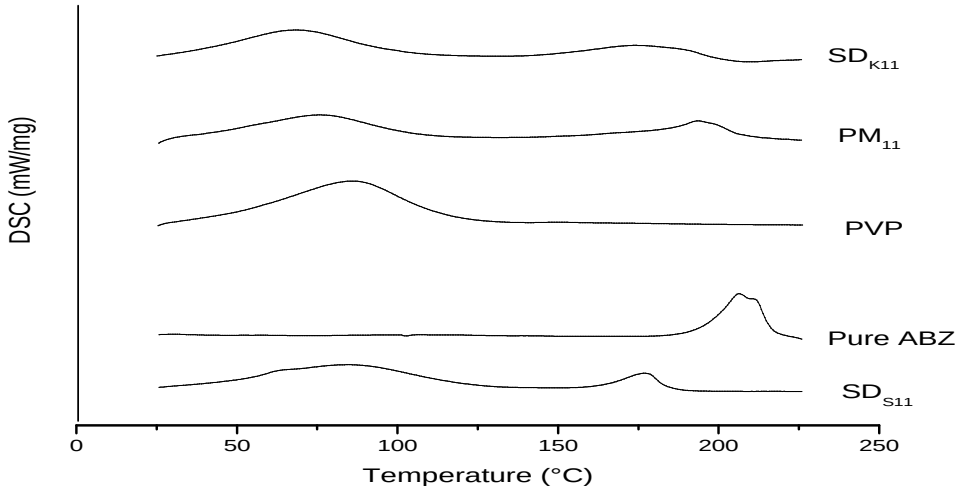

Figure 3. 19: Thermogram of Pure ABZ, PVP, PM_{11}, SD_{K11} and SD_{S11} (Key: PM_{11}: Physical mixture of ABZ, PVP and polysorbate 80; SD_{K11}: Solid dispersion of ABZ, PVP and polysorbate 80 prepared by kneading method; SD_{S11}: Solid dispersion of ABZ, PVP and polysorbate 80 prepared by solvent evaporation method).

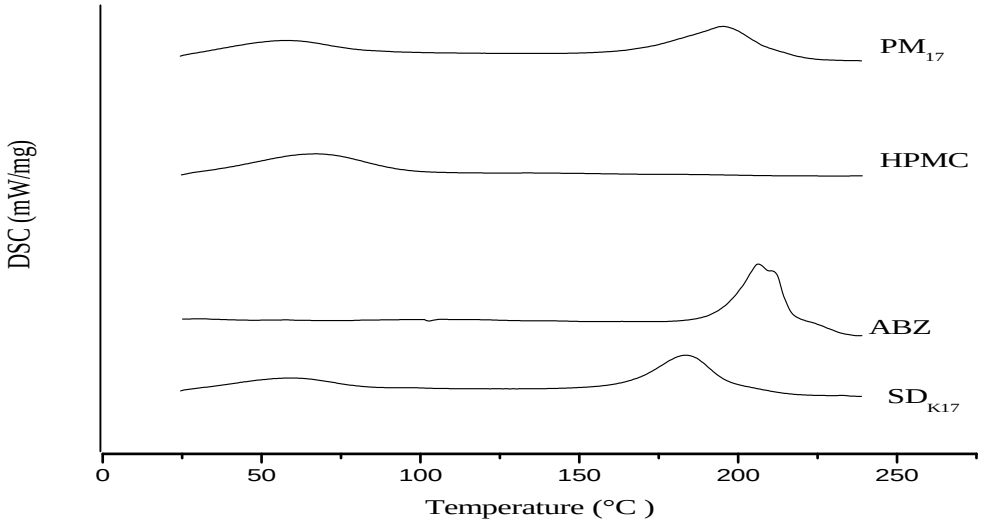

Figure 3. 20: DSC Thermogram of Pure ABZ, HPMC, PM_{17} and SD_{K17} (Key: PM_{17}: Physical mixture of ABZ, HPMC and polysorbate 80; SD_{K17}: Solid dispersion of ABZ, HPMC and polysorbate 80 prepared by kneading method).

3.5. Powder characterization of solid dispersions

The powder characteristics (flow property and compressibility) have to be evaluated if SDs are intended for solid dosage forms. Flow properties and compressibility were determined for the ternary SDs, since in all formulations the ternary system has been shown to be superior in dissolution profile. The results are shown in Table 3.4.

In general, the SDs prepared showed good to fair flowability (angle of repose ranging from 29.16 ± 0.74 to 39.91 ± 1.41, Hausner ratio from 1.03 ± 0.04 to 1.19 ± 0.03 and Carr index from 7.01 ± 0.19 to 18.21 ± 0.22). As shown in Table 3.4, the flow property of the SDs prepared by kneading method was superior to SDs prepared by solvent evaporation method. In addition, significant improvement in flow property was observed when the carrier proportion increased from 1:0.5 to 1:2. The SDs with PVP showed better flow property than the two carriers followed by PEG.

The compressibility study demonstrated that the SDs compressed at 10 KN and 20 KN compression force had hardness ranging from 43.67 ± 1.25 to 68.33 ± 2.05, and from 60.67 ± 1.25 to 87.67 ± 2.05, respectively. Tablets that have hardness greater than 50 N and that loss less than 1% of their weight after friability test are generally considered acceptable (BP, 2000).

The SDs prepared with PEG compressed at 10 KN resulted in tablet hardness greater than 50 N. The SDs with PVP and HPMC has also shown hardness greater than 50 N except with the lowest drug to carrier ratios used (1:0.5). The hardness was shown to increase with increasing carrier proportion which could be related to the carrier's property to aid as direct compression binders (Rowe *et al.*, 2006). All the tablets with the higher carrier proportion (drug to carrier ratio of 1:2) resulted in percent friability of less than one.

Table 3. 4: Powder characteristics study of ternary SDs.

Formulations	Flow rate (g/sec) ± STD	Angle of repose (°) ± STD	Hausner ratio ± STD	Carr's index (%) ± STD	Hardness (N) ±STD		Friability (%)±STD	
					at 10 KN CF	at 20 KN CF	at 10 KN CF	at 20 KN CF
SD_{K4}	NF	34.77 ± 1.33	1.16 ± 0.04	16.00 ± 0.49	50.67 ± 1.70	69.00 ± 2.00	1.23 ± 0.02	1.08 ± 0.02
SD_{K5}	NF	33.22 ± 1.46	1.13 ± 0.02	15.40 ± 0.51	55.67 ± 1.70	72.33 ± 2.08	1.11 ± 0.01	0.89 ± 0.01
SD_{K6}	3.57 ± 0.27	31.41 ± 1.18	1.12 ± 0.02	11.03 ± 0.33	68.33 ± 2.05	87.67 ± 2.05	0.98 ± 0.03	0.73 ± 0.02
SD_{SE4}	NF	38.04 ± 0.99	1.15 ± 0.01	18.21 ± 0.22	46.22 ± 1.29	62.33 ± 2.08	1.26 ± 0.03	1.09 ± 0.03
SD_{SE5}	NF	36.91 ± 0.84	1.16 ± 0.02	15.35 ± 0.42	50.11 ± 1.64	69.33 ± 2.52	1.09 ± 0.02	0.87 ± 0.01
SD_{SE6}	NF	34.32 ± 1.19	1.19 ± 0.03	14.43 ± 0.11	60.00 ± 2.16	75.67 ± 2.52	0.99 ± 0.02	0.76 ± 0.03
SD_{K10}	NF	32.17 ± 1.47	1.14 ± 0.02	11.70 ± 0.39	47.00 ± 2.16	67.97 ± 2.08	0.98 ± 0.01	0.81 ± 0.01
SD_{K11}	4.01 ± 0.21	31.90 ± 1.36	1.10 ± 0.01	8.99 ± 0.17	54.67 ± 1.67	71.33 ± 2.52	0.96 ± 0.03	0.70 ± 0.02
SD_{K12}	4.34 ± 0.41	29.16 ± 0.88	1.08 ± 0.01	7.01 ± 0.19	72.56 ± 1.75	88.67 ± 2.52	0.73 ± 0.01	0.55 ± 0.01
SD_{SE10}	NF	34.98 ± 0.93	1.03 ± 0.04	13.23 ± 0.41	43.67 ± 1.25	60.67 ± 1.25	1.03 ± 0.02	0.89 ± 0.03
SD_{SE11}	NF	33.37±1.39	1.12± 0.03	10.8 ± 0.28	50.89 ± 1.64	69.33 ± 2.52	1.01 ± 0.04	0.73 ± 0.02
SD_{SE12}	NF	31.6 ± 1.20	1.15 ± 0.03	9.40 ± 0.41	65.56 ± 2.04	73.00 ± 2.00	0.89 ± 0.02	0.51 ± 0.02
SD_{K16}	NF	39.91 ± 1.21	1.17 ± 0.01	17.7 ± 0.51	47.33 ± 1.7	65.33 ± 1.53	1.02 ± 0.03	0.80 ± 0.03
SD_{K17}	NF	38.44 ± 1.28	1.16 ± 0.04	15.94 ± 0.24	53.89 ± 2.45	73.67 ± 2.52	0.97 ± 0.03	0.67 ± 0.03
SD_{K18}	NF	36.05 ± 1.10	1.19 ± 0.04	15.34 ± 0.17	68.33 ± 2.62	85.33 ± 2.08	0.84 ± 0.02	0.58 ± 0.01

Key: SD: Solid dispersion, K: Kneading, SE: Solvent evaporation, NF: Does not pass through the funnel, CF: Compression force

3.6. Preparation and evaluation of tablets

Disintegration or dissolution is the rate-limiting step in absorption of poorly soluble active pharmaceutical ingredient (API) from tablets. The tablets prepared by direct compression disintegrate into API particles instead of granules that directly come into contact with dissolution fluid and exhibits comparatively faster dissolution (Dokala and Pallavi, 2013). Although simple in terms of unit process involved, the direct compression process is highly influenced by powder characteristics such as powder flowability and compressibility which may require a very critical selection of excipients (Sanjay and Natvarlal, 2009).

Even though in this study the solvent evaporation method has shown significantly higher dissolution profile ($p < 0.5$) than kneading method, it resulted in powders with inferior compressibility and flow property (Table 3.4). In addition this method has been identified to be expensive (Kapoor *et al.,* 2012) and removal of the solvent is difficult (Singh *et al.,* 2011). It may be necessary to evaporate hundreds of liters of organic solvent required to prepare SD for kilogram quantities of the drug. Considering the fact that ABZ is a cheap drug using a manufacturing method that is expensive may not be appropriate choice from economic point of view. As a result, kneading method was selected for tablet compression and optimization.

The powder characteristics study of the SDs prepared with kneading method demonstrated that the SDs with HPMC resulted in powders with inferior flow property than the two carriers. Using PVP resulted in superior flow property followed by PEG. However, SDs of ABZ with PEG were found to be better in dissolution profile than with PVP ($p < 0.5$). Thus, the ternary SDs of ABZ, PEG and polysorbate 80, prepared by kneading method were selected for tablet compression and optimization.

The selected SD tablets were prepared by direct compression method. Accordingly the SDs were weighed and mixed with direct compression excipients (Table 2.3). SSG was selected as a superdisintegrant. Effect of the amount of SSG on the disintegration of the tablets was studied to select the disintegrant level which could result in minimum disintegration time. Based on this, 2%, 4%, 6% and 8% SSG were evaluated. The 4% SSG gave optimum disintegration time, thus it was used throughout the study. SSG and MCC were mixed with the SDs in a TURBULA®

Mixer (Willy A. Bachofen AG, Turbula®2TF, Basel, Switzerland) for 10 min at a speed of 49 rpm. Then magnesium stearate and Aerosil® were added and mixed for additional 5 min.

3.6.1. Effect of glidants

Aerosil® (0.5%, 1% and 2%) alone was used as a flow promoter initially but no significant change was observed in flow property (SD_{k4}, the SDs containing lower amount of carrier couldn't pass through the funnel). MCC with different concentration (15, 20 and 30%) was used along with Aerosil® to improve the flow. MCC is the commonly used direct compression vehicle which has good flow and compressible characteristics. In addition MCC is self-disintegrating with low lubricant requirement even though those properties do not replace the need for disintegrant and lubricant (Iyer *et al.*, 2013). No significant change in flow was observed when 15% MCC combined with 0.5, 1 or 2% Aerosil®. However, 20% MCC along with 1% Aerosil® resulted in a significant improvement in flow than the SDs powder alone. (SD_{K4}) passed through the funnel with a flow rate of 3.46 ± 0.12. No significant change in flow property was observed between 20% MCC combined with 1% Aerosil® and 20% MCC with 2% Aerosil®. As a result the Aerosil® content was maintained at1%. The flow property was shown to increase significantly when MCC level was increased from 20% to 30% (Table 3.5). Consequently, the amount of MCC was kept between 20% and 30% for further studies.

3.6.2. Effect of drug to carrier ratio

SD blends for tablet compression, containing the largest amount of carrier proportion showed better flow property and compressibility (Table 3.5), which was also confirmed in powder characterization of SDs (Table 3.4). To determine the effect of drug to carrier ratio on tablet characteristics, tablets with the higher (1:2) and lower (1:0.5) carrier proportions were compressed at 10 KN.

As can be seen in Table 3.5, the lower carrier proportions (F1 - F3) resulted in a significantly ($p < 0.5$) lower disintegration time and hardness than the corresponding higher carrier proportions used (F4 - F6), which could be due to the binding effect of PEG (Rowe *et al.*, 2006).

Table 3. 5: Effect MCC amount and drug to carrier ratio on tablet characteristics.

Formulation	Flow rate (g/sec)	Angle of repose (°)	Hausner ratio	Carr's index (%)	Disintegration time (Min)	Hardness (N)	Friability (%)	Drug released (%)	
								10 min	30 min
F1	NF	34.01 ± 0.93	1.15 ± 0.03	15.94 ± 0.62	2.96 ± 0.66	51.00 ± 1.63	1.19 ± 0.03	50.81 ± 2.65	71.34 ± 0.51
F2	3.46 ± 0.12	32.72 ± 0.74	1.13 ± 0.04	13.95 ± 0.29	3.14 ± 0.11	60.33 ± 1.25	1.04 ± 0.02	51.03 ± 1.6	72.31 ± 1.69
F3	4.02 ± 0.11	29.26 ± 0.66	1.11 ± 0.04	11.16 ± 0.51	3.56 ± 0.13	73.33 ± 1.70	0.85 ± 0.01	52.94 ± 1.07	71.24 ± 2.19
F4	3.31 ± 0.11	31.01 ± 0.59	1.12 ± 0.05	10.97 ± 0.42	4.08 ± 0.09	68.00 ± 2.45	0.97 ± 0.01	54.13 ± 1.07	79.27 ± 2.52
F5	4.39 ± 0.17	30.02 ± 0.99	1.09 ± 0.02	9.17 ± 0.39	4.95 ± 0.11	73.00 ± 2.05	0.90 ± 0.02	55.17 ± 1.6	82.86 ± 1.70
F6	5.11 ± 0.19	28.01 ± 0.87	1.01 ± 0.03	8.09 ± 0.28	5.61 ± 0.23	98.00 ± 2.45	0.55 ± 0.01	56.48 ± 0.80	81.04 ± 1.80

Key: F1: Solid dispersion of ABZ, PEG and polysorbate 80 prepared with kneading method in 1:0.5:0.1 ratio and mixed with 15% MCC, 1% Aerosil, 4% SSG and 0.5% magnesium sterate; **F2:** Solid dispersion of ABZ, PEG and polysorbate 80 prepared with kneading method in 1:0.5:0.1 ratio and mixed with 20% MCC, 1% Aerosil, 4% SSG and 0.5% magnesium sterate; **F3:** Solid dispersion of ABZ, PEG and polysorbate 80 prepared with kneading method in 1:0.5:0.1 ratio and mixed with 30% MCC, 1% Aerosil, 4% SSG and 0.5% magnesium sterate; **F4:** Solid dispersion of ABZ, PEG and polysorbate 80 prepared with kneading method in 1:2:0.1 ratio and mixed with 15% MCC, 1% Aerosil, 4% SSG and 0.5% magnesium sterate; **F5:** Solid dispersion of ABZ, PEG and polysorbate 80 prepared with kneading method in 1:2:0.1 ratio and mixed with 20% MCC, 1% Aerosil, 4% SSG and 0.5% magnesium sterate; **F6:** Solid dispersion of ABZ, PEG and polysorbate 80 prepared with kneading method in 1:2:0.1 ratio and mixed with 30% MCC, 1% Aerosil, 4% SSG and 0.5% magnesium stearate.

As shown in Table 3.5 the amount of drug released from SD tablets was lower than the SD powder in the initial period (10 min) which is due to a lag time period resulting from tablet disintegration. However, there was no significant difference in the final release of the drug between the powder and the tablets, i.e., the amount released at 30 min was found to be similar ($p < 0.5$). Significantly higher ($p < 0.5$) amount of drug release was achieved from tablets with larger carrier proportion (drug to carrier ratio of 1:2). Thus the drug to carrier proportions 1:0.5 and 1:2 were considered for optimization.

3.6.3. Effect of compression force

The effect of compression force was studied on the formulations that contain the lowest amount of carrier proportion and MCC (F1). Tablets were compressed at 7.5, 10, 15 and 20 KN. Increasing compression force resulted in a significant increase ($p < 0.5$) in hardness and disintegration time, and decrease in friability. Tablets compressed at 7.5 KN showed hardness less than < 50 N and friability of 1.31 ± 0.005 (Table 3.6). As a result, 10 KN was taken as the minimum compression force for optimization, 20 KN was considered as the highest compression to be used since it resulted in percent friability <1 (0.88 ± 0.02).

Table 3. 6: Effect of compression force on tablet characteristics.

Formulation	Compression force (KN)	Hardness (N)	Friability (%)	Disintegration time (min)
F1a	7.5	43.33 ± 2.08	1.31 ± 0.05	1.96 ± 0.06
F1b	10	50.67 ± 1.53	1.11 ± 0.03	2.90 ± 0.10
F1c	15	65.33 ± 2.52	1.00 ± 0.03	3.26 ± 0.10
F1d	20	73.00 ± 2.00	0.88 ± 0.02	3.57 ± 0.09

3.7. Optimization of formulations

The use of advanced techniques of optimization such as response surface methodology (RSM) avoids problems of the traditional approach in that it provides best possible optimized solution

and work efficiently at very few number of experiments to be performed that minimizes time, as well as cost. The traditional approach requires determination of the dependent variable at each and every combination of independent variables just varying only one at a time. The main problems with this approach are the requirement to carry out a large number of experiments and the uncertainty of actually finding the optimal conditions, because the interactions between factors are not taken into account (Bezerraa *et al.*, 2008).

RSM is a collection of statistical and mathematical techniques useful for developing, improving, and optimizing processes in which a response of interest is influenced by several variables and the objective is to optimize this response (Ghanim, 2013). Before applying the RSM, identifying the important factors among a wider set of possible controllable factors is the first stage in optimization followed by selection of an experimental design (Bas *et al.*, 2007).

The factors studied during tablet formulation of ABZ SD by direct compression method include compression force, drug to carrier ratio and amount of MCC which were shown to significantly affect the responses such as flow property and compressibility. In addition, in the preparation of SDs the amount of carrier used was shown to affect drug release profile. The other independent variables such as percentage of SSG, Aerosil® and magnesium sterate were kept constant at 4%, 1% and 0.5%, respectively. Thus, the three factors, drug to carrier ratio, compression force and amount of MCC were considered for optimization. A full factorial design was used in which the three factors were studied at two levels resulting in 8 experiments (Table 3.7).

Table 3. 7: Design layout of full factorial design to formulate ABZ tablets.

Formulation	Carrier/drug	Amount of MCC (%)	Compression force (KN)
OF1	0.5 (-1)	20 (-1)	10 (-1)
OF2	0.5 (-1)	30 (+)	10 (-1)
OF3	2 (+1)	20 (-1)	10 (-1)
OF4	2 (+1)	30 (+)	10 (-1)
OF5	0.5 (-1)	20 (-1)	20 (+1)
OF6	0.5(-1)	30 (+)	20 (+1)
OF7	2 (+)	20 (-1)	20 (+)
OF8	2 (+)	30 (+)	20 (+)

Accordingly, SDs with the selected drug to carrier ratio were prepared using kneading method, mixed with different excipients, characterized, compressed using direct compression method and the tablet characteristics were studied. The responses were optimized using Design-Expert® 9.0.6 software.

3.7.1. Characterization of solid dispersion powder mixtures

In order to perform direct compression without any problems, it is necessary to consider certain parameters such as flow property which is to be maintained in optimum range (Dokala and Pallavi, 2013). Thus, the SD powder mixtures were evaluated for various pre-compression characteristics such as flow rate, angle of repose, Hausner's ratio and Carr's index (Table 3.8).

Table 3. 8: Characterization of SD powder mixtures of optimization formulations for tablet compression.

Formulation	Flow rate (g/s)	Angle of repose (degree)	Hausner ratio	Carr's index (%)
OF1	3.51 ± 0.11	32.81 ± 0.37	1.13 ± 0.03	14.02 ± 0.62
OF2	4.05 ± 0.07	29.16 ± 0.36	1.11 ± 0.04	11.05 ± 0.29
OF3	4.35 ± 0.16	30.12 ± 0.73	1.1 ± 0.03	9.22 ± 0.62
OF4	5.03 ± 0.08	27.71 ± 1.08	1.01 ± 0.04	8.15 ± 0.29
OF5	3.26 ± 0.12	32.63 ± 0.63	1.13 ± 0.01	13.88 ± 0.41
OF6	3.94 ± 0.12	29.47 ± 1.73	1.11 ± 0.005	11.12 ± 0.35
OF7	4.31 ± 0.12	31.06 ± 1.07	1.08 ± 0.005	9.41 ± 0.16
OF8	5.16 ± 0.12	27.03 ± 0.79	1.00 ± 0.01	8.27 ± 0.12

As can be seen in Table 3.8 the SD powder mixtures for tablet compression resulted in a significant improvement in flow property than the SD alone. All the powder mixtures passed through the funnel with significant increase in flow rate. The SD prepared in drug to carrier ratio of 1:0.5, which couldn't to pass through the funnel, exhibited flow rate of 3.51 ± 0.11g/sec (OF1) and 3.26 ± 0.12g/sec (OF5). The Carr's index and Hausner ratio were between 8.15 ± 0.29 - 14.02 ± 0.62 and 1.01 ± 0.04 - 1.13 ± 0.03, respectively demonstrating good to excellent flow

property (USP30-NF25, 2007). The angle of repose values were also in the range of 27.03 ± 0.79 - 32.81 ± 0.37, which also indicate excellent to good flow properties of the prepared SD powder mixtures.

3.7.2. Characterization of solid dispersion tablets

Post compression analysis was done for the eight formulations prepared for optimization. As can be seen in Table 3.8., the hardness of all the tablets were > 50 N (between 59.00 ± 1.63 and 129.67 ± 3.40 N) indicating the hardness is above the acceptable limit reference (BP, 2000). Tablets with the lower carrier proportion and concentration of MCC (OF1) compressed at 10 KN resulted in the lowest hardness (59.00 ± 1.63 N), and disintegration time (3.17 ± 0.11 min). On the contrary OF8, compressed at 20 KN with the highest carrier proportion and concentration of MCC resulted in tablets with the highest hardness (129.67 ± 3.40 N) and disintegration time (7.28 ± 0.16 min). The friability was < 1 % for all the formulations except for OF1.

The amount of drug released within 10 min was shown to decrease with increasing compression force, amount of carrier proportion and concentration of MCC (Table 3.9), which is related to the lag time period due to disintegration. However, the amount of the drug released within 30 min was not affected by disintegration time rather the amount of drug released from the tablets was higher than the corresponding SD. There has been an increase in percent release of the drug from 69.10 ± 0.84 to 73.19 ± 1.04% for the 1:0.5 drug to carrier proportion and from 75.39 ± 0.66 to 83.02 ± 2.80% for the 1:2 drug to carrier proportion. This could be due to the effect of MCC on enhancing dissolution behavior. MCC has been shown to significantly improve the dissolution behavior of drugs from PMs and SDs (Barzegar-Jalali *et al.*, 2014; Chowdary and Rao, 2000)

Fig 3.19 shows the *in vitro* dissolution profiles of the eight formulations. Four of the formulations containing the higher amount of carrier proportions (OF3, OF4, OF6 and OF8) have released more than 80% of the drug meeting the pharmacopeial requirement which states that not less than 80% of the label claim of ABZ tablet should be released in 30 min (USP30-NF25, 2007).

Table 3. 9: Characterization of SD tablets.

Formulation	Hardness	Friability (%)	Disintegration time (min)	Amount of ABZ released (%)	
				10 min	30 min
OF1	59.00 ±1.63	1.03 ± 0.02	3.17 ± 0.11	52.15 ± 1.87	73.19 ± 1.04
OF2	72.67 ± 1.25	0.86 ± 0.04	3.54 ± 0.13	51.38 ± 2.06	71.11 ± 1.99
OF3	71.67 ± 1.70	0.89 ± 0.03	4.91 ± 0.11	56.96 ± 1.08	80.09 ±1.93
OF4	97.00 ± 3.56	0.58 ± 0.02	5.70 ± 0.23	57.33 ± 0.60	82.19 ± 2.11
OF5	83.33 ± 2.05	0.74 ± 0.02	5.61 ± 0.08	47.25 ± 1.33	72.19 ± 1.73
OF6	95.00 ± 3.27	0.54 ± 0.02	6.21 ± 0.16	44.30 ± 1.80	71.08 ± 2.02
OF7	108.00 ± 4.32	0.49 ± 0.02	6.60 ± 0.08	52.90 ± 0.70	80.26 ± 1.66
OF8	129.67 ± 3.40	0.20 ± 0.01	7.28 ± 0.16	51.21 ± 1.10	83.02 ± 2.80

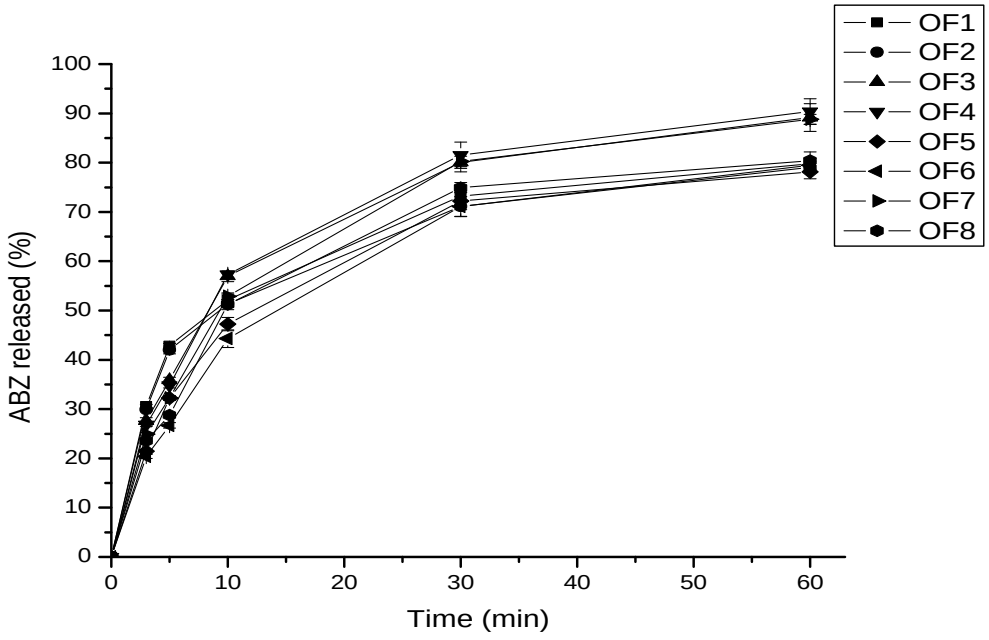

Figure 3. 21: Dissolution profiles for optimizing ABZ SD tablet formulation.

The drug release data obtained after the *in vitro* release study of the eight formulations was further analyzed by various kinetic models. The models included zero-order, first-order, Higuchi, and Hixson Crowell model. The model that best fitted the release data was selected based on the correlation coefficient (R^2) values of the various models, i.e., the model that gave the highest 'R^2' value was considered the best fit for the release data.

Table 3. 10: Rate constants and correlation coefficients of the fits of different drug release kinetic models for ABZ SD tablets.

Formulation	Zero order		First order		Higuchi equation		Hixson-crowell	
	Slope	R^2	Slope	R^2	Slope	R^2	Slope	R^2
OF1	-4.157	0.679	-0.024	0.860	0.100	0.901	-0.044	0.806
OF2	-4.055	0.678	-0.023	0.855	0.097	0.900	-0.042	0.802
OF3	-4.655	0.701	-0.031	0.889	0.110	0.915	-0.053	0.835
OF4	-4.955	0.723	-0.034	0.895	0.117	0.922	-0.057	0.845
OF5	-4.504	0.754	-0.024	0.880	0.105	0.939	-0.045	0.843
OF6	-4.695	0.797	-0.026	0.919	0.107	0.959	-0.048	0.883
OF7	-5.125	0.769	-0.035	0.930	0.118	0.946	-0.059	0.885
OF8	-5.249	0.770	-0.036	0.904	0.124	0.942	-0.061	0.867

As shown in Table 3.10, all the formulations exhibited best fit for Higuchi equation with R^2 values greater than 0.909. To find out the mechanism of drug release, the first 60% drug release data was fitted in Korsmeyer-Peppas model. The Korsmeyer-Peppas equation is used to analyse the release of pharmaceuticals from polymeric dosage forms, when the release mechanism is not well known or when more than one type of release phenomena could be involved (Costa and Sousa Lobo, 2001). The mechanism is determined by n value, for cylindrical tablets; n = 0.45 corresponds to Fickian diffusion, $0.45 < n < 0.89$ to non-Fickian (anomalous) transport, n = 0.89 to case-II transport and n > 0.89 to super case II transport (Singhvi and Singh, 2011). Table 3.11 shows the n values and R^2 of the Korsmeyer-Peppas model of the various formulations.

Table 3. 11: Drug release mechanism of the optimized formulations using Korsmeyer-Peppas model.

Formulation	K	n	R^2
OF1	19.84	0.433	0.945
OF2	19.20	0.441	0.947
OF3	13.97	0.605	0.995
OF4	13.37	0.631	0.999
OF5	10.78	0.651	0.989
OF6	10.11	0.643	0.999
OF7	12.16	0.631	0.991
OF8	11.26	0.650	0.992

As shown in Table 3.11, the n value for OF1 and OF2 is less than 0.45 indicating the drug release from these formulations is rapid and follows Fickian diffusion mechanism. For the remaining formulations, the n value was found to be between 0.45 and 0.89 which shows the anomalous mechanism of drug release.

3.7.3. Model selection

Analysis of variance for selected factorial models (Table 3.12) displays statistics such as P-value, multiple correlation coefficient (R^2), adjusted multiple correlation coefficient ("adj $R^{2"}$) and Predicted R-squared ("pred $R^{2"}$) values, provided by Design-Expert® 9.0.6 software. The best fitting mathematical model was selected based on comparisons of these statistical parameters.

As shown in Table 3.12, for ABZ released within 10 min the selected model is RMain effect with R^2 value of 0.9509, which shows that 95.09% of the variability in response could be explained by the model and there is only 4.91% of the total variation which cannot be explained by this model. The "pred R^2", 0.8743 is in reasonable agreement with the "adj R^2" of 0.9313.

Table 3. 12: Statistical parameters for selection of response model.

Response	Source	R-Squared	Adjusted R-Squared	Predicted R-Squared	Adeq. Precision
ABZ released within 10 min	RMain effects	0.9509	0.9313	0.8743	16.06
ABZ released within 30 min	RMain effects	0.9509	0.9428	0.9128	15.25
Angle of repose	RMain effects	0.9757	0.9659	0.9377	22.49
Hardness	R2FI	0.9988	0.9957	0.9808	55.31
Friability	R2FI	0.9993	0.9977	0.9895	76.32

Similarly, the selected model for ABZ released within 30 min and angle of repose is RMain effect. The R^2 values were found to be 0.9509 and 0.9757, respectively which all indicate the goodness of fit of the model. Furthermore, the pred R^2 is in reasonable agreement with adj R^2 for the two responses, the difference being less than 0.2 (Table 3.12). Thus based on the results of these statistical parameters it can be concluded the Rmain effect model could explain the relationship between the independent variables and these responses.

Reduced 2FI was the model selected for hardness and friability with R^2 of 0.9988 and 0.9993, respectively, demonstrating that 99.88% of the variability in hardness and 99.93% of the variability in friability could be well explained by the model. As shown in Table 3.12 there was also agreement between pred R^2 and adj R^2 values for both hardness and friability.

3.7.4. Model adequacy checking

ANOVA is the most important tool for the evaluation of significance and goodness of fit of the regression model and significance of individual model coefficients (Noordin *et al.*, 2004). Thus ANOVA tables were applied to summarize the test for significance of the selected models and model coefficients for the respective responses (ABZ released within 10 min, ABZ released within 30 min, hardness, friability and angle of repose). The regression model and the terms in the model are considered to be significant when a *p*-value is less than 0.05.

Table 3.13 depicts that the RMain effect model for ABZ released within 10 min and the terms in the model are statistically significant (p = 0.0005). In addition the Model F-value of 48.42 implies the model is significant. There is only a 0.05% chance that an F-value this large could occur due to noise. A-compression force (p = 0.0011) and C-carrier/ratio (p = 0.0008) are the significant model terms found to affect the response. On the other hand the statistically significant model term for ABZ released within 30 min was found to be only the C-carrier/drug ratio (p < 0.0001) (Table 3.13). The Model F-value of 116.29 implies the model is significant. There is only a 0.01% chance that an F-value this large could occur due to noise.

Table 3. 13: Summary of ANOVA results of response surface RMain effect model for ABZ released within 10min and ABZ released within 30 min.

Response	Source	Sum of Squares	df	Mean square	F-value	p-value	Remark
ABZ released within	Model	129.38	2	64.69	48.42	0.0005	Significant
10 min	A-CF	61.05	1	61.05	45.70	0.0011	Significant
	C-Carrier/drug	68.33	1	68.33	51.14	0.0008	Significant
	Residual	6.68	5	1.34			
	Cor Total	136.06	7				
ABZ released within	Model	180.41	1	180.41	116.29	<0.0001	Significant
30 min	C-Carrier/drug	180.41	1	180.41	116.29	<0.0001	
	Residual	9.31	6	1.55			
	Cor Total	189.71	7				

As shown in table 3.14, the selected model (RMain effect) for angle of repose was significant (p < 0.0001). The Model F-value of 100.24 implies the model is significant and there is only a 0.01% chance that an F-value this large could occur due to noise. The significant model terms for angle of repose includes B-percent of MCC (P < 0.0001) and C-Carrier/ratio (p = 0.0007).

Table 3. 14: Summary of ANOVA results of response surface RMain effect model for angle of repose.

Response	Source	Sum of Squares	df	Mean square	F-value	p-value	Remark
Angle of Repose	Model	30.25	2	15.12	100.24	<0.0001	Significant
	B- Concentration of MCC	21.95	1	21.95	145.46	<0.0001	Significant
	C-Carrier/drug	8.30	1	8.30	55.03	0.0007	Significant
	Residual	0.75	5	0.15			
	Cor Total	31.00	7				

The significant model terms for hardness were found to be A-compression force (p = 0.0013) B-concentration of MCC (p = 0.0034), C-carrier/ratio (p = 0.0019), AC-interaction effect of compression force and carrier to drug ratio (p = 0.0349) and BC-interaction effect of concentration of MCC and carrier to drug ratio (p = 0.0347). The selected Reduced 2FI model F-value of 327.89 infers the model is significant. There is only a 0.30% chance that an F-value this large could occur due to noise. Similarly the selected Reduced 2FI model F-value of 611.52 for friability implies the model is significant and only a 0.16% chance that an F-value this large could occur due to noise. A-compression force (p = 0.0007) B- concentration of MCC (p = 0.0014), C-carrier/ration (p = 0.0013), AB-interaction effect of compression force and concentration of MCC (p = 0.0422) and BC-interaction effect of concentration of MCC and carrier to drug ratio (p = 0.0237) were found to be the significant model terms that affect friability (Table 3.15).

Table 3. 15: Summary of ANOVA results of surface response Reduced 2FI model for hardness and friability.

Response	Source	Sum of Squares	Df	Mean square	F-value	p-value	Remark
Hardness	Model	3606.45	5	721.29	327.89	0.0030	Significant
	A-CF	1679.97	1	1679.97	763.69	0.0013	Significant
	B-concentration of MCC	645.30	1	645.30	293.34	0.0034	Significant
	C-Carrier/drug	1161.38	1	1161.38	527.94	0.0019	Significant
	AC	59.68	1	59.68	27.13	0.0349	Significant
	BC	60.12	1	60.12	27.33	0.0347	Significant
	Residual	4.40	2	2.20			
	Cor total	3619.67	7				
Friability	Model	0.50	5	0.097	611.52	0.0016	Significant
	A-CF	0.24	1	0.24	1486.23	0.0007	Significant
	B- concentration of MCC	0.12	1	0.12	723.77	0.0014	Significant
	C-Carrer/drug	0.13	1	0.13	784.64	0.0013	Significant
	AC	3.613E-003	1	3.613E-003	22.23	0.0422	Significant
	BC	6.613E-003	1	6.613E-003	40.69	0.0237	Significant
	Resdual	3.250E-004	2	1.625E-003			
	Cor Total	0.50	7				

Plots related to residuals: the normal probability plot of residuals and the plot of internally studentized residuals versus predicted values were considered as additional tests of model adequacy checking tools. Thus the normal probability plots of the residuals and the plots of the residuals versus the predicted response for the different responses including ABZ released within 10 min, ABZ released within 30 min, Angle of repose, hardness and friability are shown in Figs 3.20 to 3.29.

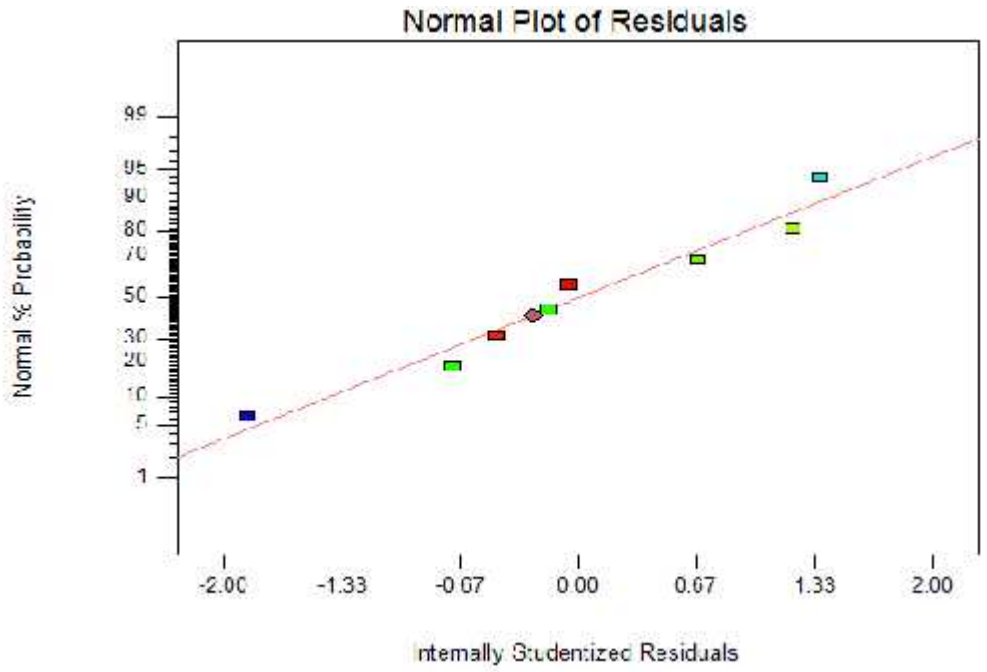

Figure 3. 22: Normal probability plot of residuals of ABZ released within 10 min.

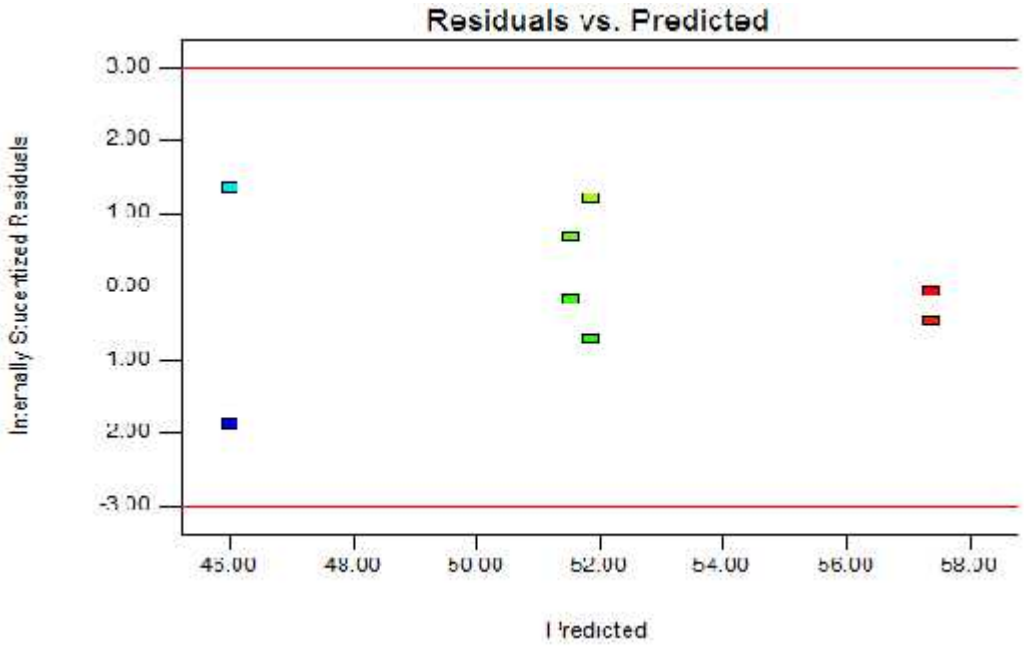

Figure 3. 23: Plots of the residuals against predicted response of ABZ released within 10 min.

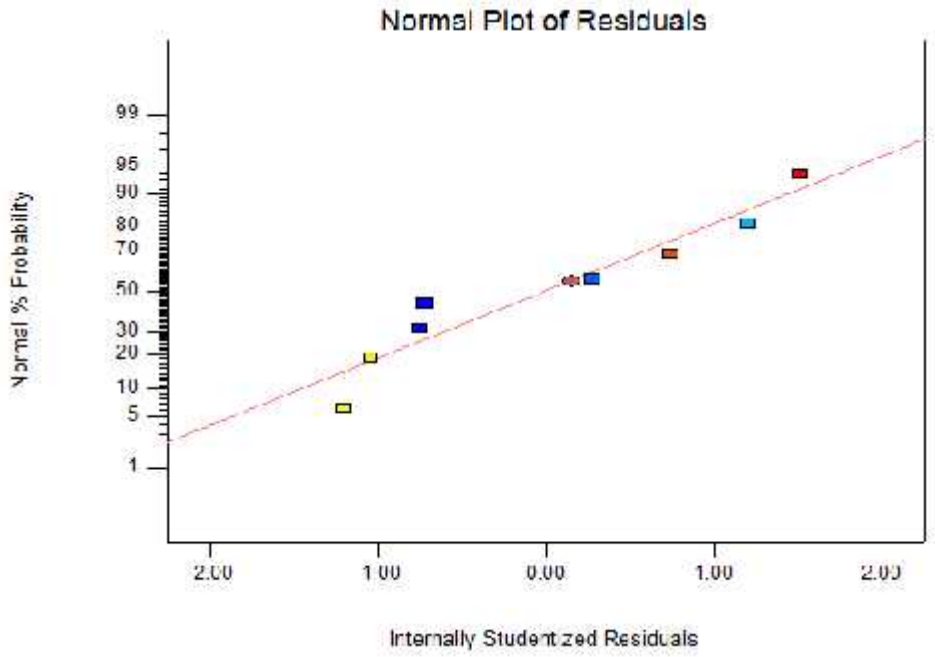

Figure 3. 24: Normal probability plot of residuals of ABZ released within 30 min.

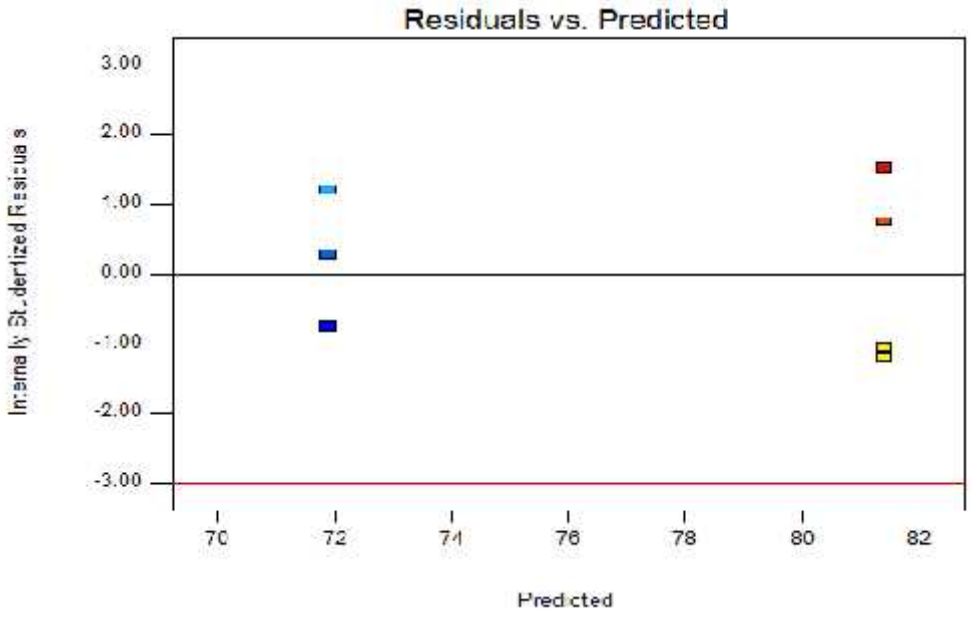

Figure 3. 25: Plots of the residuals against predicted response for ABZ released within 30 min.

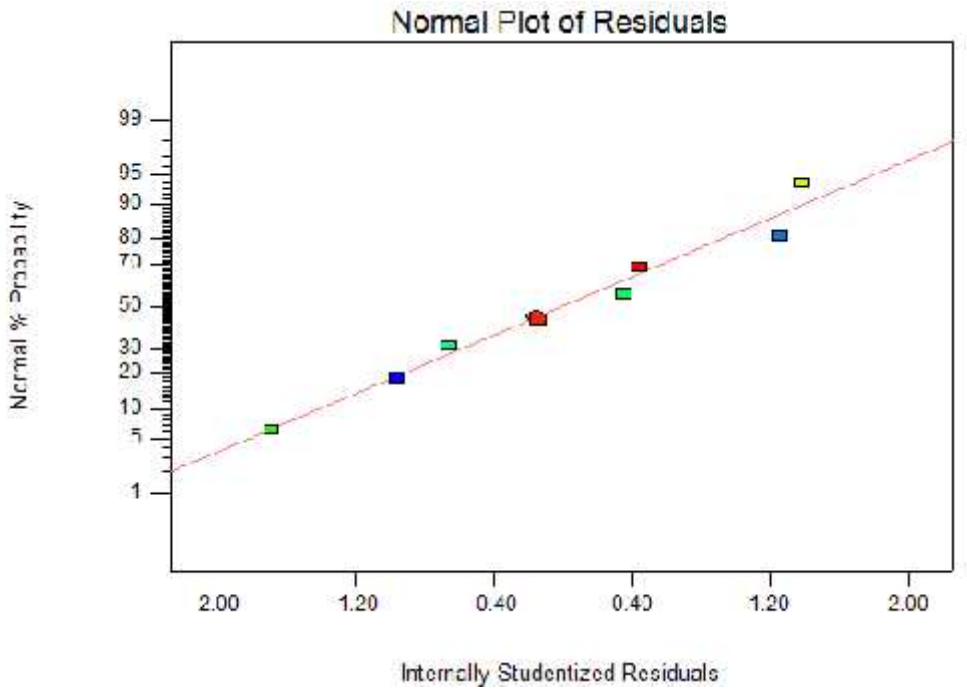

Figure 3. 26: Normal probability plot of residuals for angle of repose.

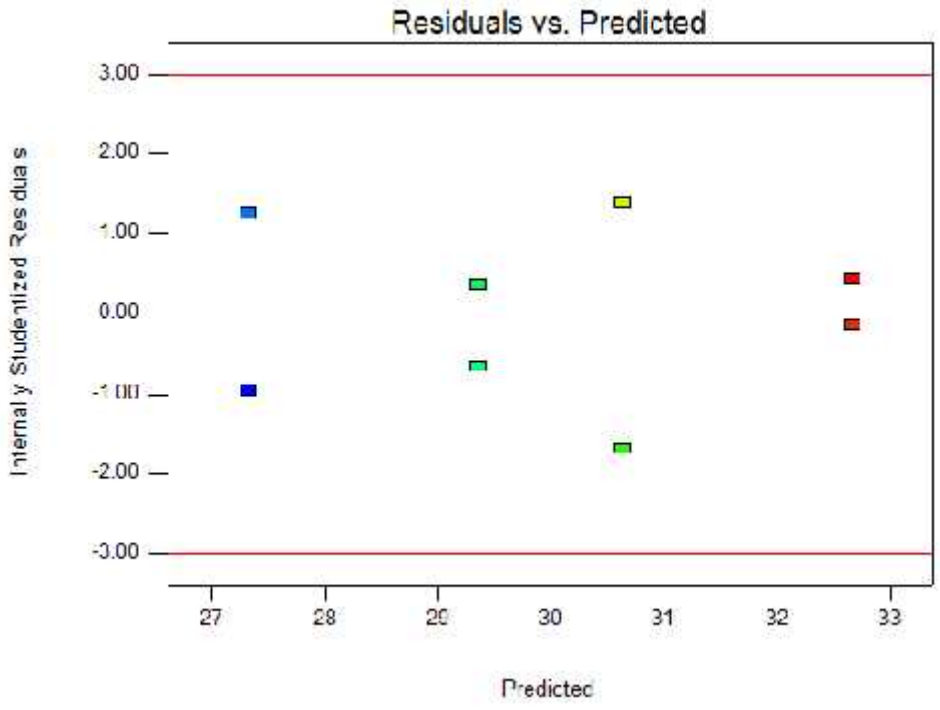

Figure 3. 27: Plots of the residuals against predicted response for angle of repose.

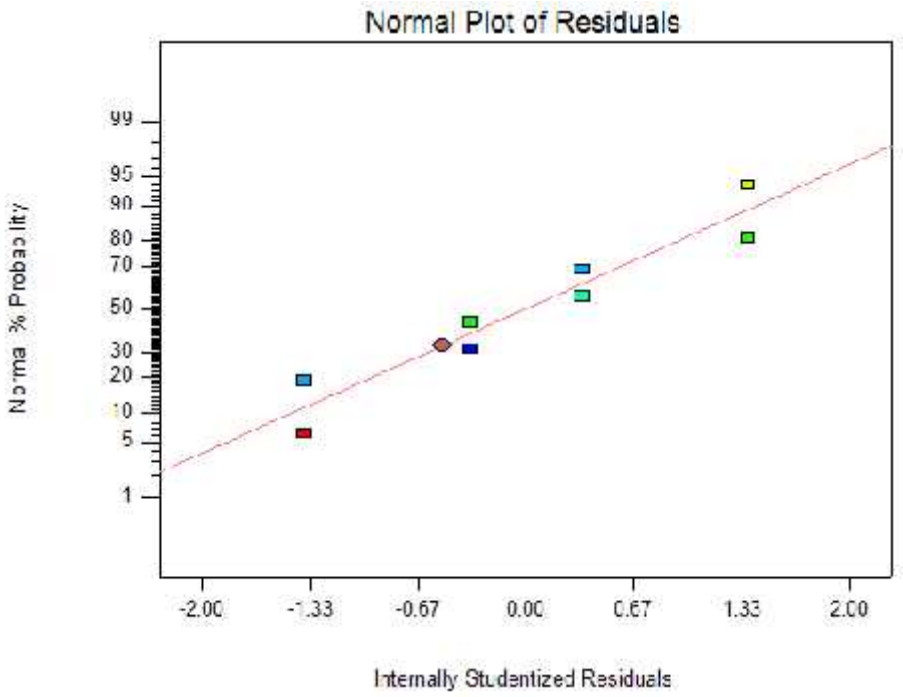

Figure 3. 28: Normal probability plot of residuals for hardness.

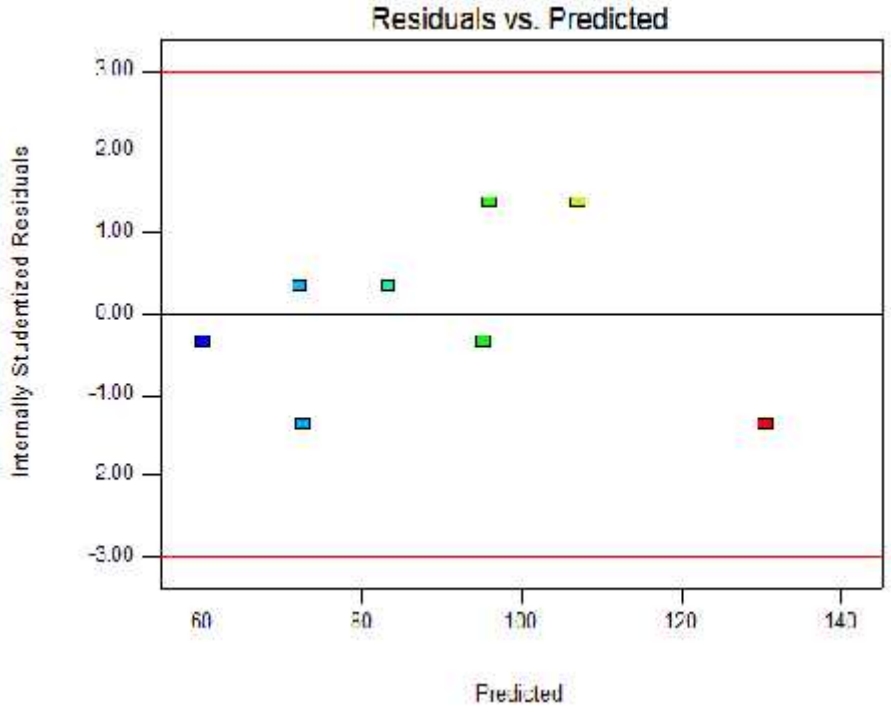

Figure 3. 29: Plots of the residuals against predicted response for hardness.

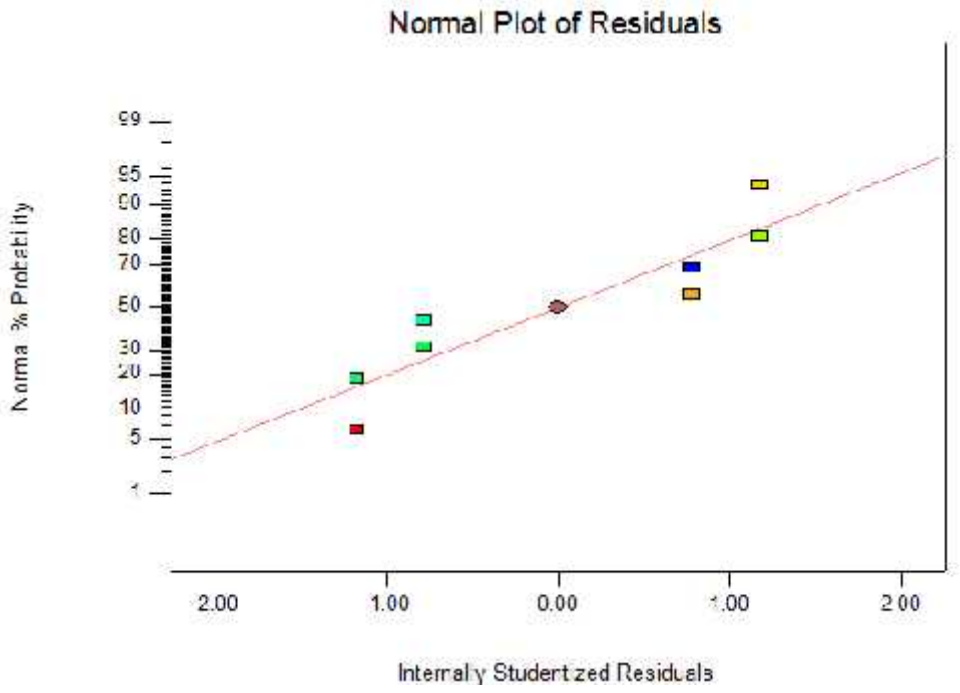

Figure 3. 30: Normal probability plot of residuals for friability.

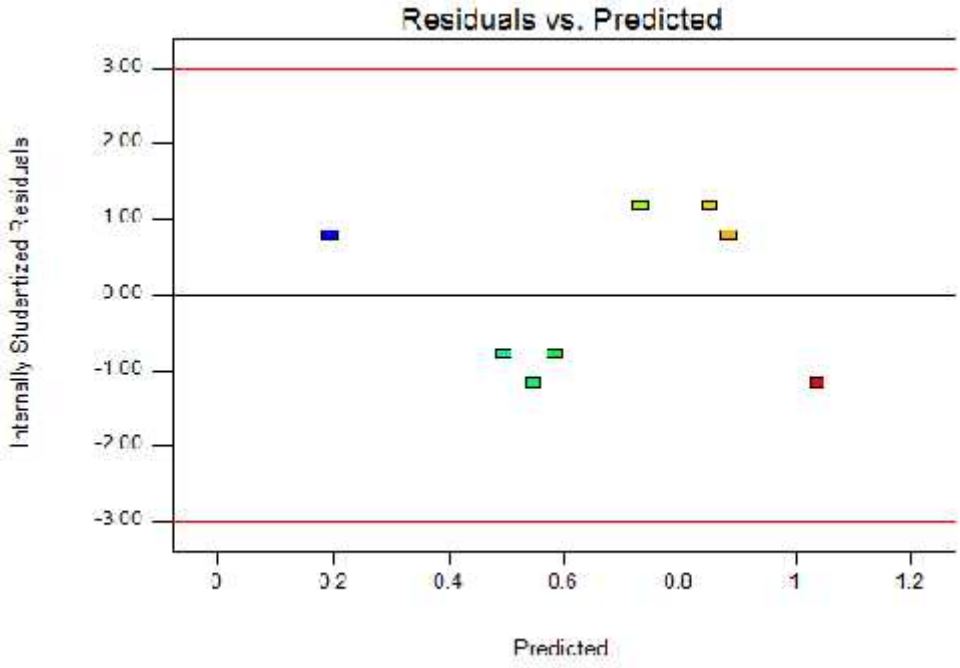

Figure 3. 31: Plots of the residuals against predicted response for friability.

The results in the normal probability plots of the residuals (Fig. 3.20, 3.22, 3.24, 3.26, 3.28) indicate that the residuals can be considered to fall on a straight line implying that the errors follow a normal distribution for all responses. Plots of the residuals versus the predicted response (Fig. 3.21, 3.23, 3.25, 3.27, 3.29) displayed that points are randomly scattered, with no obvious pattern or structure, and all values lie within the recommended range of −3 and +3 (values between −3 and +3 are considered as the top and bottom outlier detection limits). The equal scatters of the residual data above and below the x-axis indicate that the variances were independent of the value of the responses which again support the assumptions of the model. Hence, the models were used for further analysis. The final mathematical regression models in terms of coded factors (Equation 3.4 - 3.8) were developed using model term coefficients.

ABZ released within 10 min = + 51.69 - 2.76*A + 2.92*C Eq. 3.4

ABZ released within 30 = +76.64 + 4.75* C Eq. 3.5

Angle of repose = + 30.00 -1.66 * B -1.02* C Eq. 3.6

Hardness = + 89.51 + 14.49 * A + 8.98* B + 12.05* C + 2.73 * AC + 2.74* BC Eq. 3.7

Friability = + 0.67 - 0.17 * A - 0.12* B - 0.13* C - 0.02* AC - 0.03* BC Eq. 3.8

Where, A is compression force, B is concentration of MCC and C is carrier/ratio

Positive sign before a factor in polynomial equations represent that the response increases with the factor. On the contrary, a negative sign means the response and factors have reciprocal relation. The negative sign before the factor compression force (A) shows that compression force has decreased the amount of ABZ released within 10 min (Equation 3.4). Conversely, as shown in Equations 3.4 and 3.5 the carrier to drug ratio has a positive effect on amount of ABZ released within 10 and 30 min, the magnitude of the coefficient being higher for the amount of ABZ released within 30 min. The positive sign of the coefficients indicate increasing carrier concentration increases the amount of drug released.

Concentration of MCC (B) and carrier to drug ratio (C) are the two parameters that negatively affect the angle of repose (Equation 3.6). The magnitude of coefficient of concentration of MCC was found to be higher than carrier to drug ratio for the response, indicating the stronger effect of MCC on flow property.

From Equations 3.7 and 3.8, it can be observed that compression force (A), Concentration of MCC (B), carrier to drug ratio (C), interaction effect of compression force and carrier to drug ratio (AC) and interaction effect of concentration of MCC and carrier to drug ratio (BC) have a significant effect on tablet hardness and friability. As indicated by the sign of the coefficients, all the factors have positive effect on hardness and negative effect on friability. The compression force (A) was the strongest factor for both hardness (+14.49) and (-0.17) friability.

3.7.5. Contour plot and surface response analysis

The regression models developed are represented in contour and response surface plots, used to characterize the response surface graphically and determine the optimal parameter-setting (Tsai *et al.*, 2010). The contour plot is a two dimensional (2D) representation of the response across the factors displayed on an axis and response surface plot is a three dimensional (3D) Surface plot which is a projection of the contour plot giving shape in addition to the color and contour.

The combined effect of carrier to drug ratio and compression force on the amount of ABZ released within 10 min is shown in Figs 3.30 (A) and (B). The diagonal parallel lines in Fig. 3.30 (A) indicate that there is no interaction effect of compression force and carrier to drug ratio on the amount of ABZ released. The non-twisted response surface in Fig.3.30 (B) also indicates that there was no interaction effect of the two parameters on the amount released.

However, the plots show that the linear model components individually affect the amount released significantly, with the effect of compression force being pronounced. This result confirms what has been found in the ANOVA (Table 3.13), where compression force showed more significant effect ($p < 0.0001$) than carrier to drug ratio ($p = 0.0001$) on the amount of ABZ released.

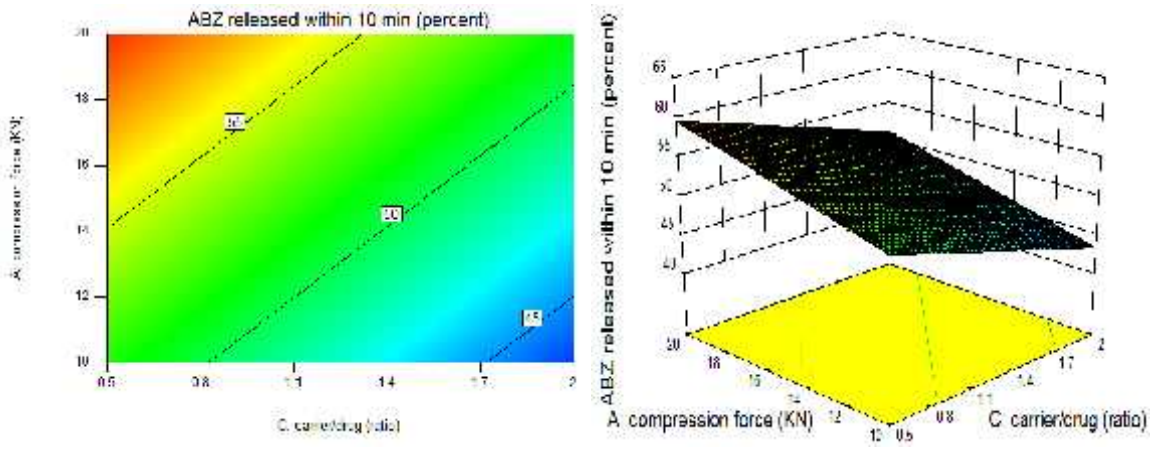

(A) **(B)**

Figure 3. 32: A: Contour; B: Surface response plot of compression force and carrier to drug ratio on ABZ released within 10 min.

Figs 3.31 (A) and (B) show the combined effect of compression force and carrier to drug ratio on the amount of ABZ released within 30 min. The vertical parallel straight lines in Fig 3.31 (A) and the non-twisted response surface in Fig 3.31 (B) show that carrier to drug ratio is the only factor that affects amount of ABZ released within 30 min. Compression force has no effect on amount of ABZ released within 30 min, which was not the case for the amount ABZ released within 10 min, that could be due to a lag time period resulting from tablet disintegration.

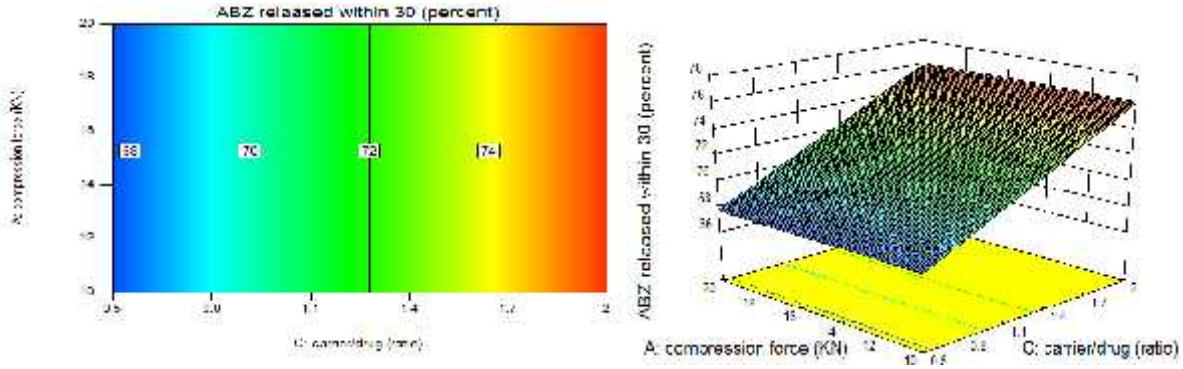

(A) **(B)**

Figure 3. 33: A: Contour B: Surface response plot of compression force and carrier to drug ratio on ABZ released within 30 min.

The 2D contour plot and surface response plot for angle of repose is displayed in Fig 3.32, demonstrating the combined effect of concentration of MCC and carrier to ratio on the response. The diagonal parallel lines in the contour plot (Fig 3.32 A) indicate that there is no interaction effect of concentration of MCC and carrier to drug ratio on angle of repose. However the linear model components individually affect the response significantly, with a relatively more significant effect of concentration of MCC than carrier to drug ratio. According to Fig. 3.32, the lowest value of angle of repose was found at the highest level of carrier to drug ratio and concentration of MCC.

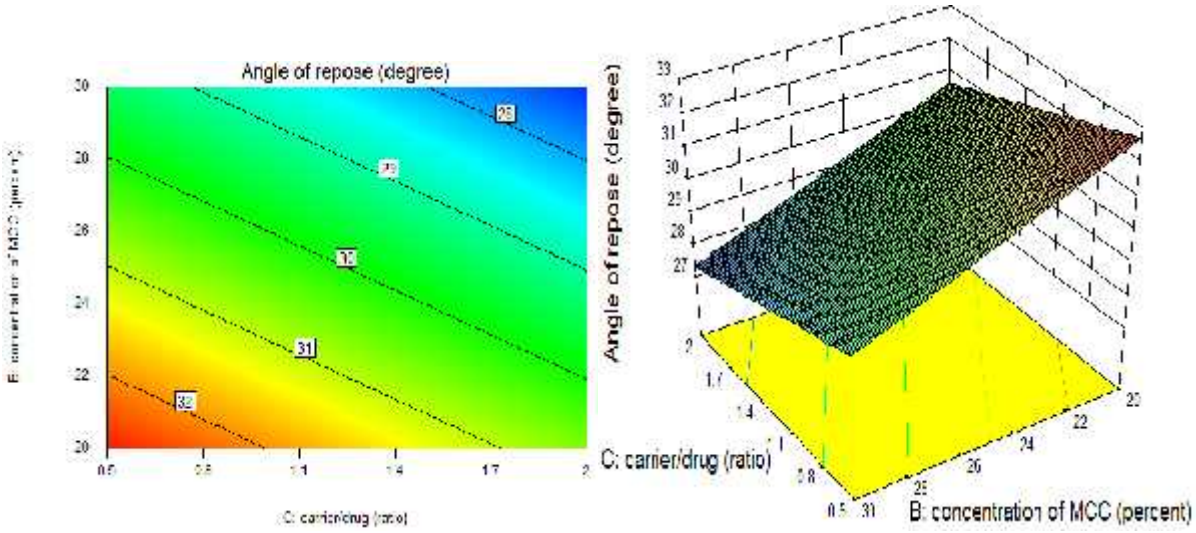

(A) (B)

Figure 3. 34: A: Contour B: Surface response plot of carrier to drug ratio and concentration of MCC on angle of repose.

Figs 3.33 (A) and (B) show the combined effect of the two selected factors, compression force (p = 0.0013) and carrier to drug ratio (p = 0.0019) on hardness. The two factors were selected based on their significance and the third significant factor concentration of MCC (p = 0.0034) was kept at level zero (that is mid-point). Likewise the two significant factors for friability was also selected based on the ANOVA result (Table 3.15), compression force (0.0007) and carrier to drug ratio (0.0013) than the third factor concentration of MCC (0.0014). For both the responses, in addition to the individual significant effect, a significant interaction effect between compression force and carrier to drug ratio was observed in the contour plots (Figs 3.33 and 3.34

A) characterized by formation of elliptical contours (Zhao *et al.*, 2012). The highest level of compression force and carrier to drug ratio resulted in the hardest tablets with lowest amount of percent friability (Figs 3.33 and 3.34).

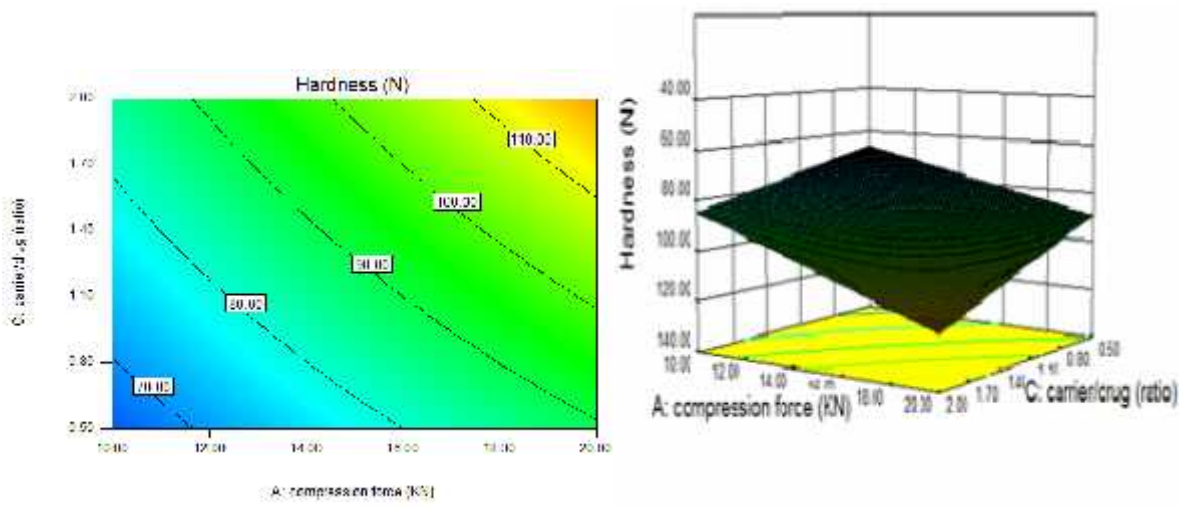

(A) **(B)**

Figure 3. 35: A: Contour B: Surface response plot of compression force and carrier to drug ratio on hardness.

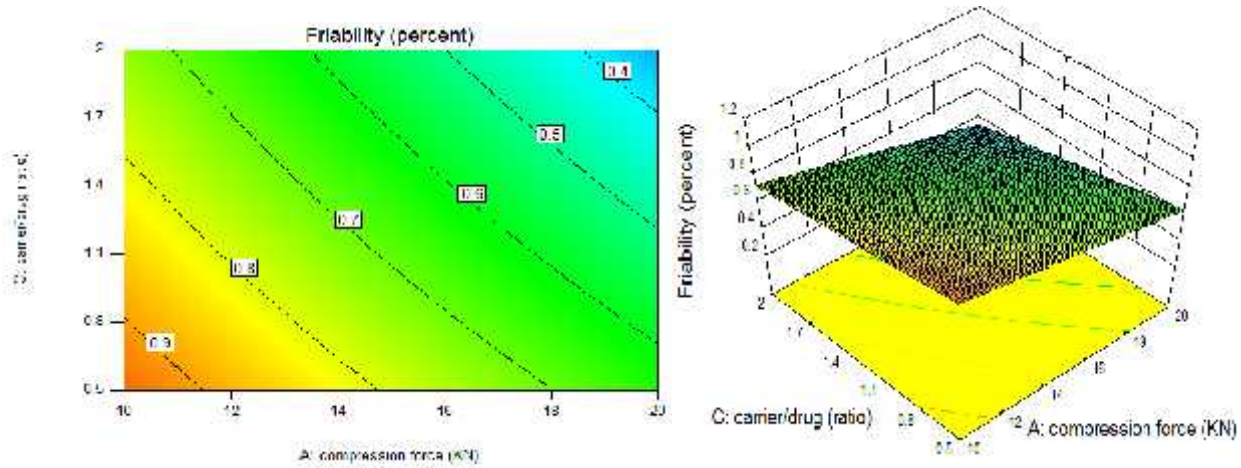

(A) **(B)**

Figure 3. 36: A: Contour B: Surface response plot of compression force and carrier to drug ratio on friability.

3.7.6. Simultaneous optimization of the response variables

Numerical and graphical optimization techniques provided by Design-Expert 9.0.6 was used to obtain the final optimal experimental parameters that optimize the five responses simultaneously by sustaining the requirement for all the responses. The criteria defined for factors and responses during optimization by both techniques are presented in Table 3.16.

Table 3. 16: Criterion settings of factors and responses for optimization by numerical and graphical optimization.

	Upper limit	Lower limit		
Factors				
Compression force	20	10		
Carrier/drug	2	0.5		
Concentration of MCC	30	20		
	Goal	Upper limit	Lower limit	Importance
Responses				
ABZ released within 10 min	Range	100	50	3
ABZ released within 30 min	Range	100	80	5
Angle of repose	Range	30	25	5
Hardness	Range	100	70	5
Friability	Range	1	0	5

3.7.6.1. Numerical optimization

The desirability function approach is one of the most widely used methods for optimization of multiple responses (Raissi and Farsani, 2009). Thus a numerical optimization technique based on the desirability function approach was employed to develop a new formulation. This function searches for a combination of factor levels that jointly optimize a set of responses by supporting the requirements for each. The predicted optimum values and the corresponding levels of parameters are shown in Fig. 3.35 in which the best solution is indicated by a highlighted point.

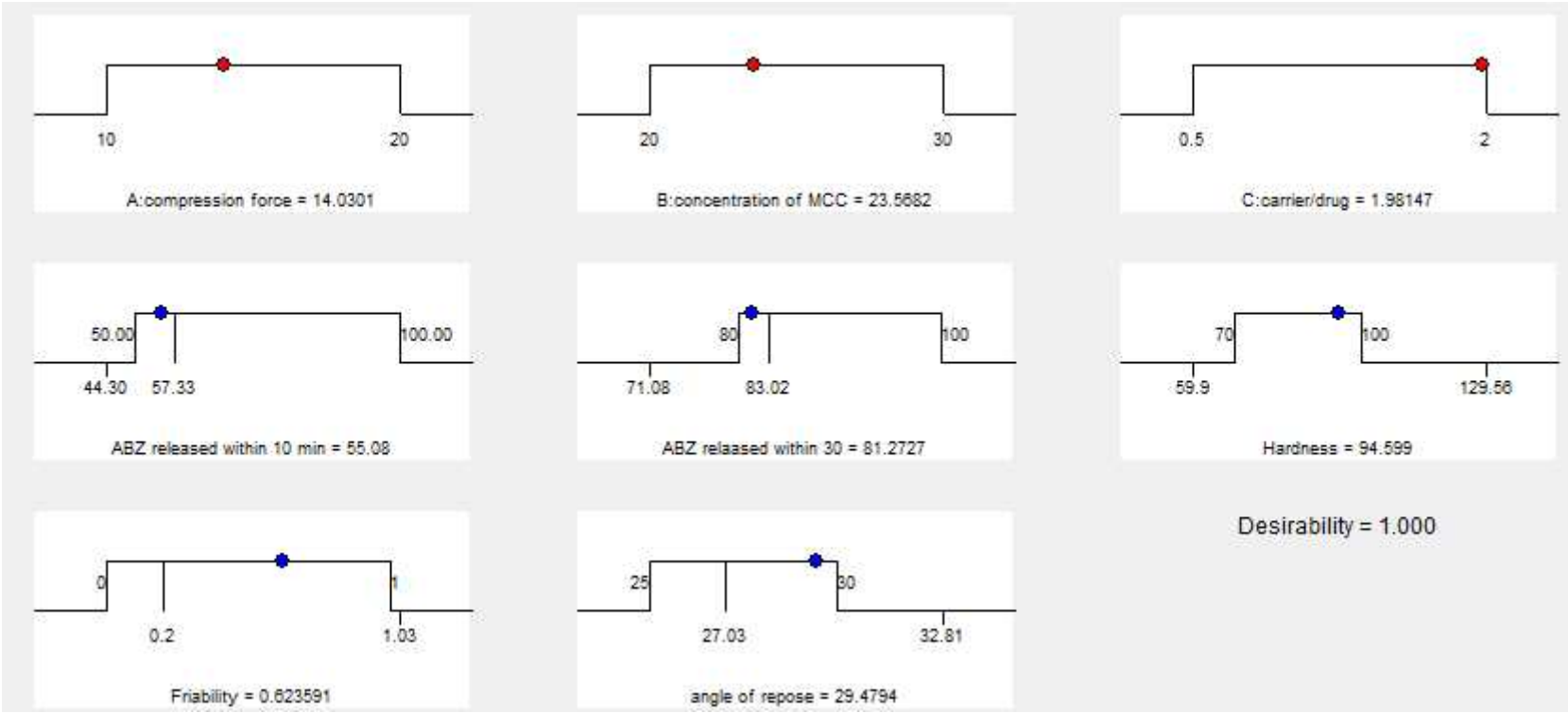

Figure 3. 37: Graphical representation of the constraints accepted for the determination of global desirability and obtained optimal conditions.

As shown in Fig. 3.35 the optimal points for the responses were found to be 55.09% for the amount of ABZ released within 10 min, 81.27% for amount of ABZ released within 30 min, 29.48° for angle of repose, 94.60 N for hardness and 0.62% for friability when the factors are set at compression force of 14.03 KN, carrier to drug ratio of 1.98 and concentration of MCC of 23.57%.

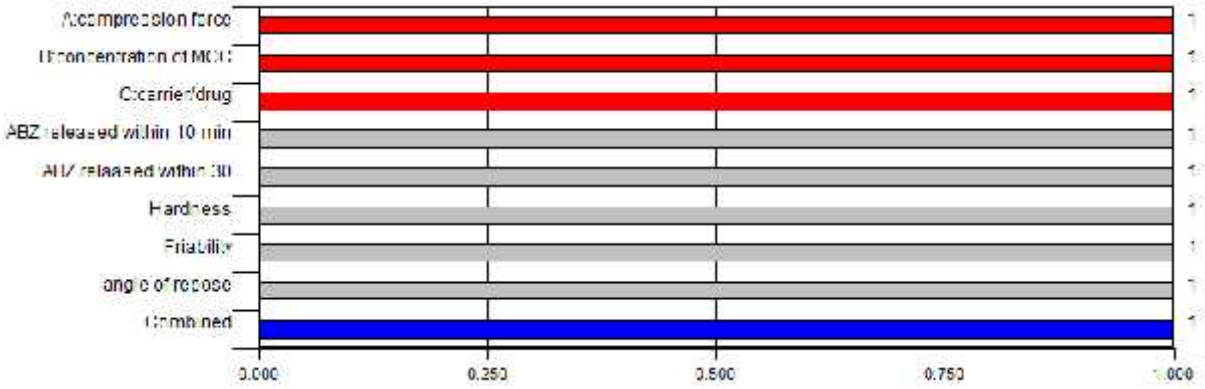

Figure 3. 38: Bar graph showing individual desirability values (di) of various objective responses.

As shown in Fig. 3.36, the individual desirability functions (di) of the responses were found to be 1. Desirability function ranges from zero to one (least to most desirable, respectively) (Raissi and Farsani, 2009). Thus, the individual desirability functions (di) of the responses indicate that, fully desired responses were achieved for all the responses. The global desirability function (D) was then obtained from the individual desirability functions to be 1.00 from the software solver calculated based on equation 3.9.

$$D = (d_1^{r_1} \times d_2^{r_2} \times \ldots \times d_i^{r_i})^{1/\sum r_i} \qquad \text{Eq. 3.9}$$

Where i is the number of responses, di the individual desirability functions and r_i is the relative importance of i^{th} response which varies from the least important (+), a value of 1, to the most important (+++++) a value of 5.

For better visualization of the results, the global desirability function D is presented in the form of a three dimensional plots (Figs 3.37 A - C). The third factor was set up at the optimum constant level.

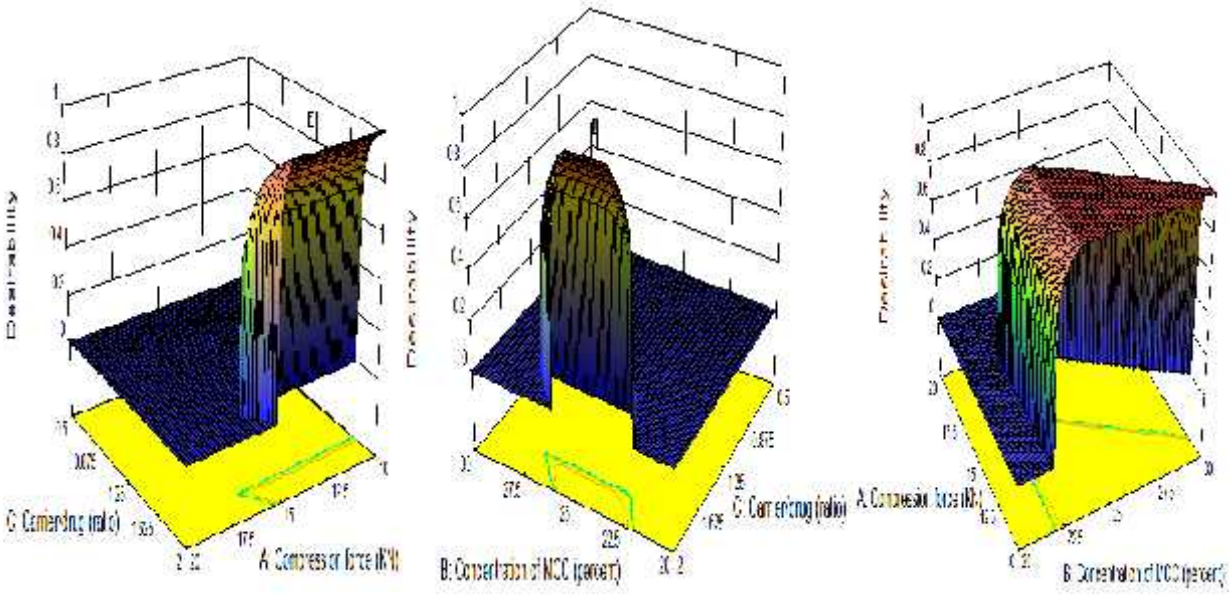

(A) **(B)** **(C)**

Figure 3. 39: Three dimensional graphs: (A) D = *f* (carrier to drug ratio, compression force) with concentration of MCC held at 23.57%; (B) D = *f* (concentration of MCC, carrier to drug ratio) with compression force held at 14.03 KN; (C) D = *f* (compression force, concentration of MCC) with carrier to drug ratio held at 1.98.

3.7.6.2. Validation of optimum formulation

Validation is intended to be used to confirm that the model can predict actual outcomes at the optimal settings determined from the analysis. Three batches of ABZ tablets were prepared according to the optimized formulation. Thus, ABZ SD was prepared in1:1.98:0.1 ABZ: PEG : polysorbate 80 proportion using kneading method and experiments were carried out at the optimal combinations of the other factors including compression force of 14.03 KN, and concentration of MCC of 23.57%. Then the amount of drug released within 10 and 30 min, angle

of repose, hardness and friability were determined (Table 3.17). The average results of the three batches were compared to the predicted values.

Table 3. 17: Experimentally prepared formulations based on the predicted values and evaluation of the various responses.

Responses	Predicted value	Experimental value	Percentage error
ABZ released within 10 min (percent)	55.08	53.79 ± 1.25	2.34%
ABZ released within 30 min (percent)	81.27	80.09 ± 0.67	1.45%
Angle of repose (degree)	94.60	90.67 ± 1.70	1.83%
Hardness (KN)	29.48	28.84 ± 0.61	4.15%
Friability (percent)	0.62	0.60 ± 0.02	3.23%

From the results presented in Table 3.17, the values of percentage errors falling below 5%, showed that the experimental values of the optimized formulations agreed well with the predicted value. The good correlation between predicted and experimental values justified the validity of the response model. The optimized formulations were further evaluated for different characteristics as shown in Table 3.18. Powder characterization of the optimized SD powder mixtures showed excellent flow property with Hausenr ratio and Carr's index value of 1.08 ± 0.02 and 9.01 ± 0.01, respectively. Percentage drug content was found to be 95.84 ± 3.40 % which lies within the range (not less than 90 percent and not more than 110 percent) (USP30-NF25,2007), indicating that the drug was uniformly distributed throughout the prepared formulations. Percent yield of the SD was also determined and found to be 96.69 ± 2.25.

Table 3. 18: Characteristic properties of optimized ABZ SD powder mixture and tablet.

parameters	Experimental values
Flow rate (g/sec)	4.68 ± 0.15
Hausenr ratio	1.08 ± 0.02
Carr's index (%)	9.010 ± 0.01

Yield (%)	96.69 ± 2.25
Drug content (%)	95.84 ± 3.4
Disintegration (min)	5.91 ± 0.14

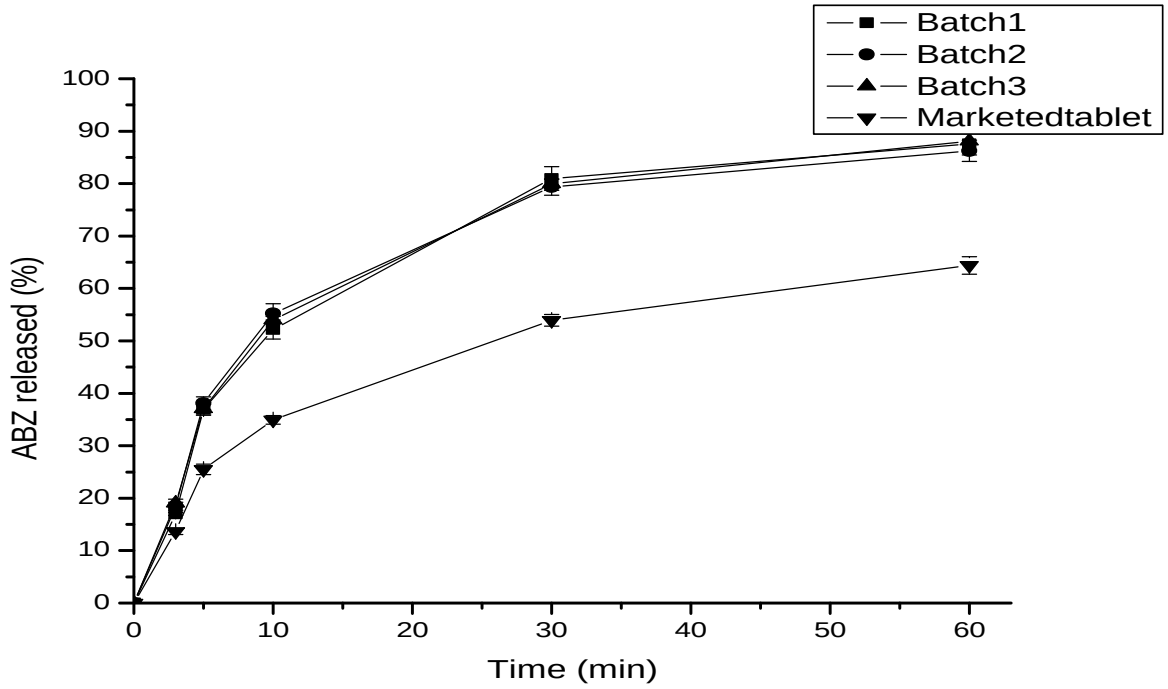

Figure 3. 40: Dissolution profiles of the three batches of the optimized ABZ SD tablets and 200mg marketed tablet.

As shown in Fig. 3.38 the release profiles of the three batches were similar and there was no statistically significant difference ($p > 0.05$) which indicates that the optimal formulation could yield reproducible results. The release profiles of the optimized formulation of the three batches were compared with marketed tablet. As shown in Fig 3.38 the optimized ABZ SD tablet provided superior dissolution profile than the 200 mg marketed tablet.

As shown in Table 3.19 all the three batches showed the best fit for Higuchi equation with R^2 values of 0.948, 0.965 and 0.966 with anomalous mechanism of drug release. The average n value of the three batches (0.631) indicated the drug release mechanism is erosion controlled.

Table 3. 19: Drug release kinetic and mechanism of release from the three batches of the optimized formulation.

Batch	Zero order		First order		Higuchi matrix		Hixson crowel		Koresmeyer-Peppas		
	K	R^2	K	R^2	K	R^2	K	R^2	K	n	R^2
Batch 1	-5.004	0.748	-0.034	0.914	0.116	0.937	-0.058	0.868	12.72	0.632	0.948
Batch 2	-4.802	0.722	-0.032	0.902	0.113	0.924	-0.055	0.850	13.33	0.633	0.965
Batch 3	-4.951	0.745	-0.034	0.928	0.115	0.938	-0.058	0.877	13.15	0.628	0.969

4. CONCLUSION

This study has shown that the dissolution profile of ABZ is enhanced to a greater extent through SD technique. The type and proportion of the carriers used, the preparation method, and the presence of surfactant were the critical variables impacting dissolution profiles among formulations. The ternary system provided significantly higher percentage of drug release (up to 100%) than the corresponding binary systems (87.07%). Solvent evaporation system provided higher extent and rate of dissolution as compared to kneading method; the PEG containing SDs being higher than those containing PVP for both methods. In the kneading method of preparation, the highest drug release was observed for the SDs prepared with HPMC (88.8% released within 60 min) followed by PEG (81.4% released within 60 min). In all the formulations, increasing the proportion of the carriers resulted in enhanced dissolution profiles. Powder characteristics study (flow property and compressibility) showed that the SDs can be used for manufacturing of acceptable solid dosage forms.

In compression of SD tablets carrier to drug ratio, compression force and concentration of MCC were found to be the important factors influencing tablet properties such as hardness and friability as well as dissolution profiles. RSM based on 2^3 full factorial design provided an optimum tablet formulation and compression force which released 55.09% and 81.27% ABZ at 10 and 30 min, respectively. The responses obtained from the experiment were in close agreement with the predicted values for the optimized formulation. The dissolution profile of the tablets prepared exhibited superior dissolution profile (87.3% in 60 min) than 200 mg marketed tablet (64.4% in 60 min).

Results from FTIR spectroscopy revealed interaction trough hydrogen bonding between the drug and carriers employed. DSC thermograms of the PMs and SDs indicated decrease crystallinity and stabilized amorphous structure of the drug, ABZ. Therefore, based on these results it can be concluded that the practically insoluble drug ABZ can be formulated into a dosage form with the required dissolution profile using SD techniques.

5. SUGGESTIONS FOR FURTHER WORK

- Characterization of the SDs using X-ray Diffraction;
- Surface characterization of the formulations with Scanning Electron Microscope;
- Stability study; and
- In vivo evaluation of the formulation.

REFERENCES

AKILADEVI, D., SHANMUGAPANDIYANI, P., JEBASINGHI, D. & BASAK, S. 2011. Preparation and evaluation of paracetamol by solid dispersion technique. *Int J Pharm Pharm Sci.,* 3**,** 188-191.

ALANAZI, K. F., BADRY, E. M., AHMED, O. M. & ALSARRA, A. I. 2007. Improvement of albendazole dissolution by preparing microparticles using spray-drying technique. *Sci. Pharm.,* 75**,** 63-79.

ANKUSH, C., GEETA, A., FOZIYAH, Z. & VARINDER, K. 2011. Mini review: Journey of solid dispersion technique from bench to scale. *IRJP,* 2**,** 46-51.

ANUPAMA, S., SURINDER, G., BIRENDRA, S. & GOYAL, N. 2011a. Design, optimization, preparation and evaluation of solid dispersions of albendazole using factorial design. *Der Pharmacia Sinica,* 2**,** 30-42.

ANUPAMA, S., SURINDER, G., BIRENDRA, S. & GOYAL, N. 2011b. Formulation and optimization of solid dispersion tablets of albendazole using response surface methodology *RJPBCS,* 2**,** 740-754.

ARUNACHALAM, A., KARTHIKEYAN, M., ASHUTOSHKUMAR, S., MANIDIPA, S., KONAM, K., PRASAD, H. P., SETHURAMAN, S. & SENTHILRAJ, R. 2011. Preparation and invitro evaluation of solid dispersion of Proxicam with HPMCV K100M by using spray drying technique. *JGTPS,* 2**,** 43-54.

BAKSHI, S. K., VIVEK, K., VERMA, K. R., KRISHNA, B. M., NARRAVULA, S., SINGH, B. R. & SINGLA, K. A. 2012. Investigation on the impact of core and barrier layer compostion on the drug release from a triple layer tablet. *IJPSR.,* 3**,** 2168-2179.

BARZEGAR-JALALI, M., GHANBARZADEH, S., ADIBKIA, K., VALIZADEH, H., BIBAK, S., MOHAMMADI, G. & SIAHI-SHADBAD, R. M. 2014. Development and characterization of solid dispersion of piroxicam for improvement of dissolution rate using hydrophilic carriers. *BioImpacts.,* 4**,** 141-148.

BAS, D., ISMAIL, H. & BOYAC, H. I. 2007. Modeling and optimization I: Usability of response surface methodology. *J Food Eng.,* 78 836–845.

BEZERRAA, A. M., SANTELLI, E. R., OLIVEIRAA, P. E., VILLAR, S. L. & ESCALEIRAA, A. L. 2008. Response surface methodology (RSM) as a tool for optimization in analytical chemistry. *Talanta.,* 76**,** 965–977.

BISWAS, R. G. & MAITY, S. 2011. Solubility enhancement of poorly water soluble drug amoxycillin trihydtate by modified Gum Karaya using solid dispersion technique. *IJDFR.,* 2**,** 235-249.

BP 2000. British Pharmacopoeia. *Her majesty's stationary office.,* 1.

CASTRO, G. S., BRUNI, S. S., LANUSSE, E. C., ALLEMANDI, A. D. & PALMA, D. S. 2010. Improved albendazole dissolution rate in pluronic 188 solid dispersions. *AAPS PharmSciTech.,* 11**,** 1518-1525.

CAVALCANTI, T. C., SOUSA, D. G., TABOSA, M. A., SOBRINHO, S. L., LEAL, B. L. & SANTANA, P. D. 2012. Assay and physicochemical characterization of the antiparasitic albendazole. *Brazilian J Pharm Sci.,* 48**,** 281-290.

CHADHA, R., KAPOOR, K. V. & KUMAR, A. 2006. Analytical techniques used to characterize drug-polyvinylpyrrolidone systems in solid and liquid states-an overview. *J Sci Ind Res,* 65**,** 459-469.

CHAUHAN, B., SHIMPI, S. & PARADKAR, A. 2005. Preparation and characterization of etoricoxib solid dispersions using lipid carriers by spray drying technique. *AAPS Pharm SciTech,* 6 405-412.

CHHATER, S. & PRAVEEN, K. 2013. Solvent evaporation method for amorphous solid dispersions: Predictive tools for improve the dissolution rate of pioglitazone hydrochloride. *IJPCBS* 3 350-359.

CHOWDARY, K. P. & RAO, S. S. 2000. Investigation of dissolution enhancement of Itraconazole by solid dispersion in superdisintegrants. *Drug Dev Ind Pharm.,* 26**,** 1207-1211.

CHOWDARY, R. P., SHANKAR, R. K. & SUBBALAKSHMI, M. 2014. Recent research in solid dispersions – a review. *JGTPS,* 5**,** 1612-1623.

COSTA, P. & SOUSA LOBO, M. J. 2001. Modeling and comparison of dissolution profiles. *Eur J Pharm Sci.,* 13**,** 123–133.

DABBAGH, A. M. & TAGHIPOUR, B. 2007. Investigation of solid dispersion technique in improvement of physicochemical characteristics of ibuprofen powder. *IJPS,* 3**,** 69-76.

DASH, S., MURTHY, N. P., NATH, L. & CHOWDHURY, P. 2010. Kinetic modeling on drug release from controlled drug delivey system. *Acta Poloniae Pharmaceutica - Drug Research.,* 67**,** 217-223.

DAYAN, D. A. 2003. Albendazole, mebendazole and praziquantel.Review of non-clinical toxicity and pharmacokinetics. *Acta Tropica.,* 86**,** 141-159.

DHIRENDRA, K., LEWIS, S., UDUPA, N. & ATIN, K. 2009. Solid dispersions: A review. *Pak. J Pharm Sci.,* 22**,** 234-246.

DOKALA, K. G. & PALLAVI, C. 2013. Direct Compression - an overview. *IJRPBS.,* 4**,** 155-158.

EL-BADRY, A., AL-JUHANI, A., IBRAHIM EL, K. & AL-ZUBIANY, S. 2008. Distribution of sand flies in El-Nekheil province, in Al-Madinah Al-Munawwarah region, western of Saudi Arabia. *Parasitol Res.,* 103**,** 151-6.

EL-RAHMAN, A. M., OMRAN, A. M., ABDEL-NABI, M. I. & MOHAMED, F. M. 1999. Assessment of albendazole (antiparasitic drug) effects on the physiological activities of the cardiac, smooth and skeletal muscles of some experimental animals. *Egypt J Biol.,* 1**,** 30-44.

EL HARTI, J., ANSAR, M. & TAOUFIK, J. 2014. Albendazole and its analogues. *IJPSR,* 5**,** 102-107.

ESLAMI, A., RASSOULI, A., MESHKI, B. & SHAMS, R. G. 2006. A bioequivalence study of an albendazole oral suspension produced in Iran and a reference product in sheep. *Intern J Appl Res Vet Med.,* 4**,** 109-114.

FERNANDO, D. S., WICKRAMASINGHE, P. V., DEWASURENDRA, R. L. & KAPILANANDA, G. M. 2011. Comparative effect of albendazole and diethylcarbamazine in the treatment of toxocariasis in children from Sri Lanka: A preliminary study. *J Clin Med Res.,* 3**,** 46-51.

GAFOURIAN, T., SAFARI, A., ADIBKIA, K., PARVIZ, F. & NOKHODCHI, A. 2007. A drug release study from hydroxypropylmethylcellulose (HPMC) matrices using QSPR modeling. *JPS.,* 96**,** 3334-3351.

GAWAI, K. S., DESHMANE, V. S., PUROHIT, N. R. & BIYANI, R. K. 2013. In vivo-In vitro evaluation of solid dispersion Containing Ibuprofen. *AJADD.,* 1**,** 066-072.

GHANIM, A. N. 2013. Application of response surface methodology to optimize nitrate removal from wastewater by electrocoagulation. *IJSER.,* 4**,** 1410-1416.

GIRI, K. T., ALEXANDER, A. & TRIPATHI, K. D. 2010. Physicochemical classification and formulation development of solid dispersion of poorly water soluble drugs: an updated review. *Int J Pharm Biol Sci Arch.,* 1**,** 309-324.

HASNAIN, S. M. & NAYAK, K. A. 2012. Solubility and dissolution enhancement of ibuprofen by solid dispersion technique using PEG 6000-PVP K 30 combination carrier. *Bulg J Sci Educ.,* 21**,** 118-132.

HORTON, J. 2000. Albendazole: a review of anthelmintic efficacy and safety in humans. *Parasitology.,* 12**,** 113-132.

HOWLADER, I. S., CHAKRABARTY, K. J., FAISAL, S. K., KUMAR, U., SARKAR, R. & KHAN, F. 2012. Enhancing dissolution profile of diazepam using hydrophilic polymers by solid dispersion technique. *Int Curr Pharm J.,* 1**,** 423-430.

HUANG, Y. & DAI, G. W. 2014. Fundamental aspects of solid dispersion technology for poorly soluble drugs. *Acta PharmaceuticaSinica.,* 4**,** 18–25.

IYER, R. S., SIVAKUMAR, R., SIVA, P. & SAJEETH, I. C. 2013. Formulation and evaluation of fast dissolving tablets of risperidone solid dispersion. *IJPCBS.,* 3**,** 388-397.

JAHAN, T. S., KHAN, R. S., RAHMAN, R. M., SADAT, A. M. & JALIL, U. R. 2011. Enhancement of dissolution profile for oral delivery of fexofenadine hydrochloride by solid dispersion (solvent evaporation) technique. *Am J Sci Ind Res.,* 2**,** 112-115.

JATWANI, S., RANA, C. A., SINGH, G. & AGGARWAL, G. 2011. Solubility and Dissolution enhancement of simvastatin using synergistic effect of hydrophilic carriers. *Der Pharmacia Lettre.,* 3**,** 280-293.

KADAJJI, G. V., BETAGERI, V. G. & 2011. Water soluble polymers for pharmaceutical applications. *Polymers.,* 3**,** 1972-2009.

KALYANWAT, R. & PATEL, S. 2010. Solid dipersion: A method for enhancing drug dissolution. *IJDFR.,* 1**,** 1-14.

KAPOOR, H., KAUR, R., BEHL, H. S. & KOUR, S. 2012. Solid dispersion: an evolutionary approach for solubility enhancement of poorly water soluble drugs. *Int J Recent Adv Pharm Res.,* 2**,** 1-16.

KAROLEWICZ, B., GORNIAK, A., OWCZARE, K. A., NARTOWSKI, K., ŻURAWSKA-PŁAKSEJ, E. & PLUTA, J. 2012. Solid dispersion in pharmaceutical technology. Part II.

The methods of analysis of solid dispersions and examples of their application. *Polim Med.,* 42**,** 97–107.

KAUR, J., AGGARWAL, G., SINGH, G. & RANA, C. A. 2012. Improvement of Drug solubility using solid dispersion. *Int J Pharm Pharm Sci.,* 4**,** 47-53.

KIM, T. K., LEE, Y. J., LEE, Y. M., SONG, K. C., CHOI, J. & KIM, D. D. 2011. Solid dispersions as a drug delivery system. *J Pharm Invest.,* 41 125-142.

KOMMAVARAPU, P., MARUTHAPILLAI, A., PALANISAMY, K., SALADI, N. V. & KOYA, T. R. 2014. Solid Dispersions for solubility and bioavailability enhancement of poorly aqueous soluble drugs: a review. *IJACSA.,* 2**,** 8-15.

KONNO, H. & TAYLOR, L. S. 2006. Influence of different polymers on the crystallization tendency of molecularly dispersed amorphous felodipine. *J Pharm Sci.,* 95**,** 2692-2705.

MA, C., LIN, P. & LIU, P. 1999. Statistical Evaluation of dissolution similarity. *Statistical sinica.,* 1011-1027.

MAHAPATRA, K. A., MURTHY, N. P., RANI, R. E., SOUJANYA, P. S. & PATRA, K. R. 2012. An update review on technical advances to enhance dissolution rate of hydrophobic drugs. *IRJP.,* 3**,** 1-7.

MAHLER, G., DAVYT, D., GORDON, S., INCERTI, M., NÚÑEZ, I., PEZAROGLO, H., SCARONE, L., SERRA, G., SILVERA, M. & MANTA, E. 2008. Synthesis of an albendazole metabolite: characterization and HPLC determination. *J Chem Educ.,* 85**,** 1652-1654.

MANOHARA, C., SANGANAL, S. J., PREM KUMAR, G., SWAMY, K. B. & PHANI, A. R. 2014. Improved dissolution rate of piroxicam by fusion solid dispersion technique. *Sci Technol Arts Res J.,* 3**,** 44-47.

MARQUES, P. M., TAKAYANAGUI, M. O. & LANCHOTE, L. V. 2002. Albendazole metabolism in patients with neurocysticercosis: antipyrine as a multifunctional marker drug of cytochrome P450. *Braz J Med Biol Res.,* 35**,** 261-269.

MASTERS, K. 1991. Spray drying handbook Wiley, New York.

MORIWAKI, C., COSTA, L. G., FERRACINI, N. C., MORAES, F. F., ZANIN, M. G., PINEDA, G. A. & MATIOLI, G. 2008. Enhancement of solubility of albendazole by complexation with β-cyclodextrin. *Braz J Chem Eng.,* 25**,** 255 – 267.

NAGABANDI, K. V., RAMARAO, T. & JAYAVEERA, N. K. 2011. Liquisolid compacts: a novel approach to enhance bioavailability of poorly soluble drugs. *Int J Pharm biol sci.,* 1**,** 89-102.

NIKGHALB, A. L., SINGH, G., SINGH, G. & KAHKESHAN, F. K. 2012. Solid dispersion: methods and polymers to increase the solubility of poorly soluble drugs. *JAPS.,* 2**,** 170-175.

NOORDIN, Y. M., VENKATESH, C. V., SHARIF, S., ELTING, S. & ABDULLAH, A. 2004. Application of response surface methodology in describing the performance of coated carbide tools when turning AISI 1045 steel. *J Mater Process Technol.,* 145**,** 46–58.

OKONOGI, S. & PUTTIPIPATKHACHORN, S. 2006. Dissolution improvement of high drug-loaded solid dispersion. *AAPS PharmSciTech.,* 7**,** 1-6.

PATIDAR, K., SHIRSAGAR, D. M., SAINI, V., JOSHI, B. P. & SONI, M. 2011a. Solid dispersion technology: a boon for poor water soluble drugs. *IJNDD.,* 3**,** 83-90.

PATIDAR, K., SHIRSAGAR, D. M., SAINI, V., JOSHI, B. P. & SONI, M. 2011b. Solid dispersion technology: a boon for poor water soluble drugs. *IJNDD.,* 3**,** 83-90.

PEHLIVAN, B. S., SUBASI, B., VURAL, O., UNLU, N. & CAPAN, Y. 2011. Evaluation of drug excipient interaction in the formulation of celecoxib tablets. *Acta Pol Pharm -Drug Res.,* 68**,** 423-433.

PRANZO, B. M., SHANK, C. D., CORUZZI, M., CAIRA, R. M. & BETTINI, R. 2010. Enantiotropically related albendazole polymorphs. *J Pharm Sci.,* 99**,** 3731-3743.

RAISSI, S. & FARSANI, E. R. 2009. Statistical process optimization through multi-response surface methodology. *WASET.,* 3 03-25.

RAJESH, K., RAJALAKSHMI, R., UMAMAHESWARI, J. & KUMAR, A. K. 2011. Liquisolid technique a novel approach to inhance solubility and bioavailability. *IJB.,* 2**,** 8-13.

RAMESH, B. 2011. Method development and validation for dissolution testings. *RJPBCS.,* 2**,** 561-575.

ROWE, C. R., SHESKEY, J. P. & OWEN, C. S. 2006. Handbook of pharmaceutical excipients. *Pharmaceutical Press, London.***,** p 549.

RUPAL, J., KAUSHAL, J., MALLIKARJUNA, C. S. & DIPTI, P. 2009. Preparation and evaluation of solid dispersions of aceclofenac. *IJPSDR.,* 1**,** 32-35.

SAMEER, S., RAVIRAJ, S.B. & YADAV, L. 2011. A review on solid dispersion. *IJPLS,* 2**,** 1078-1095.

SANJAY, S.P. & NATVARLAL, M.P. 2009. Developmecnt of directly compressible co-processed excipient for dispersible tablets using 3^2 full factorial design. *Int J Pharm Pharm Sci.,* 1**,** 125-148.

SAPKAL, S., BABHULKAR, M., RATHI, A., MEHETRE, G. & NARKHEDE, M. 2013. An overview on the mechanisms of solubility and dissolution rate enhancement in solid dispersion. *Int J PharmTech Res.***,** 31-39.

SEKIGUCHI, K. & OBI, N. 1961. Studies on absorption of eutectic mixture. I. a comparison of the behavior of eutectic mixture of sulfathiazole and that of ordinary sulfathiazole in man. *Chem Pharmaceut Bul,* 9**,** 866-872.

SHINDE, S. S., PATIL, S. S., MEVEKARI, F. I. & SATPUTE, A. S. 2010. An approach for solubility enhancement: solid dispersion. *IJAPR.,* 1**,** 299-308.

SIMONE, D. I., COCEANI, N., FARRA, R., FIORENTINO, M. S., GRASSI, G., LAPASIN, R., HASA, D., PERISSUTTI, B., GRASSI, M. & VOINOVICH, D. 2012. Study on polymer-surfactant interactions for the improvement of drug delivery systems wettability. *Chem Biochem Eng Q.,* 26**,** 405–415.

SINGHVI, G. & SINGH, M. 2011. Review: in-vitro drug release characterization models. *IJPSR.,* 2**,** 77-84.

TACHIBANA, T. & NAKAMURA, A. 1965. "A methode for preparing an aqueous colloidal dispersion of organic materials by using water-soluble polymers: dispersion ofβ-carotene by polyvinylpyrrolidone,". *Colloid and Polymer Science,* 203**,** 130-133.

TANTISHAIYAKUL, V., KAEWNOPPARATV, N. & INGKATAWORNWONG, S. 1999. Properties of solid dispersions of piroxicam in polyvinylpyrrolidone. *Int J Pharm.,* 181**,** 143-151.

TEJAS, P., TAMIR, P., SUNIL, M. & TUSHAR, P. 2010. Enhancement of dissolution of fenofibrate by solid dispersion technique. *Int J Res Pharm Sci.,* 1**,** 127-132.

THAKUR, K., NAGPAL, M., AGGARWAL, G., KAUR, R., SINGH, S., BEHL, T. & JAIN, K. U. 2014. A review on solid dispersion. *WJPPS.,* 3**,** 173-187.

THORAT, S. Y., GONJARI, D. I. & HOSMANI, H. A. 2011. Solubility enhancement techniques: a review on conventional and novel approaches. *IJPSR.,* 2**,** 2501-2513.

TIWARI, R., TIWARI, G., SRIVASTAVA, B. & AWANI, K. 2009. Solid dispersions: an overview to modify bioavailability of poorly water soluble drugs. *Int J PharmTech Res.,* 1**,** 1338-1349.

TSAI, W. C., TONG, I. L. & WANG, H. C. 2010. Optimization of multiple responses using data envelopment analysis and response surface methodology. *Tamkang J Sci Eng.,* 13**,** 197-203.

ULLAH, S. S., ULLAH, K. S., ABDUL, W., HAROON, K. & MAJID, G. K. 2011. Formulation and evaluation of directly compressed ofloxacin ethocel controlled release tablets: a kinetic approach. *IJRAP.,* 2**,** 801-809.

USP30-NF25 2007. United State Pharmacopoeia 30-National Formulary 25. The United States Pharmacopoeial Convention. *The United States Pharmacopoeial Convention.*

VARMA, V., SOWMYA, C. & TABASUM, S. G. 2012. Formulation and evaluation of piroxicam solid dispersion with suitable carrier. *RJPBCS.,* 3**,** 929-940.

VASKULA, S., VEMULA, K. S., BONTHA, K. V. & GARREPALLY, P. 2012. Liquisolid compacts: an approach to enhance the dissolution rate of nimesulide. *JAPS.,* 2**,** 115-121.

VAZQUEZ, N. G., YEPEZ, L., CAMPOS, H. A., TAPIA, A., LUIS, H. F., CEDILLO, R., GONZALEZ, J., FERNANDEZ, M. A., GRUEIRO, M. M. & CASTILLOA, R. 2003. Synthesis and antiparasitic activity of albendazole and mebendazole analogues. *Bioorg Med Chem.,* 11**,** 4615–4622.

VENKATESAN, P. 1998. Albendazole. *J Atimicrob Chemother.,* 41**,** 145–147.

VENKATESH, N. G., SANGEETHA, S., SAMANTA, K. M., SURESH, N., RAMESH, M., FAISAL, M., ILAHI, A. A., ABUTHAHIR, S. S., HAQ, I. M. & ELANTHIRAYAN, S. 2008. Dissolution enhancement of domperidone using water soluble carrier by solid dispersion technology. *Int J Pharm Sci Nanotech.,* 1**,** 221-226.

YADAV, B. & TANWAR, S. Y. 2015. Applications of solid dispersions. *J Chem Pharm Res.,* 7**,** 965-978.

YAGOUB, M. M., ABDOUN, S. & SERI, I. H. 2013. In use stability studies of two veterinary medicinal products: albendazole and oxytetracycline. *Assiut Vet Med J.,* 59**,** 11-14.

ZHAO, C. L., HE, Y., XIN , DENG, X., YANG, L. G., LI, W., LIANG, J. & TANG, L. Q. 2012. Response surface modeling and optimization of accelerated solvent extraction of four lignans from fructus schisandrae. *Molecules.,* 17**,** 3618-3629.